ICEBE
IMAGINEERING
NATURE

DIPLOMARBEIT

The positive effect of calcite as bed material for dual fluidized bed steam gasification

ausgeführt zum Zwecke der Erlangung des akademischen Grades eines
Diplomingenieurs (Dipl.-Ing.) unter der Leitung von

Univ.Prof. Dipl.-Ing. Dr.techn. Hermann Hofbauer

am

Institut für Verfahrenstechnik, Umwelttechnik und Technische Biowissenschaften

betreut von

Dipl.-Ing.(FH) Dr.techn. Johannes Schmid, MBA

Dipl.-Ing. Florian Benedikt

eingereicht an der Technischen Universität Wien
Fakultät für Maschinenwesen und Betriebswissenschaften
von

Fatemeh Hassanli
Matrikelnummer 01634850

Wien, am 28.05.2018

Ich habe zur Kenntnis genommen, dass ich zur Drucklegung meiner Arbeit unter der Bezeichnung

Diplomarbeit

nur mit Bewilligung der Prüfungskommission berechtigt bin.

Ich erkläre weiters an Eides statt, dass ich meine Diplomarbeit nach den anerkannten Grundsätzen für wissenschaftliche Abhandlungen selbstständig ausgeführt habe und alle verwendeten Hilfsmittel, insbesondere die zugrunde gelegte Literatur, genannt habe.

Weiters erkläre ich, dass ich dieses Diplomarbeitsthema bisher weder im In- noch Ausland (einer Beurteilerin/einem Beurteiler zur Begutachtung) in irgendeiner Form als Prüfungsarbeit vorgelegt habe und dass diese Arbeit mit der vom Begutachter beurteilten Arbeit übereinstimmt.

Wien, am 28. Mai 2018

Fatemeh HASSANLI

Acknowledgment

First, I proudly and wholeheartedly thank my very dear and kind parents, who have always loved and supported me in all aspects of emotional and financial of my life. They have always advised and encouraged me on four things: Always to hope, to be honest, to be a generous human and to keep education. My dear parents it have made possible for me to continue my education in abroad at my favorite university, TU Wien, in Austria.

I heartily thank so much Mr. Prof. Hermann Hofbauer for this valuable opportunity to carry out my master thesis in the “Gasification and Gas Cleaning” research team at the Institute of Chemical, Environmental and Biological Engineering of TU Wien.

Mr. Prof. Hermann Hofbauer helped me a lot during my studies as dean of study for Chemical Engineering and also as Professor. I learned so much from his courses. He is a prominent and humble professor. At the beginning of my studies at TU Wien, he helped me a lot regarding paper work and he always was kind to me.

A very special thank goes to Mr. Dr. Johannes C. Schmid to invest time to edit my master thesis. Indeed, writing my master thesis was impossible without the guidance, supports and advices of him. He always replied my questions with patience and open ear. I learned a lot from him during my work. He is one of the best person in charge.

I would like kindly to thank Dipl.-Ing. Florian Benedikt to invest time to edit my master thesis as well as to help me regarding my work.

Furthermore, I would like to thank Dipl.-Ing. Anna Magdalena Mauerhofer, Dipl.- Ing. Josef Fuchs , Mr. Dr. Stefan Müller and also everyone who helped me directly and indirectly regarding my work in the research group “Gasification and Gas Cleaning”.

I had a very useful and good working time with this team. To study at TU Wien as well as to work with this research team was really my pleasure and I am really so happy for that.

Abstract

A promising key technology for the sustainable (renewable) production of electricity, heat, synthetic chemicals and fuels is steam gasification of biomass in a dual fluidized bed (DFB) gasification system. Therefore, gasification of softwood at temperatures between 750 – 850 °C was carried out at an advanced 100 kW_{th} pilot plant at TU Wien to investigate the effects of calcite admixtures to different bed materials on the performance of the DFB steam gasification process regarding product gas composition and the concentration of condensable hydrocarbons (tars) in it. In this respect, olivine, silica sand and feldspar were used as pure bed materials and also mixed with calcite in mass ratios of 100/0, 90/10, 50/50 and 0/100. The gasifier system consists of gasification and combustion reactor, which are thermodynamically connected via a circulating bed material. The bed material has two functions (i) as a heat carrier from the combustion to the gasification reactor and (ii) as a catalyst for gasification reactions to improve the product gas quality. The product gas consists mainly of H_2, CO, CO_2, CH_4 and C_2H_4. For the use as synthesis gas in subsequent processes tar, char and inorganic fines in the product gas have to be removed by suitable cleaning and filtering equipement. Pure steam was used as fluidization and gasification agent at a range of steam to fuel ratios between 0.7 – 1 $kg_{H_2O}/kg_{fuel,daf}$. During the gasification operation, extensive gas analyses were performed at the outlet of the gasification reactor (sample point A). Experimental results were validated via IPSEpro software by calculation of mass- and energy balances. A good agreement between simulation and experimental results was achieved. It was observed that the admixture of calcite to olivine, silica sand and feldspar as bed material shifted the product gas compositions towards higher hydrogen and carbon dioxide and lower carbon monoxide contents. Additionally, the tar content (GC-MS tar and gravimetric tar) in the product gas was decreased and the tar composition changed, resulting in lower calculated tar dew points. The pure calcite as bed material led to the product gas with the highest H_2 and the lowest tar content as well as the lowest calculated tar dew point compared to all mass ratios of other bed materials. These results can be explained by enhanced water-gas shift reactions and improved steam reforming reactions of hydrocarbons. Pure calcite compared to pure olivine, pure silica sand and pure feldspar as bed material caused an increase of the H_2 content of up to 25 %. The tar content was decreased up to 93 %. Additionally, the lowest content of higher hydrocarbons, CH_4 and C_2H_6, in the product gas was found by applying pure calcite as bed material.

Table of Contents

1 Introduction

1.1 Biomass as a renewable energy source

With the energy crisis caused by high demand and ecological environment deterioration produced from fossil energy, it is urgent to look for new alternative energy to realize saving energy and reducing emissions. Biomass as the third largest natural source of energy in the world has attracted widespread attention with the advantage of rich in resources, environmentally friendly and easy to develop (Mirkouei A. et al., 2017). Since approximately 1850, global use of fossil fuels (coal, oil and gas) has increased to dominate energy supply, leading to a rapid growth in carbon dioxide (CO_2) emissions (IEA, 2014; IPCC, 2011; UNDP, 2001). Bioenergy can be produced from a variety of biomass feed stocks, including forest, agricultural and livestock residues; short rotation forest plantations; energy crops; the organic component of municipal solid waste; and other organic waste streams. To mitigate climatic change caused by green- house gas emissions, the developed world is working to substitute fossil fuels with renewable energy sources. To stabilize the atmospheric concentration of CO_2, global emissions must be reduced by at least 60% from the current levels. Approximately 80% of the total emissions come from use of fossil fuels, mostly from industrialized nations. Much of the remaining 20% is believed to come from deforestation, mostly from tropical nations (Swisher J. N., 1994). Furthermore, there are indications that forestland could contribute more to global CO_2 stabilization through sustained production chains of fuel for biomass energy systems to replace fossil fuels (State of the World's Forests, 2001). Figure 1 (World Energy Council, 2017) shows the share of bioenergy in the primary energy world consumption. The total global potential of biomass is estimated 500 EJ/year, which represents 30% of global energy demand. At this moment, for energy purposes almost 30 EJ of energy from biomass is consumed per year (British Petroleum, 2017).

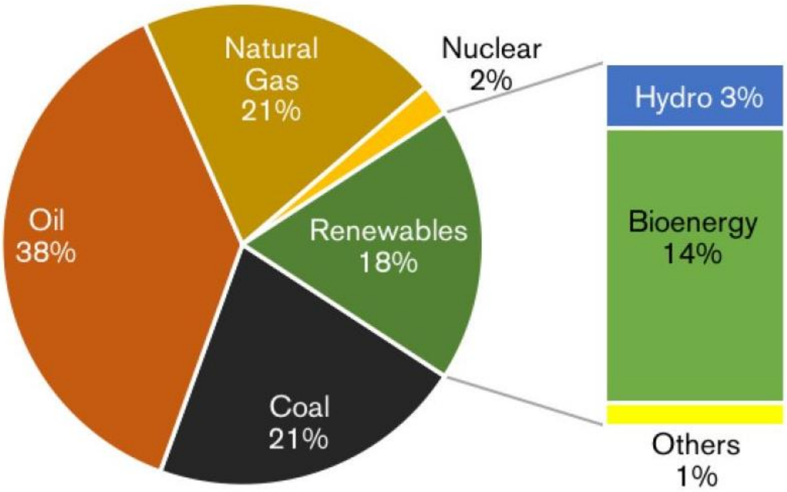

Figure 1: Share of bioenergy in the primary energy world

1.2 Polygeneration concept of biomass gasification

Since the early 2000s global research on energy extraction from renewable sources has risen considerably. The awareness of global warming caused by combustion of fossil fuels has increased the development of technologies using biomass since it is considered as a major source of renewable energy. Biomass is suitable for use in pyrolysis, combustion and gasification as CO_2-neutral feedstock [Van Swaaij W. et al., 2015]. Gasification transforms the solid feedstock into a gaseous secondary energy carrier, which is referred to as product gas. Biomass gasification as a thermochemical partial oxidation is an advanced and important technology to produce useful convenient gaseous fuels with low cost and high efficiency (Basu P., 2010; Van der Stelt M. J. C., 2011 and Ruiz J. et al., 2013). Figure 2 (Koppatz S et al., 2011) represents the polygeneration concept from biomass gasification. The thermo-chemical conversion of biogenic feedstock is a promising option to advance the eco-friendly and efficient production of heat and power, as well as the generation of valuable products for the chemical industry or transportation fuels based on renewable sources. Fluidized bed processing is applied by preference for the gasification of various carbonaceous fuels, and therefore also for biomass. This technology intensely promotes the conversion of the solid feedstock into a valuable gas by an excellent gas–solid contact and heat transfer. The application of biomass derived product gas as precursor for various syntheses might increase the share of renewables in the chemical industry in contrast to fossil fuels (Schmid J. C. et al., 2012a and 2012b).

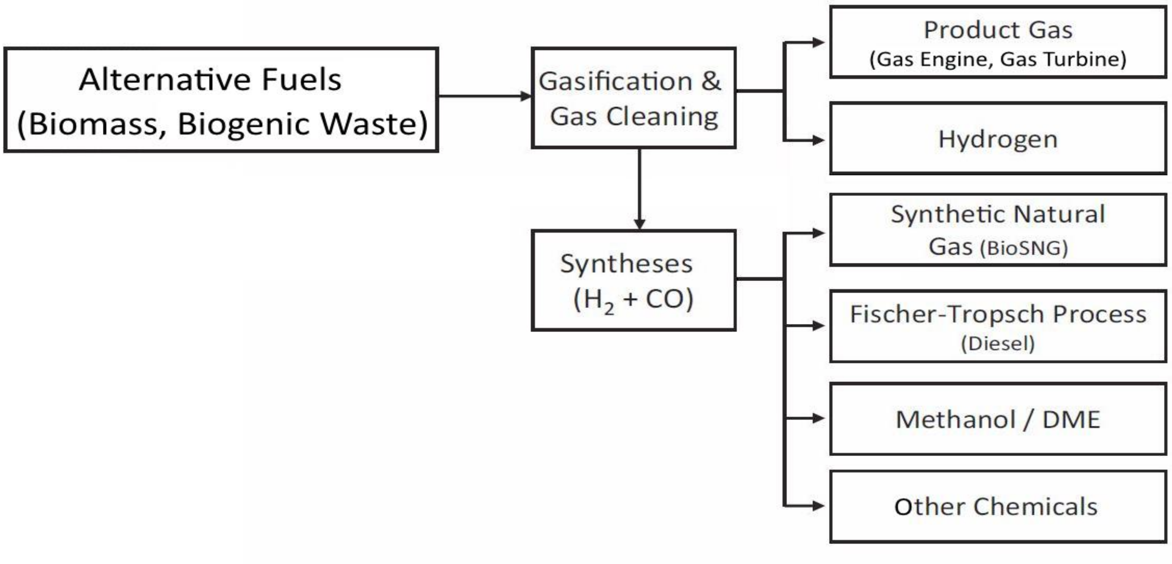

Figure 2: Polygeneration concept of biomass gasification

1.3 Objective and methodology

This research focuses on the effect of calcite in mixing with other bed materials on the performance of dual fluidized bed (DFB) steam gasification in the advanced 100 kW_{th} pilot plant at TU Wien. In this regard, calcite is added to different bed materials such as olivine, silica sand and feldspar. For comparison, also test runs with pure calcite, olivine, silica sand and feldspar are performed additionally. H. Hofbauer et al. (Hofbauer H. et al.,1995 and 1997) developed DFB technology for steam gasification of biomass at TU Wien in the 1990s. This master thesis responds to the research questions that are the purpose of this study;

- What effect has the applying calcite as pure bed material or as mixture with other bed materials on the DFB gasifier system?
- How is the product gas composition and tar content in the gasification of softwood pellets?
- What are the key figures of the process simulation?
- What effects have different mass ratios of bed materials on the product gas composition?

This master thesis explains the presented work in a clear way. The work is divided into the following chapters:

- Chapter 2 gives an overview on the fundamentals of DFB steam gasification at TU Wien;
- Chapter 3 presents the advanced 100 kW_{th} pilot plant at TU Wien as well as the applied extensive measurement systems;
- Chapter 4 provides the results of softwood gasification test runs with different bed materials and subsequently discusses the results;
- Chapter 5 answers the research questions of this investigation and provides a proposal for future experimental gasification test runs at TU Wien.

2 Fundamentals of DFB steam gasification

2.1 Bioenergy

Bioenergy is energy from organic matter (biomass), i.e. all materials of biological origin that is not embedded in geological formations (fossilised) [World Energy Council, 2017]. Woody biomass is used for production of electricity and heat for industries, towns and cities and production of liquid biofuels. The primary energy supply of forest biomass used worldwide is estimated at about 56 EJ, which means woody biomass is the source of over 10% of all energy supplied annually. Overall woody biomass provides about 90% of the primary energy annually sourced from all forms of biomass [WBA, 2017]. Woody biomass used is in the form of cut branches and twigs, wood chip and bark, and pellets made from sawdust and other residues. Some of it is wood from demolition and construction, from urban parks and gardens and from industrial wood waste streams (broken pallets, building form work and industry packing crates) [World Energy Council, 2017]. In the current work, softwood pellets are used as feedstock. Schmid et al. reported that softwood pellets have a very good cohesion behavior during the gasification process (Schmid et al., 2012a). Equation 1 shows that the water content (w) is defined as the mass of water in the biomass referring to the total mass:

$$w = \frac{m_w}{m_w + m_f} \qquad \text{Eq. 1}$$

Where m_w is mass of water and m_f is mass of dry substance.

2.2 Gasification of biomass

Gasification is one of the paths to extract energy from biomass. Efficient conversion of biomass to a medium calorific product gas by means of steam gasification allows the combined production of heat and power. Gasification is divided into three steps: drying, devolatilisation and gasification (Kaushal P. et al., 2008). In Figure 3 (Kaltschmitt M. et al., 2016) the process steps for gasification of a single biomass particle are shown. The overall gasification process of biomass is endothermic. Therefore, the particle has to be heated up and goes through the following process steps:

- Drying occurs at temperatures between 100 °C and 150 °C. The biomass particle as feedstock loses the water and steam is released from it. Due to the high vaporization enthalpy of water, the average temperature increase is low;
- Devolatilisation occurs at temperatures between 200 °C and 650 °C, without free oxygen from gasification agent. The macromolecules of the biomass structure break up and release as gases. The reaction between gasification agent and residual particle is negligible. The residual particle consists of char and ash;
- Gasification occurs at temperatures between 700 °C and 1000 °C, with steam as gasification agent. The remaining char reacts at higher temperatures with steam to product gas. In this atmosphere volatiles can further react in homogenous gas-gas reactions. The inorganic matter or ash remains.

A gasification agent like air, oxygen, steam, carbon dioxide, or a mixture of oxygen and steam can convert the residual char into product gas. In fluidized beds, gasification takes place at temperatures between 700 C and 1000 C (Kern S. et al., 2013).

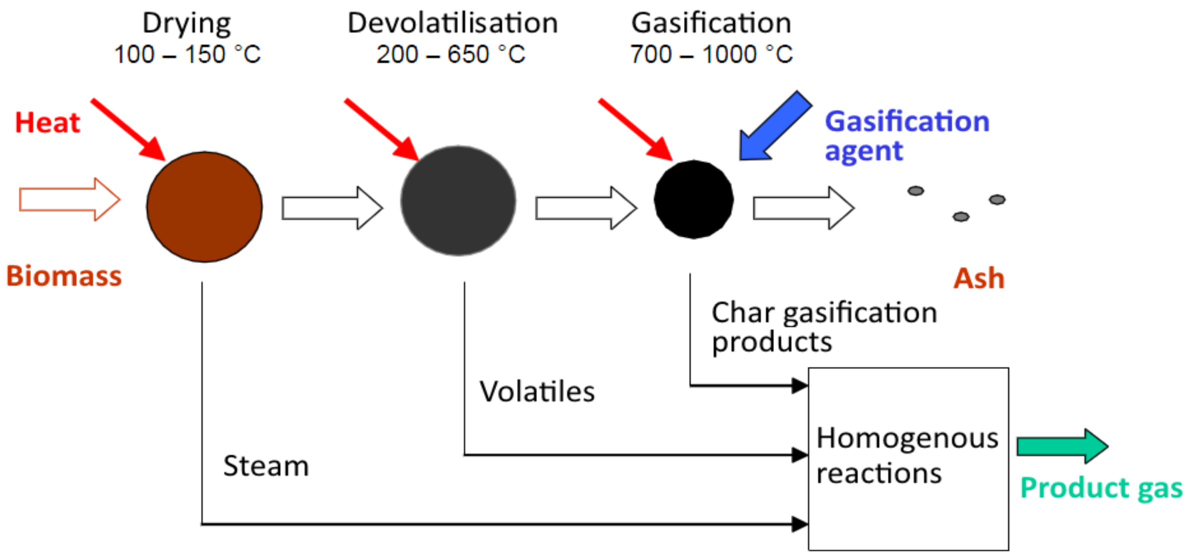

Figure 3: Process during the gasification of a single biomass particle

In many applications for gasification of solid feedstock, air is used as gasification agent, as it is cheap as well as drives the process auto-thermally. The drawback of using air is that a lot of nitrogen is introduced, dilutes the product gas, and lowers the heating value of the product gas down to about 3 – 6 $\mathrm{MJ/Nm^3_{db}}$ (Zainal Z. A. et al., 2002). When steam or CO_2 is used as a gasification agent, the product gas is free of nitrogen and the calorific value of the gas is higher: for steam, gasification values from 10 – 18 $\mathrm{MJ/Nm^3_{db}}$ can be reached (Rapagna S., 2000). The advantage using steam instead of CO_2 is that the reactivity of steam is on average about four times higher than that of CO_2. If CO_2 was used as gasification agent, residence times of the char in the gasification section would have to be longer and the gasification efficiency would suffer. With H_2O or CO_2 as a gasification agent, the process becomes allo-thermal, so the heat for the endothermic gasification reactions has to be provided externally (Schuster G., 2001; Molina A., Mondrago F, 1998). Several investigations with previous test plants at TU Wien focused on the increase of the lower heating value as well as the hydrogen content of the product gas. Therefore, steam is used as a gasification agent in a dual fluidized bed gasifier (see Pasteiner H. A., 2015).

The main heterogeneous and homogeneous gasification reactions are shown in Table 1 (Schmid J. C., 2014; M. Kaltschmitt et al., 2009). Eq. 2 and Eq. 3, which are exothermic reactions, represent the total and partial oxidation of carbon reactions. The required heat for the endothermic reactions Eq.4 and Eq. 5 is provided by these reaction (Eq. 2 and Eq. 3). The methanation reaction (Eq. 6) is slightly exothermic. Homogeneous gasification reactions (Eq. 8 – Eq. 12) influence the product gas composition depending on temperature and pressure. During devolatilisation, vapor of condensable hydrocarbons (tar) is released from the fuel particle. The tar content of the product gas can be analyzed gravimetrically and by gas chromatography coupled with mass spectrometry (GC-MS). Tar causes problems in downstream equipment due to the deposition at lower temperatures. Therefore, the reduction of tar in the product gas due to steam (Eq. 11) and dry reforming (Eq. 12) is a central goal of the advanced dual fluidized bed gasifier concept (Pasteiner H. A., 2015).

Table 1: Important reactions in the gasification process

Heterogeneous reactions (gas-solid)			**Eq.**
Oxidation of carbon	$C + O_2 \rightarrow CO_2$	H. Exothermic	2
Partial oxidation of carbon	$C + \frac{1}{2} O_2 \rightarrow CO$	Exothermic	3
Water-gas reaction	$C + H_2O \rightarrow CO + H_2$	Endothermic	4
Boudouard	$C + CO_2 \rightarrow 2\,CO$	Endothermic	5
Methanation	$C + 2\,H_2 \rightarrow CH_4$	S. Exothermic	6
Steam gasification of solid fuel	$C_xH_yO_z + (x - z)H_2O \rightarrow x\,CO + \left(x - z + \frac{y}{2}\right) H_2$	Endothermic	7
Homogeneous reactions (gas-gas)			
Oxidation of hydrogen	$2\,H_2 + O_2 \rightarrow 2\,H_2O$	H. Exothermic	8
Water-gas-shift reaction	$CO + H_2O \leftrightarrow CO_2 + H_2$	S. Exothermic	9
Methanation	$CO + 3\,H_2 \leftrightarrow CH_4 + H_2O$	Exothermic	10
Steam reforming of hydrocarbons	$C_xH_y + x\,H_2O \rightarrow x\,CO + \left(x + \frac{y}{2}\right) H_2$	Endothermic	11
Dry reforming of hydrocarbons	$C_xH_y + x\,CO_2 \rightarrow 2x\,CO + \frac{y}{2}\,H_2$	Endothermic	12

H.: Highly
S.: Slightly

2.3 Fluidized Bed technology

Fluidization is associated with solid particles being transformed into a fluid-like state by an upwards flowing fluid. One of the first industrial applications was documented in the early 1940s with fluid catalytic cracking (Jahnig C. E. et al., 1980) and has since been implemented in many other industrial applications, including solid-catalyzed gas-phase reactions, non-catalytic reactions and physical processes. Gas – solid fluidized beds have Advantageous features such as excellent gas – solid contacting, efficient and uniform heat transfer, temperature uniformity, and suitability for processing a wide range of feedstocks, which have led to widespread industrial applications including coal/biomass, combustion/gasification/pyrolysis, drying, coating, ore roasting, catalytic processes such as acrylonitrile, aniline and Fischer-Tropsch synthesis, and gas-phase polyolefin production (Kunii D. and Levenspiel O., 1991; Grace J. R. et al., 1997).

2.3.1 Flow types of fluidized beds

If a granular material is present in a cylindrical container with a porous bottom, and if a. gas flows through it from bottom to top, then different states may occur depending on the gas velocity. It has been assumed $\rho_g < \rho_p$, which ρ_g and ρ_p represent gas density and particle density, respectively. The possible states of flow types for gas-solid systems are qualitatively characterized in Figure 4 (Levenspiel, O., 1998).

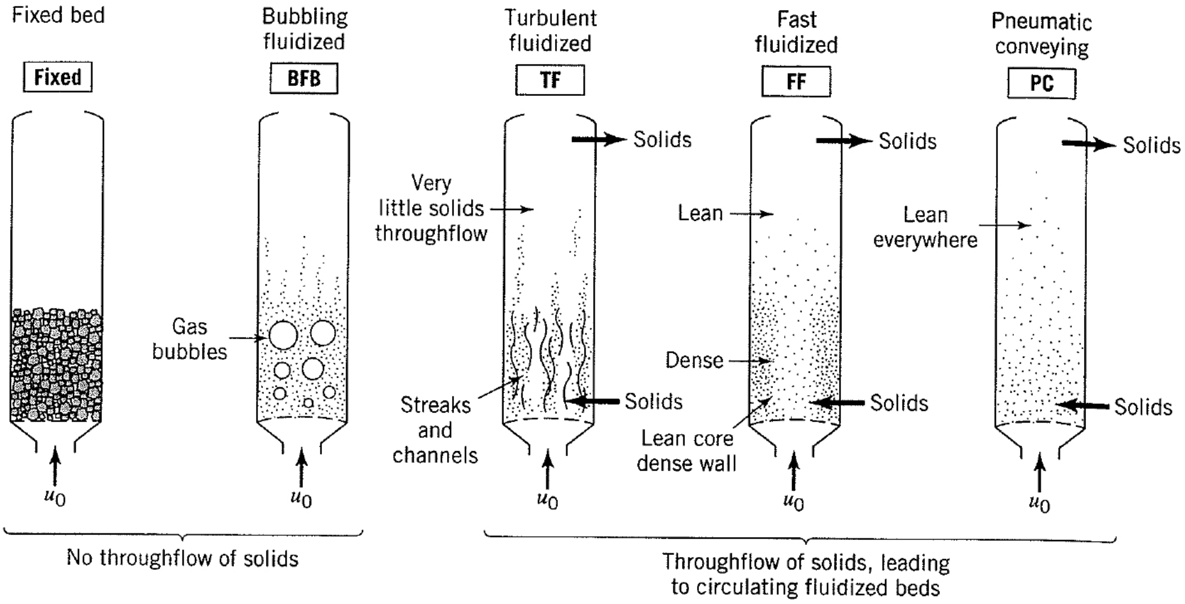

Figure 4: Fixed bed, fluidized bed and pneumatic transport

If the gas velocity is kept low, then a fixed bed is established. The solid particles have a fixed position and do not move. If the gas velocity increases, then the fixed bed begins to expand and the particles begin to move. This velocity is named minimum fluidization velocity. As the gas velocity further increases, it enters the fluidized bed region and the bed continues to expand. The bubbling fluidized bed, which mainly occur in slender fluidized bed tanks. The bubbles take on a size that fills the entire fluidized bed cross section. Fluidized beds can be maintained in a wide velocity range. On further increase, one finally approaches a velocity at which particles can be discharged from the container. This velocity is called the terminal velocity and represents the upper end of a fluidized bed. Due to the high gas volumes, the gas bubbles are combined and solid strands are observed. The literature also refers to so-called turbulent fluidized beds, since in this area, the pressure fluctuations decrease and the fluidized bed makes a distinctly quieter impression. At high velocities above the levitation velocity, which also corresponds to the rate of descent of the individual particles in the static fluid, the area of pneumatic transport is located.

2.3.2 Characterization of single particle

To characterize fluidized beds, the particle diameter (d_p) is defined. The problem is that particles have no perfect spherical shape. Therefore, the concept of the equivalent spherical diameter is introduced. This concept uses a physical property of the particle to calculate the diameter of a sphere with the same property. The physical property can be e.g. the volume of the particle (V_p). The equivalent diameter (Stieß M., 2008) is the diameter of a sphere with the same volume as the particle. The equivalent diameter is called particle volume diameter (d_v)

$$d_v = \left(\frac{6\,V_p}{\pi}\right)^{1/3}$$ Eq. 13

The particle surface diameter (d_s) (Stieß M., 2008) is calculated based on the surface of concerning particle. The particle surface diameter represents the diameter of a sphere with a similar surface as the particle.

$$d_s = \left(\frac{A_p}{\pi}\right)^{1/2}$$ Eq. 14

The shape of a particle (ϕ) (presented by Hofbauer H., 2013) is an important characteristic that influences its behavior in fluidized bed systems.

$$\phi = \frac{surface\ of\ the\ equal\ volume\ sphere}{surface\ of\ the\ particle} = \left(\frac{d_v}{d_s}\right)^2$$ Eq. 15

- For spheres: ϕ =1
- For all other particle forms: $0 < \phi < 1$

If one considers a layer of non-spherical particles and tries to simulate these by a layer with spherical particles in such a way that both layers have the same total particle surface area and the same porosity. These assumptions should result in about the same pressure drop when flowing through the layer. This results in an equivalent diameter that corresponds approximately to the sauter diameter d_{sv}. The equivalent diameter d_{sv} can be expressed by means of the shape factor as follows:

$$d_{sv} = \phi\, d_v \qquad \text{Eq. 16}$$

To determine the grain size, a sieve analysis is usually carried out, the equivalent diameter d_p being determined. However, as previously argued, most calculation formulas are mostly about d_{sv}. There is no general correlation between d_{sv} and d_p. Approximately can be used:

For particles that do not deviate too much from the spherical shape:

$$d_{sv} \approx \phi\, d_p \qquad \text{Eq.17}$$

For particles that are significantly larger in one dimension than in the other dimensions but not more than 2: 1 ("egg-shaped"):

$$d_{sv} \approx d_p \qquad \text{Eq. 18}$$

For particles that are significantly smaller in one dimension than in the others dimensions are, but not less than 1: 2 ("disk-shaped"):

$$d_{sv} \approx \phi^2\, d_p \qquad \text{Eq. 19}$$

For spherical or approximately spherical particles:

$$d_{sv} \approx d_v \approx d_p \qquad \text{Eq. 20}$$

To determine d_{sv}, the pressure drop in the fixed bed is measured. To determine d_v, a known number of particles N is weighed (total mass M) and determined by means of the following relationship d_v (presented by Hofbauer H., 2013).

$$d_v = \left(\frac{6\, M}{\pi\, \rho_P\, N}\right)^{1/3} \qquad \text{Eq. 21}$$

To describe the fluid dynamics of fluidized beds, the Reynolds number (Re) and Archimedes number (Ar) (presented by Hofbauer H., 2013) are used as follows:

$$Re = \frac{U\, \rho_g\, d_{sv}}{\mu} \qquad \text{Eq. 22}$$

$$Ar = \frac{\rho_g\, d_{sv}^3\, (\rho_p - \rho_g)\, g}{\mu^2} \qquad \text{Eq. 23}$$

2.3.4 Porosity, bulk density and particle volume fraction

Figure 5 (reproduced from Hofbauer H., 2017) presents a schematic of a container containing gas.

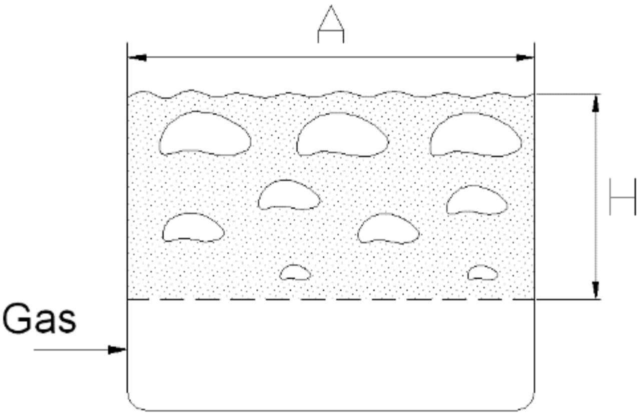

Figure 5: Schematic of a bubbling bed

The porosity (ε) is defined in the context of fluidized bed technology as follows:

$$\varepsilon = \frac{Void\ volume}{Total\ volume} = \frac{Total\ volume - Particle\ volume}{Total\ volume}$$

In symbols written this means:

$$\varepsilon = \frac{V_B - V_P}{V_B} = 1 - \frac{V_P}{V_B} = 1 - \frac{M}{\rho_p\, V_B} \qquad \text{Eq. 24}$$

- M: mass of the total particles
- ρ_P: particle density
- V_B: total bed volume

The bulk density (presented by Hofbauer H., 2017) is defined in the following equation:

$$\rho_b = \frac{M}{V_B} \qquad \text{Eq. 25}$$

From Euations 24 and 25, the relationship between fixed-bed porosity and bulk density can be calculated and is given in Equation 26

$$\varepsilon = 1 - \frac{\rho_b}{\rho_p} \qquad \text{Eq. 26}$$

Particle volume fraction (Schmid J. C., 2014) is defined as follows:

$$\varphi = 1 - \varepsilon \qquad \text{Eq. 27}$$

2.3.5 Fluidization regimes for industrial applications

Figure 6 (Schmid J.C., 2014, modified from: Grace J.R., 1986, Kunii D. & Levenspiel O., 1997) represents the most common fluidization regimes, typical for industrial applications. In bubbling fluidized beds a clear and evident surface is defined by a dense bed. This regime goes toward turbulent fluidization with increasing the superficial gas velocity (U_0). The turbulent fluidization regime shows no clear surface of the bed and a low entrainment of solids. The entrained solids have to be returned in order to ensure stationary operation. The height of the dense region is expanded compared to bubbling fluidization. Fast fluidization occurs at even higher superficiral gas velocities with higher particle entrainment and particle distribution over the total height of the reactor.

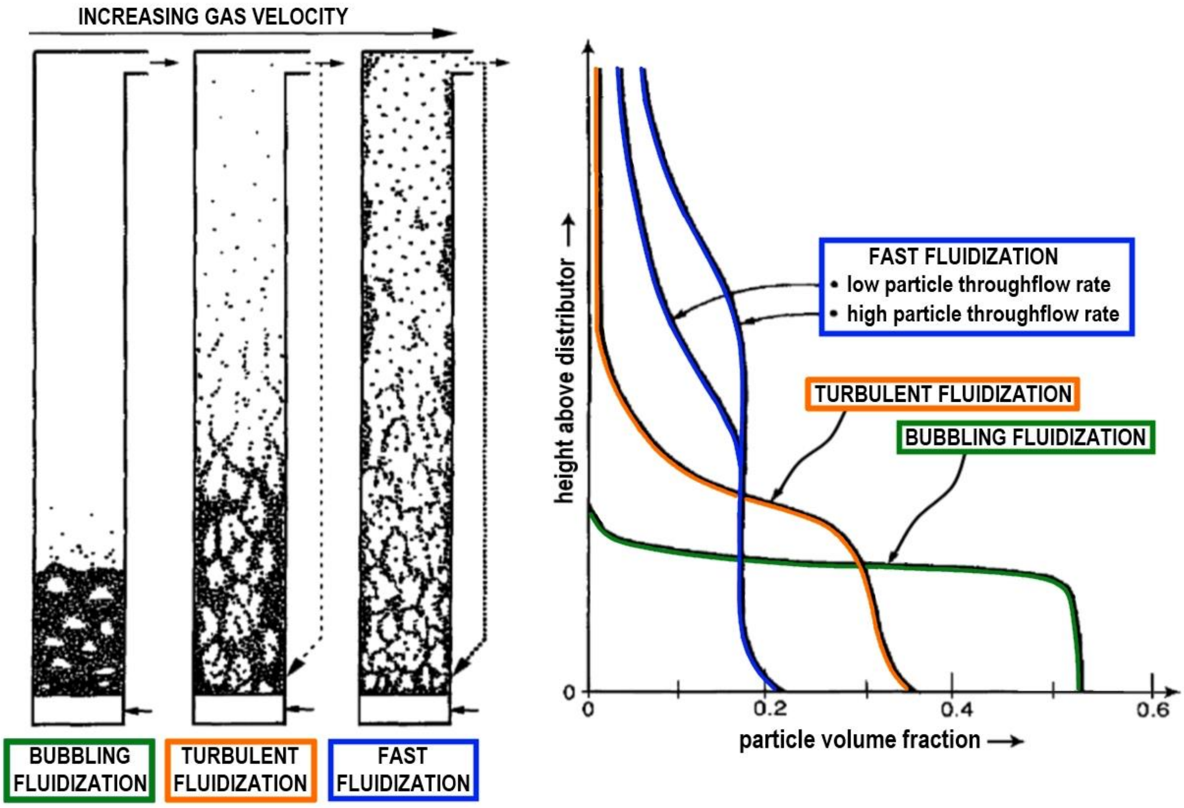

Figure 6: Common flow regims of fluidized beds for industrial applications

The superficial gas velocity U$_0$ (Geldart D., 1972) is calculated by the fluidization volume flow and the cross sectional area of the column as follows:

$$U_0 = \frac{\dot{V_g}}{A_{cs}} \qquad \text{Eq.28}$$

Geldart defined the behavior of powders fluidized by gases falls into four categories characterized by density difference ($\rho_s - \rho_f$) and mean size. Powders in group A exhibit dense phase expansion after minimum and prior to the commencement of bubbling; those in group B bubble at the minimum fluidization velocity; those in group C are difficult to fluidize at all and those in group D are of large size and/or density and spout readily (Geldart D. 1972). Each of the three regimes mentioned above occurs at a certain superficial gas velocity (Geldart D. 1972, Grace J. R., 1986). Depending on the group of particles, bubbling fluidization occurs if the superficial gas velocity (U_0) exceeds the minimum fluidization velocity (U_{mf}) or the minimum bubbling velocity U_{mb}. Minimum fluidization velocity (U_{mf}) and Reynolds number for minimum fluidization velocity (Re_{mf}) are defined as follows:

$$U_{mf} = \frac{\nu}{d_p} Re_{mf} \qquad \text{Eq. 29}$$

$$Re_{mf} = \left(\sqrt{27.2^2 + 0.0408\, Ar} - 22.7\right) \qquad \text{Eq. 30}$$

The transition from a fixed bed to a bubbling regime for group A particles is delineated by the minimum bubbling velocity U_{mb}. If U_0 exceeds U_{mb}, first bubbles appear in the bed. U_{mb} depends strongly on the particle properties. Therefore, the correlations for U_{mb} are assigned to the particle groups (Geldart D., 1972). Minimum bubbling velocity for group A particles (Bi H. T. and Grace J. R., 1995) is defined as follows:

$$U_{mb} = 33\, d_p \left(\frac{\rho_g}{\mu_g}\right)^{0.1} \qquad U_{mb} < U_{mf} \qquad \text{Eq. 31}$$

Minimum bubbling velocity for group B and D particles (Grace J. R. et al., 1997) is presented as follows:

$$U_{mb} = U_{mf} \qquad \text{Eq. 32}$$

When the superficial gas velocity (U_0) exceeds the critical fluidization velocity (U_c), the bubbling regime is changing to a turbulent regime. U_c has been extensively investigated and several correlations were found. An overview of the current state of correlations is presented in literature (Schmid J. C., 2014). The numerous correlations represent the transition area between the two regimes. For practical reasons the average critical fluidization velocity (U_{c_av}) (Schmid J. C., 2014) was introduced to describe the transition area between the two regimes:

$$U_{c\_av} = \frac{\nu}{d_p} Re_{c\_av} \qquad \text{Eq. 33}$$

Reynolds number of average critical fluidization velocity (Schmid J. C., 2014) was found as:

$$Re_{c\_av} = \frac{Ar^{19/30}}{0.85 + 0.85\, Ar^{1/5}} \qquad \text{Eq. 34}$$

The transition from a turbulent regime to the fast fluidization is delineated by the fluidization velocity with significant entrainment of solids U_{se}. When the superficial gas velocity U_0 exceeds U_{se}, the entrained solids of the fluidized bed have to be returned in order to ensure stationary operation (Pasteiner H. A. 2015). Fluidization velocity with significant entrainment of solids (Schmid J. C., 2014) and Reynolds number for U_{se} (Bi et al., 1995) are as follows:

$$U_{se} = \frac{\nu}{d_p} Re_{se} \qquad \text{Eq. 35}$$

$$Re_{se} = 1.53\, Ar^{0.5} \qquad \text{Eq. 36}$$

2.3.7 Pressure drop in the fluidized bed

A fixed bed becomes a fluidized bed when the resistance of the gas flow to the bulk material is equal to the weight of the sum of the individual particles reduced by the buoyancy. This balance of forces can be represented as follows:

$$\Delta p\ A = A\ H_L (1 - \varepsilon_L) \left(\rho_{P-}\rho_g\right) g \qquad \text{Eq. 37}$$

- A: cross section area of the fluidized bed
- H_L: height of bed at the relaxation point
- ε_L: porosity at the relaxation point
- g: gravitational constant

The results of pressure drop formula for the fluidized bed, which simultaneously represents the fundamental fluidization condition (presented by Hofbauer H., 2017):

$$\Delta p = (1 - \varepsilon_L) \left(\rho_{P-}\rho_g\right) g\ H \qquad \text{Eq. 38}$$

This pressure drop is independent of the flow rate; it therefore remains constant in the area of the fluidized bed. A flow regime map presents the flow regimes of a gas-solid two phase system based on dimensionless numbers. Grace presented a modified flow regime map of Reh (Geace J., 1986). The Grace's flow regime map uses the dimensionless superficial gas velocity U^* and the dimensionless particle diameter d_p^*. Dimensionless superficial gas velocity and dimensionless particle diameter are defined as follows:

$$U^* = U \left(\frac{\rho_g}{\upsilon\ g\ (\rho_p - \rho_g)}\right)^{1/3} = \frac{Re}{Ar^{1/3}} = \qquad \text{Eq. 39}$$

$$d_p^* = d_p \left(\frac{g\ (\rho_p - \rho_g)}{\upsilon^2\ \rho_g}\right)^{1/3} = Ar^{1/3} \qquad \text{Eq. 40}$$

This map was further modified by Schmid J. C. in 2014. Schmid implemented correlations based on an extensive literature research for the transition areas between the flow regimes and a reinterpretation of Geldart's particle classification. The modified flow regime map by Schmid is presented in Figure 7 (Schmid J. C., 2014).

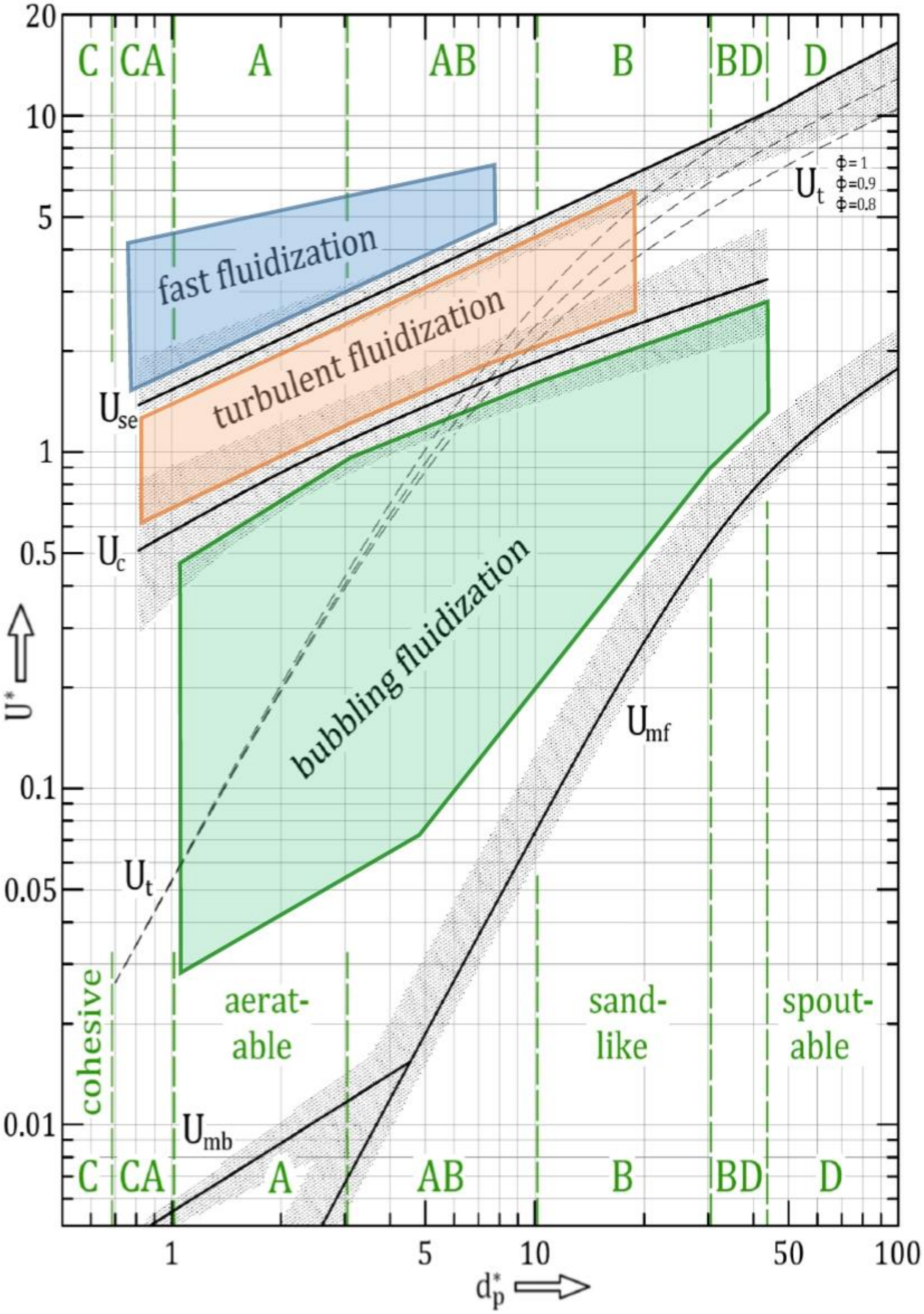

Figure 7: Flow regime map of gas-solid fluidized beds

2.4 Basic concept of DFB steam gasification at TU Wien

In Figure 8 (by Benedikt F., 2018) the basic concept of dual fluidized bed steam gasification at TU Wien is shown. This gasifier system consists of two fluidized beds; gasification reactor (GR) and combustion reactor (CR), which are thermodynamically connected via a circulating bed material. Bed material circulates from combustion to gasification reactor and supplies heat for overall endothermic gasification reactions.

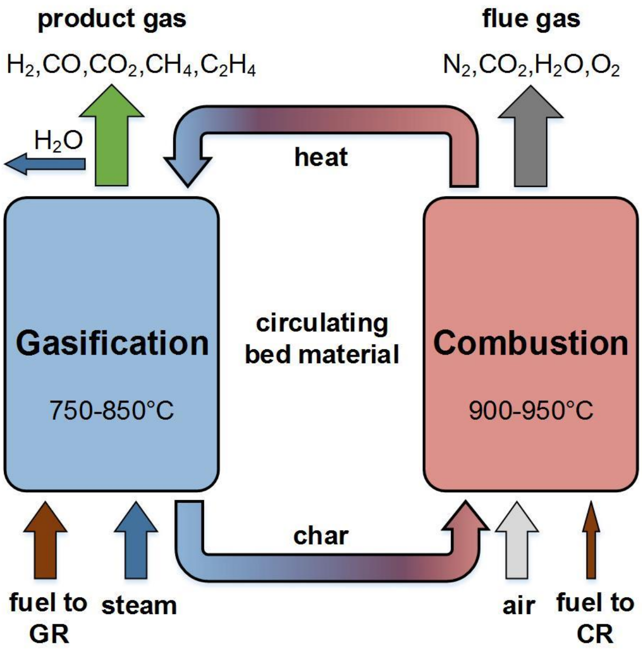

Figure 8: Basic concept of dual fluidized bed steam gasification at TU Wien

The main fuel for the combustion reactor itself is provided by the residuals of the gasification, so-called char. With the circulating bed material, this char is transported to the combustion reactor, where it is burned with air. Additional fuel can be introduced into the combustion reactor to control the gasification temperature and to compensate the relatively high specific heat losses of the experimental advanced 100 kW_{th} pilot plant. It is obvious that within this process the flue gas stream is separated from the product gas stream. This leads to a high calorific nitrogen-free product gas. The gasification reactor, where mainly endothermic gasification reactions take place, is operated in a bubbling bed regime and fluidized with steam as gasification agent. Temperature range in this part is 750 – 850 °C. As standard fuel, softwood is fed into the gasification reactor, where they dry and the volatiles are released. The product gas, which consists mainly of H_2, CO, CO_2, goes from the top of the gasification reactor to the cleaning and filtering section to remove inorganic particles, tar and char. In current industrial applications tar is removed from the product gas in a scrubber that is operated with rapeseed oil methyl ester (RME) (Kirnbauer F and Hofbauer H., 2013). The combustion reactor is operated in a fast-fluidized bed regime and in the temperature range between 900 – 950 °C. The flue gas enters a cyclone from the top of the combustion reactor to separate bed material particles from the flue gas. Then, the clean flue gas is released into the atmosphere. Bed material particles from the gravity separator flow back to the gasification reactor. There, the hot bed material provides heat for endothermic reactions. The cleaned product gas is utilized in a gas engine to generate electricity and heat at industrial scaled plants. The dual fluidized bed concept is highly qualified for “scale-up”. The technical feasibility of this gasification technology has been proven in the early 2000’s with the combined heat and power plant (CHP) Güssing in Austria. Further plants, based on the concept, went into operation in Oberwart/Austria (9 MW_{th}), Villach/Austria (15 MW_{th}), Senden/Germany (14 MW_{th}), and in Göteborg/Sweden (32 MW_{th}).

2.6 Advanced and classic DFB steam gasification at TU Wien

Figure 9 (Mauerhofer, A. M. et al., 2017) and Figure 10 (Mauerhofer, A. M. et al., 2017) represent the classic and advance design of DFB steam gasification at TU Wien. The classic design is typically used at the existing industrial-sized plants and consists of a bubbling-fluidized bed as gasification reactor and a fast – fluidized bed as combustion reactor. Pure olivine is commonly used as bed material. The reactors are connected via a loop seal in the lower part of the reactors and a loop seal in the upper part. The bed material circulates from combustion to gasification reactor at the bottom and returns at the top via a cyclone. By a cyclone bed material is separated from the flue gas. Further information regarding the classic design of the 100 kW_{th} pilot plant at TU Wien can be found in (Kern S. et al., 2013).

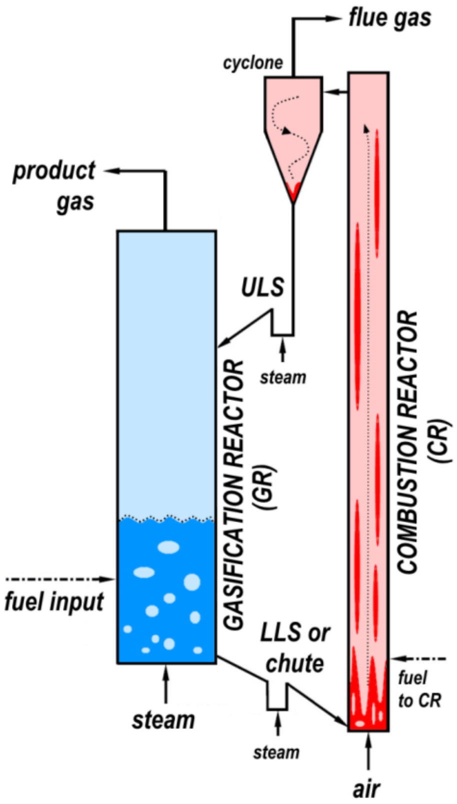

Figure 9: The classic design of DFB gasification 100 kW_{th} pilot plant at TU Wien

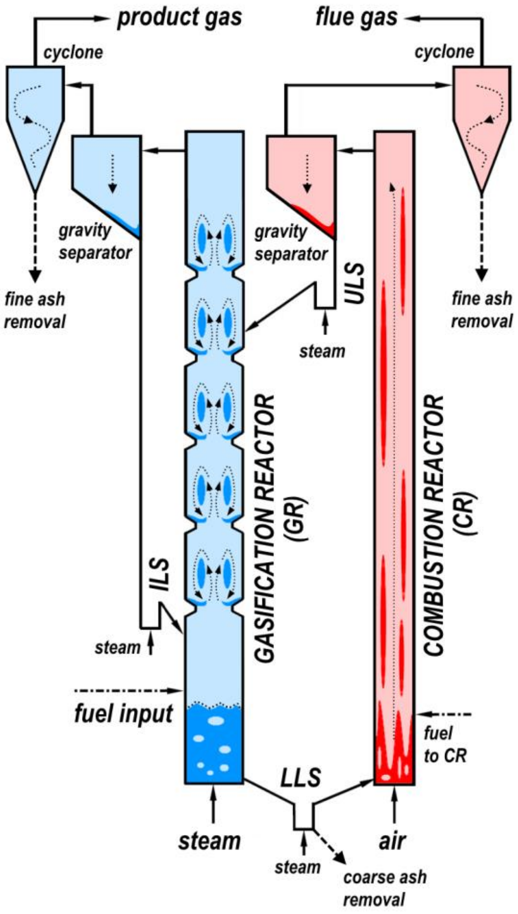

Figure 10: The advance design of DFB gasification 100 kW_{th} pilot plant at TU Wien

To improve the gas-solid contact within the gasification reactor, an advanced design of the DFB steam gasification process has been developed at TU Wien. In the advanced 100 kW_{th} pilot plant gasification is realized applying pure calcite ($CaCO_3$) as bed material. Since calcite shows relatively low abrasion resistance in comparison to silica sand and olivine (as commercial bed materials) the advanced design is equipped with two gravity separators on top of the reactors, which leads to a smooth separation of the calcite from the gas streams. Therefore, also calcite as bed material can be used in this new pilot plant without continuous replacement of the bed material. Cyclones are installed to remove fines after the gravity separators. In the advanced 100 kW_{th} pilot plant of the DFB steam gasification, the gasification reactor consists of two main parts: the lower part, which is operated as bubbling fluidized bed and the upper part, which is realized as a countercurrent column with turbulent fluidized bed zones. Feedstock is fed into the lower part of gasification reactor. The countercurrent column results from the hot bed material, which is separated from the flue gas stream and is introduced into this column from the combustion reactor. Further, the column is equipped with constrictions, which leads to an increased bed material hold-up over the height of the column. As a result, the interaction of bed material and the product gas in the upper part of the gasification reactor is increased significantly (Benedikt F. et al., 2017).

3 Experimental setup

3.1 Feedstock

The main elemental composition, volatiles, water and ash content, as well as the ash melting behavior of the softwood pellets were analyzed according to international standards at the Test Laboratory for Combustion Systems at the TU Wien. The results are shown in Table 2. For all presented test runs in this work, softwood pellets with a diameter of 6 mm according to the Austrian standard ÖNORM M 7135 were used.

Table 2 : Chemical fuel and ash analysis of softwood pellets

Proximate Analysis	**Unit**	**Value**
Water content	wt.-%	7.2
Volatiles	wt.-%$_{db}$	85.4
Residual char (incl. ash)	wt.-%$_{db}$	14.6
Lower heating value (dry)	MJ/kg$_{db}$	18.9
Lower heating value (moist)	MJ/kg	17.4
Ultimate Analysis		
Ash content	wt.-%$_{db}$	0.2
Carbon (C)	wt.-%$_{db}$	50.7
Hydrogen (H_2)	wt.-%$_{db}$	5.9
Oxygen (O_2)	wt.-%$_{db}$	43.0
Nitrogen (N_2)	wt.-%$_{db}$	0.2
Sulphur (S)	wt.-%$_{db}$	0.005
Chlorine (Cl)	wt.-%$_{db}$	0.005
Ash analysis , main components (550°C)		
SiO_2	wt.-%$_{db}$	6.62
Al_2O_3	wt.-%$_{db}$	1.63
CaO	wt.-%$_{db}$	55.2
Fe_2O_3	wt.-%$_{db}$	0.91
K_2O	wt.-%$_{db}$	13.4
Na_2O	wt.-%$_{db}$	1.07
MgO	wt.-%$_{db}$	8.35
P_2O_5	wt.-%$_{db}$	3.07
TiO_2	wt.-%$_{db}$	0.12
MnO	wt.-%$_{db}$	5.44
Ash melting behavior		
Deformation temperature	°C	1335
Spherical temperature	°C	not occurred
Hemi-spherical temperature	°C	not occurred
Flow temperature	°C	1438

3.2 Bed materials

Table 3 – Table 6 represent composition of olivine, calcite, feldspar and silica sand respectively, which were used as bed material for. Test runs during this research.

Table 3: Composition of olivine ($d_{sv} \approx 0.25$ mm)

Parameter	Unit	Value
MgO	wt.-%	48 – 50
SiO_2	wt.-%	39 – 42
Fe_2O_3	wt.-%	8.0 – 10.5
Al_2O_3+Cr_2O_3+Mg_3O_4	wt.-%	0.7 – 0.9
CaO	wt.-%	< 0.4
NiO	wt.-%	< 0.1
$CaCO_3$	wt.-%	< 0.1
Hardness	Mohs	6 – 7
particles density	kg/m³	≈ 2850

Table 4: Composition of calcite ($d_{sv} \approx 0.38$ mm)

Parameter	Unit	Value
$CaCO_3$	wt.%	95 – 97
$MgCO_3$	wt.%	1.5 -4.0
SiO_2	wt.%	0.4 – 0.6
Al_2O_3	wt.%	0.2 – 0.4
Fe_2O_3	wt.%	0.1 – 0.3
Hardness	Mohs	3
particles density	kg/m³	≈ 2650
Particles density (after full calcination)	kg/m³	≈ 1500

Table 5: Composition of potassium feldspar ($d_{sv} \approx 0.31$ mm)

Parameter	Unit	Value
SiO_2	wt.%	65.7
Al_2O_3	wt.%	17.9
K_2O	wt.%	17.74
Na_2O	wt.%	0.84
BaO	wt.%	0.33
P_2O_5	wt.%	0.
Fe_2O_3	wt.%	0.041
CaO	wt.%	0.03
TiO_2	wt.%	0.28
MgO	wt.%	0.01
Hardness	Mohs	6
Particles density	kg/m³	≈ 2600

Table 6: Composition of silica sand ($d_{sv} \approx 0.29$)

Parameter	Unit	Value
SiO_2	wt.%	99.8
Al_2O_3	wt.%	0.1
Fe_2O_3	wt.%	0.04
Hardness	Mohs	7
Particles density	kg/m³	≈ 2650

3.3 Experimental equipment

3.3.1 Main operational parameters of the DFB gasifer system

An overview of the plant equipment of the advanced 100 kW_{th} gasification pilot plant at TU Wien is shown in Figure 11 (from Schmid J. C., 2014). The arrows inside the scheme show flow paths of the solid streams and gas/fluid flows. Important plant parts of the main units are as follow:

- Solid fuel supply/hopper system
- Gasification reactor system, gas production
- Gas cooling, cleaning and utilization
- Process media supply systems
- Measurement and control technology, control station
- Safety technology

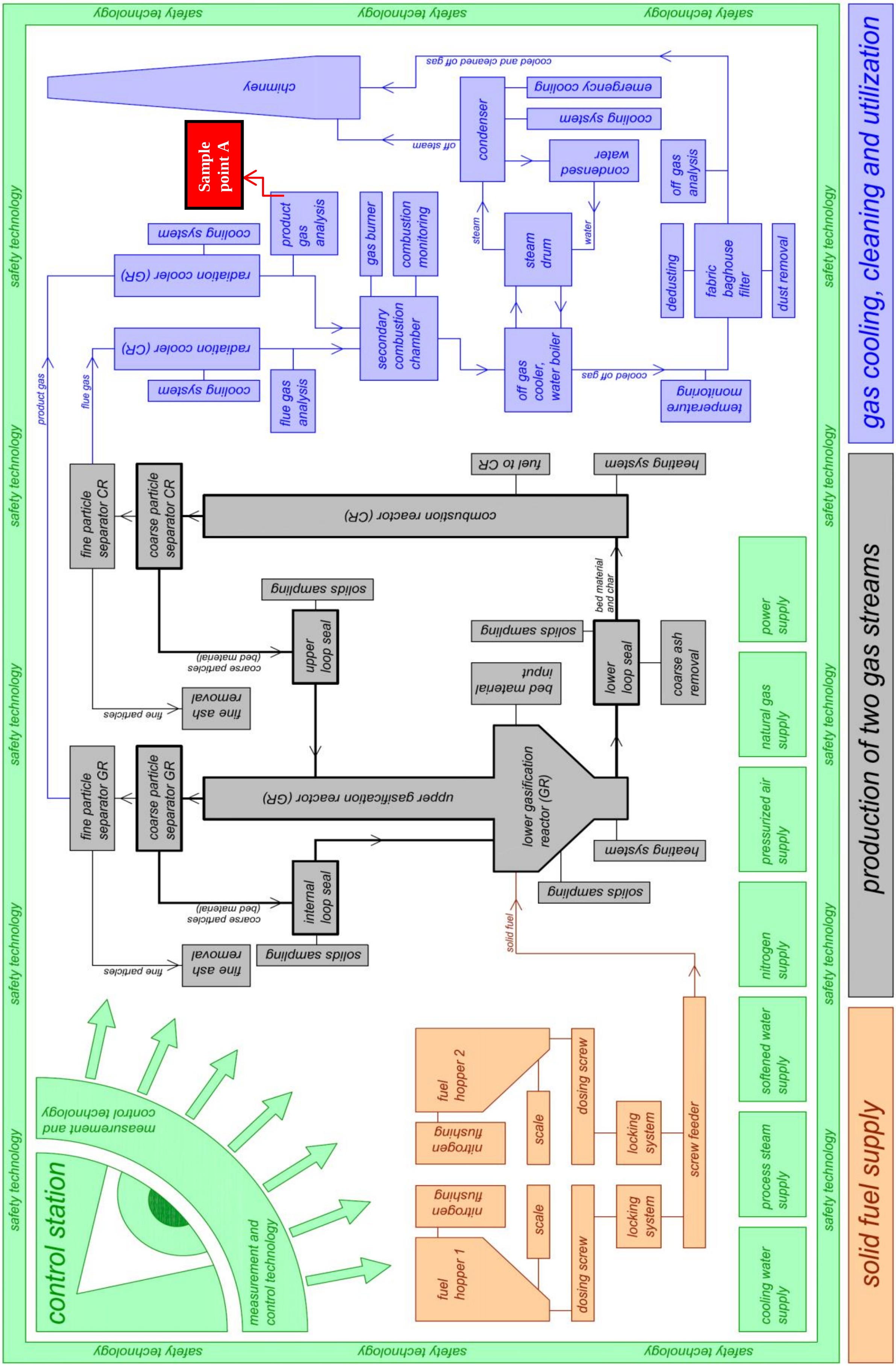

Figure 11: Overview of the plant equipment used for gasification test runs

Figure 12 and Figure 13 show different pictures of the gasification pilot plant without and with the thermal insulation.

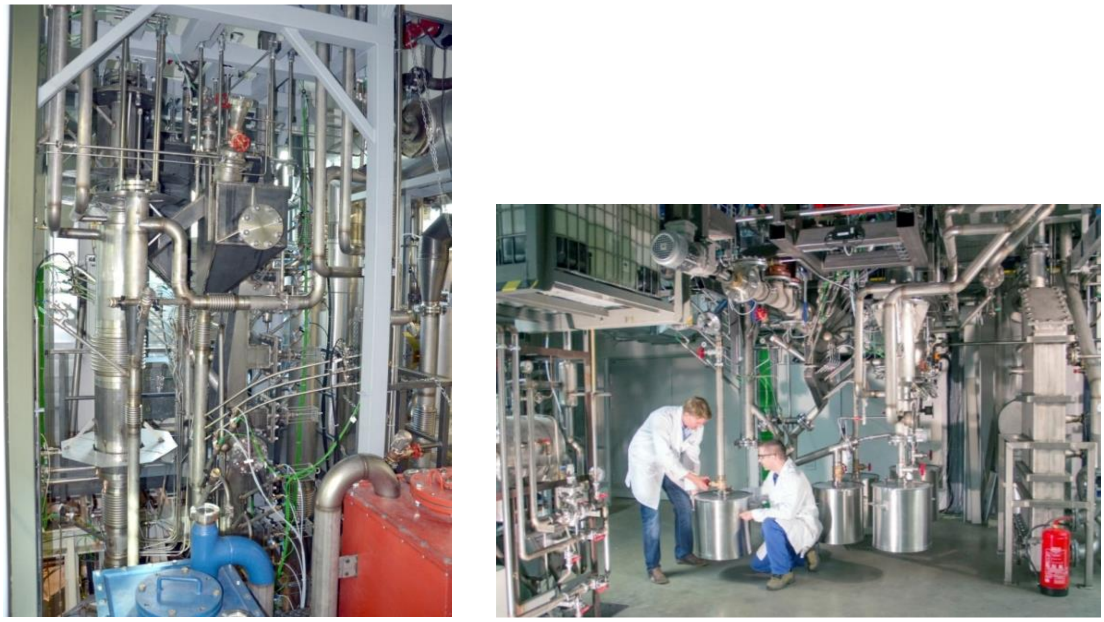

Figure 12: Pictures of the novel DFB reactor system without thermal insulation (Left: upper reactor parts and hopper system, Right: lower reactor parts)

Figure 13: Pictures of the novel dual fluidized bed reactor system with thermal insulation (Left: upper reactor parts and hopper system, Right: lower reactor parts)

3.3.2 Online measurement equipment

The product gas is filtered and washed with rapeseed methyl ester (RME) to remove tar before measurement (see Figure 14) (Kern S., 2013). Main product gas components like H_2, CO, CO_2 and CH_4 are analyzed by Rosemount NGA2000 measurement equipment; C_2H_4, C_2H_6, C_3H_8 and N_2 values are measured with a gas chromatograph "Perkin Elmer ARNEL-Clarus 500" every 12 – 15 minutes (see Figure 15) (modified from Schmalzl M., 2014). Every single value is logged with a data storage computer. A large number of temperature (thermocouples) and pressure sensors guarantee an effective process control and a smooth and continuous operation of the whole gasification facility.

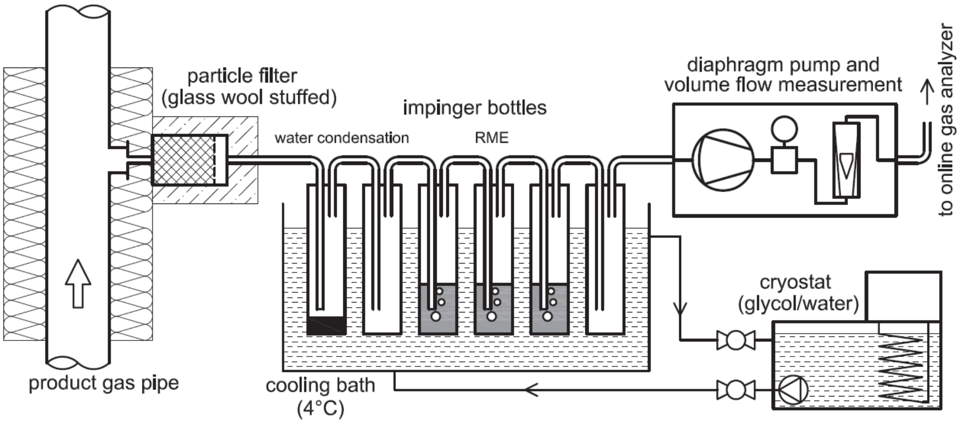

Figure 14: Gas cleaning line for online product gas measurement

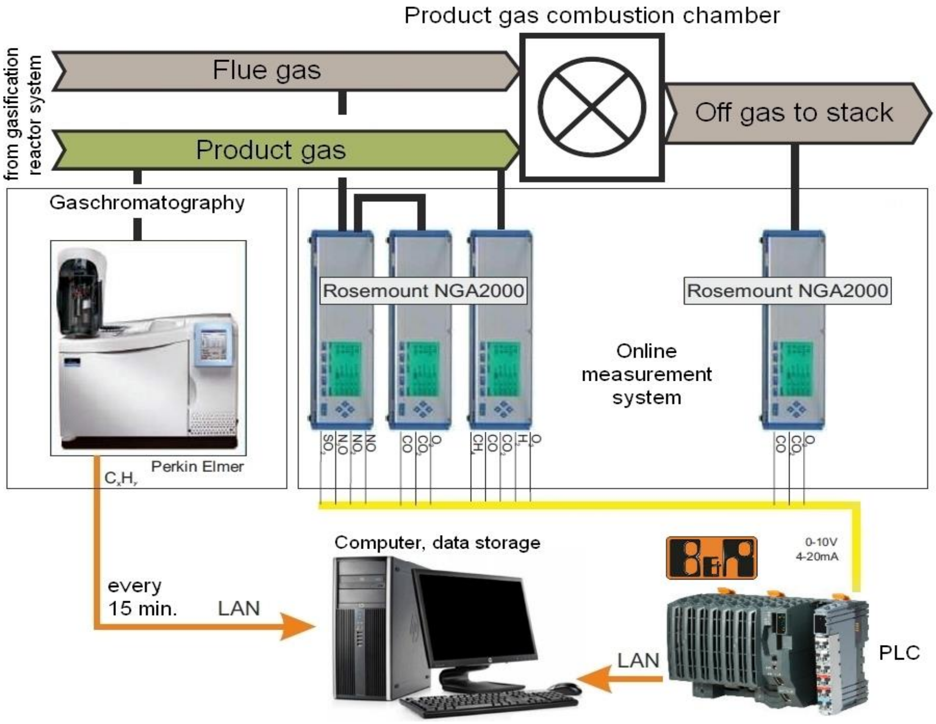

Figure 15: Online product gas measurement equipment

3.3.3 Offline measurement equipment

To analyze the content of dust, water, char and tar in the product gas stream discontinuously (offline) measurement equipment is used (see Figure 16). The high molecular weight (heavy) tar compounds are quantified as the mass of tars left after vacuum evaporation of the solvent (toluene). This is referred as "gravimetric" tar. The medium molecular weight tar compounds such as naphthalene are detected by gas chromatography coupled with mass spectrometry (GC-MS). Since toluene is used as solvent, benzene, toluene, ethyl benzene, and xylene (BTEX) values are typically not detectable GC-MS tar components, but water can be easily detected. The heat resistant ball valve (up to 450°C) and the arrangement of the sampling point in the product gas flow pipe to the secondary combustion chamber are shown in Figure 17.

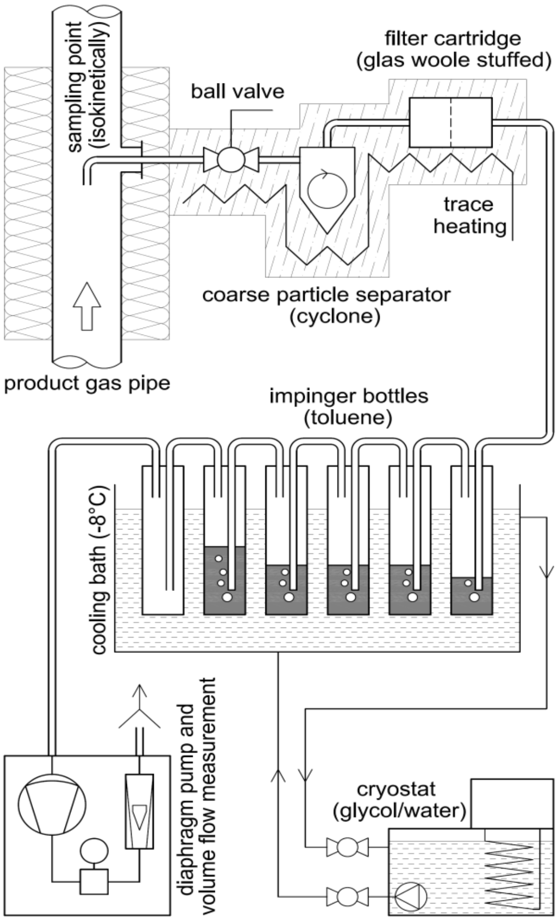

Figure 16: Dust, char, water and tar sampling scheme

Figure 17: Picture of the product gas sampling point A for offline analysis

3.3.4 IPSEpro simuation- mass and energy balance

To validate the accuracy of gathered data during the experimental tests the software package IPSEpro is used, as well as in order to compute the mass and energy balance for getting data, which cannot be measured directly. IPSEpro is a software package originating from the power plant sector, which offers stationary process simulations based on flow sheet modeling. The software uses an equation-oriented solver. IPSEpro is minimizing the general error. Following tables display also validated results of the simulation work. These validated results are highly valuable and representative for the up-scaling of DFB gasification processes. A detailed layout for the simulation work of the advanced100 kW_{th} gasification pilot plant is shown in Figure 18 (Schmid et al., 2016).

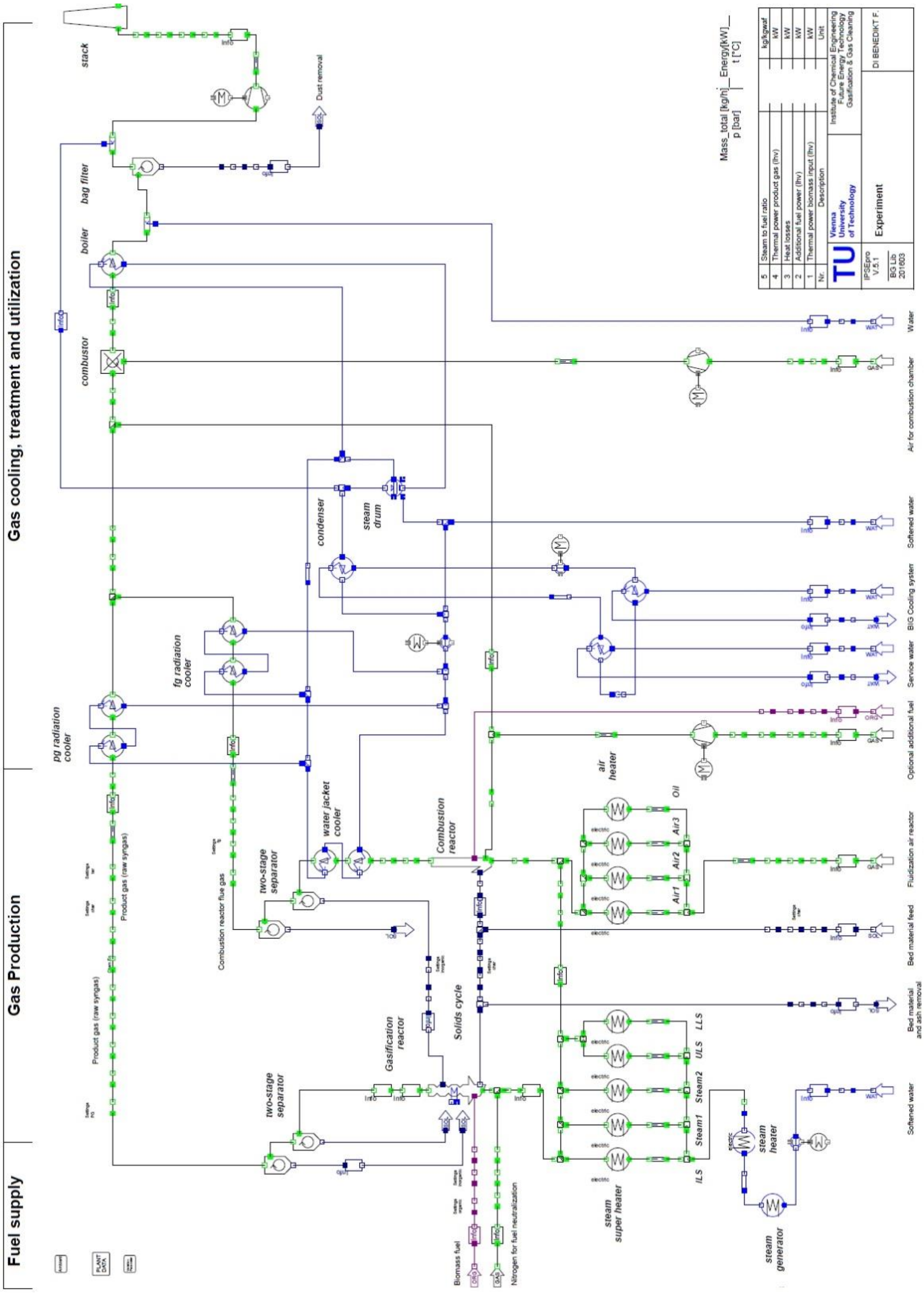

Figure 18: Flow sheet for the simulation of the advanced 100 kW$_{th}$ gasification pilot plant via IPSEpro software

4 Experimental results and discussion

This chapter represents the experimental results from the test runs, which were carried out during this research. Ten test runs of softwood gasification were performed in the advanced 100 kW_{th} gasification pilot plant at TU Wien to investigate the influence of different bed materials as well as effect of adding calcite to other bed materials on the performance of DFB steam gasification. In this research were applied different mass rations of 100 wt.-% olivine to 100 wt.-% calcite, 100 wt.-% silica sand to 100 wt.-% calcite and 100 wt.-% feldspar to 100 wt.-% calcite as bed material. In all gasification test runs, softwood pellets were used as feedstock.

4.2 Pure calcite (100 wt.- %)

In this section, results from gasification test runs of softwood with pure calcite as bed material in the advanced 100 kW_{th} pilot plant at TU Wien are presented. Figure 19 shows an overview on the temporal courses of gasification temperature in the gasification reactor (GR) at steady state operation during the softwood gasification process with pure calcite as bed material. T_GR15 and T_GR 6 are the temperature at the top and bottom of the gasification reactor in the fluidized bed region, respectively. T_GR1 is the temperature at the bottom of the gasification reactor in the bubbling bed region. During the gasification operation, it was tried to measure the gas composition at the outlet of the gasification reactor (sample point A). Table 7 presents the main results and parameters of the gasification test run. Table 8 and Table 9 display the main gaseous product gas composition and additional product gas component, respectively. Table 10 illustrates the main gaseous flue gas composition of combustion reactor. Table 11 gives detailed information on the tar components measured by gas chromatography coupled with mass spectrometry (GC-MS).

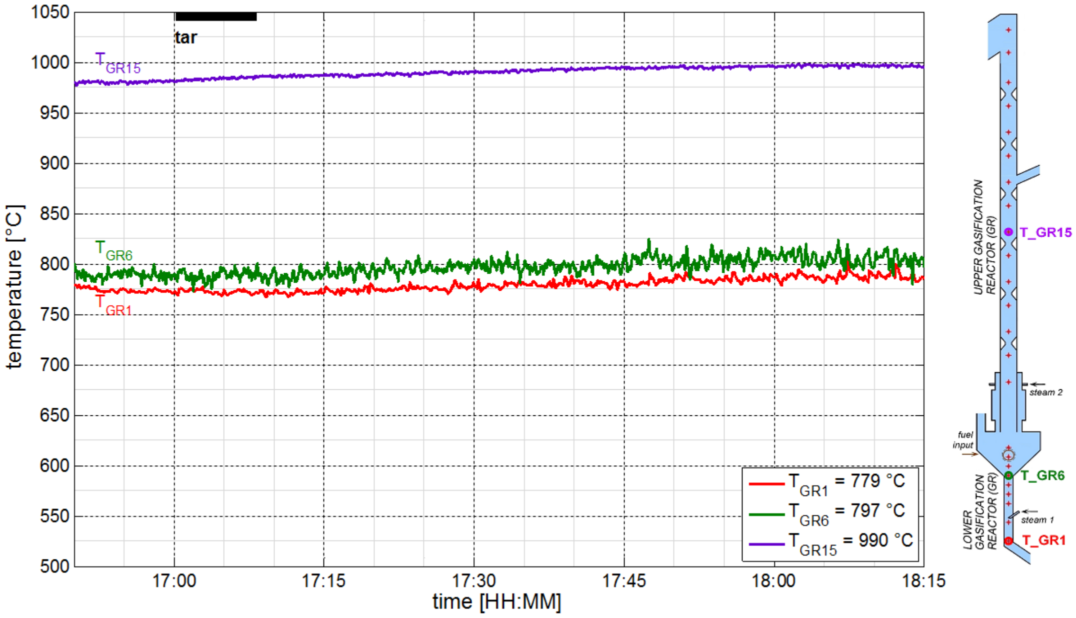

Figure 19: Overview on the temporal courses of gasification temperature for the gasification test run with softwood pellets and pure calcite as bed material

Table 7: Main results and parameters; gasification of softwood pellets with pure calcite as bed material

Parameter	Unit	Gasification reactor	Combustion reactor
Bed material types	µm	300 – 500 (calcite)	
Bed material	wt.-%	100 (calcite)	
Overall initial bed material inventory	kg	80	
Feedstock type	-	softwood	-
Feedstock/fuel analysis no.	-	PL-15065-A	-
Feedstock mass flow	kg/h	21.3	-
Feedstock/fuel power into GR	kW	100.9	-
Fuel to CR	kW	-	45.7*
Heat losses of reactor system	kW	19.64	13.10
Typical temperatures **(**lower reactor part)	°C	GR6 797	CR4 1042
Typical temperatures **(**upper reactor part)	°C	GR15 990	CR7 1008
Water content in the gas stream	vol.-%	31.55*	11.55*
Gasification steam to fuel ratio	$kg_{steam}/kg_{fuel,db,af}$	0.73*	
Gasification steam to carbon ratio	$kg_{steam}/kg_{fuel,carbon}$	1.44*	
Product gas volume flow	Nm^3_{db}/h	26.9*	
Feedstock mass flow, dry & ash free	$kg_{,db,af}/h$	19.73	
Product gas yield	$Nm^3_{db}/kg_{fuel,db,af}$	1.36*	
Steam related H_2O conversion	kg_{H2O}/kg_{H2O}	0.31*	
Fuel related H_2O conversion	$kg_{H2O}/kg_{fuel,db,af}$	0.23*	
Product gas lower heating value (free of char & tar)	MJ/Nm^3_{db}	11.24*	
Product gas power (free of char & tar)	kW	84.02*	
Cold gas efficiency	%	84.1*	
Overall cold gas efficiency, novel 100kW test plant	%	57.9*	
Overall cold gas efficiency, estimated for a 50 MW plant	%	70 – 80	
Product gas, H_2 to CO ratio	-	2.3*	

* via calculation with IPSEpro mass and energy balance

Table 8: Main gaseous product gas composition; gasification of softwood pellets with pure calcite as bed material; sample point A

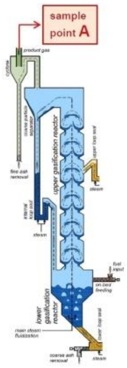

Product gas composition; sample point A				
Parameter	**Unit**	**NGA2000 online**	**PE Arnel GC TU Wien**	**IPSEpro simulation**
H_2 hydrogen	vol.-% $_{db}$	44.4	-	47.5
CO carbon monoxide	vol.-% $_{db}$	22.8	23.7	21.0
CO_2 carbon dioxide	vol.-% $_{db}$	21.1	20.3	21.3
CH_4 methane	vol.-% $_{db}$	9.5	9.9	8.7
C_2H_4 ethylene	vol.-% $_{db}$	-	1.05	0.5
C_2H_6 ethane	vol.-% $_{db}$	-	0.25	0.05
C_3H_8 propane	vol.-% $_{db}$	-	0.00	0.00

Additional gaseous product gas components			
Parameter	**Unit**	**Typical values**	**PE Arnel GC TU Wien**
N_2 nitrogen	vol.-% $_{db}$	0.5 – 2.0	0.52
Sum of C_4-.C_5-hydrocarbons, NH_3, H_2S, HCl& other comp.	vol.-% $_{db}$	0.1 – 2.0**	-

* value because of purging/flushing feedstock hoppers and temp. & press.-measuring points with nitrogen
** value range strongly depends on the fuel composition (see fuel analysis & optional offline gas analysis)

Table 9: Additional product gas component; gasification of softwood pellets with pure calcite as bed material; sample point A from test laboratory for combustion systems from TU Wien; offline tar measurement

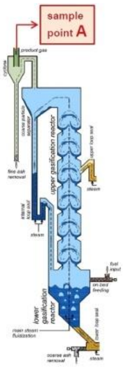

Product gas analytics, measured discontinuous, sample point A		
Parameter	**Unit**	**Solvent: toluene**
Dust content	g/Nm^3 $_{db}$	0.66
Char content	g/Nm^3 $_{db}$	1.8
Tar content GC-MS (without BTEX)	g/Nm^3 $_{db}$	1.21
Tar content BTEX	g/Nm^3 $_{db}$	8.505
Tar content gravimetric	g/Nm^3 $_{db}$	0.66
Water content, H_2O	vol.-%	31
Tar dew point*	°C	91.7

*calculated via http://www.thersites.nl/completemodel.aspx

Table 10: Main gaseous flue gas composition of the combustion reactor; gasification of softwood pellets with pure calcite as bed material

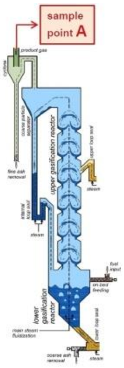

Flue gas composition			
Parameter	**Unit**	**NGA2000 online**	**IPSEpro simulation**
CO_2 carbon dioxide	vol.-% $_{db}$	16.7	16.68
O_2 oxygen	vol.-% $_{db}$	0.32	0.3
CO carbon monoxide	vol.-% $_{db}$	0.26	0.00
N_2 nitrogen	vol.-% $_{db}$	-	82.06
Ar argon	vol.-% $_{db}$	-	0.96
NO nitrogen monoxide	vol.-% ppm $_{db}$	31.7	0.00
SO_2 sulfur dioxide	vol.-% ppm $_{db}$	15.1	0.00
NO_2 nitrogen dioxide	vol.-% ppm $_{db}$	0.0	0.00
N_2O nitrous oxide	vol.-% ppm $_{db}$	5.4	0.00

Table 11: GC-MS tar components of product gas; gasification of softwood pellets with pure calcite as bed material

Solvent		Toluene
Total GC-MS (without BTEX)	**g/Nm³**	**1.210**
2-Methylpyridin	mg/Nm³	0
Phenylacetylen	mg/Nm³	0
3- und 4-Methylpyridin	mg/Nm³	0
Styrol	mg/Nm³	24
Mesitylen	mg/Nm³	0
Phenol	mg/Nm³	0
Benzofuran	mg/Nm³	0
1H-Inden	mg/Nm³	25
2-Methylphenol	mg/Nm³	0
4-Methylphenol	mg/Nm³	0
2-Methylbenzofuran	mg/Nm³	0
2,6-Dimethylphenol	mg/Nm³	0
2,5&2,4-Dimethylphenol	mg/Nm³	0
3,5-Dimethylphenol	mg/Nm³	0
2,3-Dimethylphenol	mg/Nm³	0
3,4-Dimethylphenol	mg/Nm³	0
2-Methoxy-4-Methylphenol	mg/Nm³	0
Naphthalin	mg/Nm³	894
1-Benzothiophen	mg/Nm³	0
Chinolin	mg/Nm³	0
2-Methylnaphthalin	mg/Nm³	0
Isochinolin	mg/Nm³	0
1-Methylnaphthalin	mg/Nm³	0
Eugenol	mg/Nm³	0
1-Indanon	mg/Nm³	0
Indol	mg/Nm³	0
Biphenyl	mg/Nm³	≤12
1-Vinylnaphthalin	mg/Nm³	0
Isoeugenol	mg/Nm³	0
2-Vinylnaphthalin	mg/Nm³	0
Acenaphthylen	mg/Nm³	114
Acenaphthen	mg/Nm³	14
Dibenzofuran	mg/Nm³	0
Fluoren	mg/Nm³	0
Dibenzothiophen	mg/Nm³	0
Anthracen	mg/Nm³	88
Phenanthren	mg/Nm³	12
Carbazol	mg/Nm³	0
4,5-Mehtylphenanthren	mg/Nm³	0
9-Methylanthracen	mg/Nm³	0
Fluoranthen	mg/Nm³	14
Pyren	mg/Nm³	12
Benzo[a]anthracen	mg/Nm³	0
Chrysen	mg/Nm³	0
Benzo[b]fluoranthen	mg/Nm³	0
Benzo[k]fluoranthen	mg/Nm³	0
Benzo[e]pyren	mg/Nm³	0
Benzo[a]pyren	mg/Nm³	0
Perylen	mg/Nm³	0
Dibenz[a,h]anthracen	mg/Nm³	0
Benzo[g,h,i]perylen	mg/Nm³	0
Indeno[1,2,3-cd]pyren	mg/Nm³	0
Coronen	mg/Nm³	0
BTEX components	**g/Nm³**	**8.505**
Benzol	mg/Nm³	8505
Toluol	mg/Nm³	not measurable
Ethylbenzol	mg/Nm³	0
m- und p-Xylol	mg/Nm³	0
o-Xylol	mg/Nm³	0

4.3 Olivine and mixtures with calcite

4.3.1 Pure olivine (100 wt.-%)

In this section, results from gasification test runs of softwood with pure olivine as bed material in the advanced 100 kW_{th} pilot plant at TU Wien are presented. Figure 20 shows an overview on the temporal courses of gasification temperature in the gasification reactor (GR) at steady state operation during the softwood gasification process with pure olivine as bed material. T_GR15 and T_GR 6 are the temperature at the top and bottom of the gasification reactor in the fluidized bed region, respectively. T_GR1 is the temperature at the bottom of the gasification reactor in the bubbling bed region. During the gasification operation, it was tried to measure the gas composition at the outlet of the gasification reactor (sample point A). Table 12 presents the main results and parameters of the gasification test run. Table 13 and Table 14 display the main gaseous product gas composition and additional product gas component, respectively. Table 15 illustrates the main gaseous flue gas composition of combustion reactor. Table 16 gives detailed information on the tar components measured by gas chromatography coupled with mass spectrometry (GC-MS).

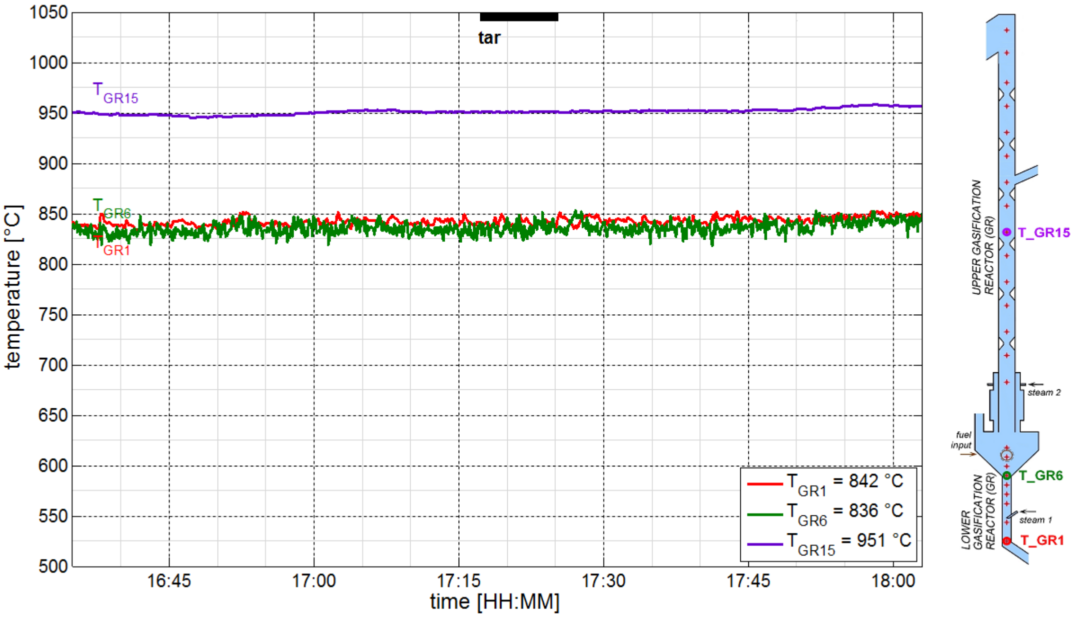

Figure 20: Overview on the temporal courses of gasification temperature for the gasification test run with softwood pellets and pure olivine as bed material

Table 12: Main results and parameters; gasification of softwood pellets with pure olivine as bed material

Parameter	Unit	Gasification reactor	Combustion reactor
Bed material types	µm	100 – 300 (olivine)	
Bed material	wt.-%	100 (olivine)	
Overall initial bed material inventory	kg	82	
Feedstock type	-	Softwood	-
Feedstock/fuel analysis no.	-	PL-15065-A	-
Feedstock mass flow	kg/h	19.3*	-
Feedstock/fuel power into GR	kW	91*	-
Fuel to CR	kW	-	46*
Heat losses of reactor system (GR & CR)	kW	19*	
Typical temperatures (lower reactor part)	°C	GR6 836	CR4 979
Typical temperatures (upper reactor part)	°C	GR15 951	CR7 954
Water content in the gas stream	vol.-%	42* – 43	14*
Gasification steam to fuel ratio	$kg_{steam}/kg_{fuel,db,af}$	1.0*	
Gasification steam to carbon ratio	$kg_{steam}/kg_{fuel,carbon}$	2.0*	
Product gas volume flow	Nm^3_{db}/h	24*	
Feedstock mass flow, dry & ash free	$kg_{,db,af}/h$	17.9	
Product gas yield	Nm^3_{db} $/kg_{fuel,db,af}$	1.35*	
Steam related H_2O conversion	kg_{H2O}/kg_{H2O}	0.22*	
Fuel related H_2O conversion	$kg_{H2O}/kg_{fuel,db,af}$	0.22*	
Product gas lower heating value (free of char & tar)	MJ/Nm^3_{db}	12.6*	
Product gas power (free of char & tar)	kW	84*	
Cold gas efficiency	%	93*	
Overall cold gas efficiency, novel 100 kW test plant	%	62*	
Overall cold gas efficiency, estimated for a 50 MW plant	%	70 – 80	
Product gas, H_2 to CO ratio	-	1.5*	

* via calculation with IPSEpro mass and energy balance

Table 13: Main gaseous product gas composition; gasification of softwood pellets with pure olivine as bed material; sample point A

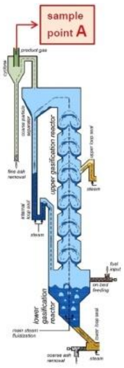

Product gas composition, sample point A				
Parameter	**Unit**	**NGA2000 online**	**PE Arnel GC TU Wien**	**IPSEpro simulation**
H_2 hydrogen	vol.-% $_{db}$	39.0	-	39.8
CO carbon monoxide	vol.-% $_{db}$	26.7	27.6	27.1
CO_2 carbon dioxide	vol.-% $_{db}$	18.7	19.3	18.7
CH_4 methane	vol.-% $_{db}$	9.93	10.50	10.66
C_2H_4 ethylene	vol.-% $_{db}$	-	1.7	1.71
C_2H_6 ethane	vol.-% $_{db}$	-	0.097	0.1
C_3H_8 propane	vol.-% $_{db}$	-	0.00	0.00

Additional gaseous product gas components			
Parameter	**Unit**	**Typical values**	**PE Arnel GC TU Wien**
N_2 nitrogen	vol.-% $_{db}$	0.5 – 2.0	1.66*
Sum of C_4-.C_5-hydrocarbons, NH_3, H_2S, HCl & other comp.	vol.-% $_{db}$	0.1 – 2.0**	-

* value because of purging/flushing feedstock hoppers and temp. & press.-measuring points with nitrogen
** value range strongly depends on the fuel composition (see fuel analysis & optional offline gas analysis)

Table 14: Additional product gas component; gasification of softwood pellets with pure olivine as bed material; sample point A from test laboratory for combustion systems from TU Wien; offline tar measurement

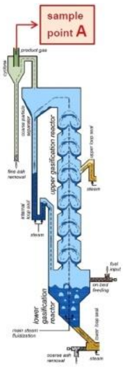

Product gas analytics, measured discontinuous, sample point A		
Parameter	**Unit**	**Solvent: toluene**
Dust content	g/Nm^3 $_{db}$	0.3
Char content	g/Nm^3 $_{db}$	2.4
Tar content GC-MS (without BTEX)	g/Nm^3 $_{db}$	11.201
Tar content gravimetric	g/Nm^3 $_{db}$	6.7
Water content, H_2O	vol.-%	43
Tar dew point*	°C	204

*calculated via http://www.thersites.nl/completemodel.aspx

Table 15: Main gaseous flue gas composition of the combustion reactor; gasification of softwood pellets with pure olivine as bed material

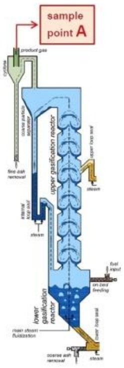

Flue gas composition			
Parameter/Name	**Unit**	**NGA2000 online**	**IPSEpro simulation**
CO_2 carbon dioxide	vol.-% $_{db}$	14.5	14.6
O_2 oxygen	vol.-% $_{db}$	1.9	1.9
CO carbon monoxide	vol.-% $_{db}$	0.0	0.0
N_2 nitrogen	vol.-% $_{db}$	-	82.6
Ar argon	vol.-% $_{db}$	-	0.96
NO nitrogen monoxide	vol.-% ppm $_{db}$	21	0.0
SO_2 sulfur dioxide	vol.-% ppm $_{db}$	17	0.0
NO_2 nitrogen dioxide	vol.-% ppm $_{db}$	0	0.0
N_2O nitrous oxide	vol.-% ppm $_{db}$	4	0.0

Table 16: GC-MS tar components of product gas; gasification of softwood pellets with pure olivine as bed material

Solvent		**Toluene**
Total GC-MS (without BTEX)	**g/Nm³**	**11.201**
2-Methylpyridin	mg/Nm³	0
Phenylacetylen	mg/Nm³	33
3- und 4-Methylpyridin	mg/Nm³	0
Styrol	mg/Nm³	211
Mesitylen	mg/Nm³	0
Phenol	mg/Nm³	0
Benzofuran	mg/Nm³	0
1H-Inden	mg/Nm³	437
2-Methylphenol	mg/Nm³	0
4-Methylphenol	mg/Nm³	0
2-Methylbenzofuran	mg/Nm³	0
2,6-Dimethylphenol	mg/Nm³	0
2,5&2,4-Dimethylphenol	mg/Nm³	0
3,5-Dimethylphenol	mg/Nm³	0
2,3-Dimethylphenol	mg/Nm³	0
3,4-Dimethylphenol	mg/Nm³	0
2-Methoxy-4-Methylphenol	mg/Nm³	0
Naphthalin	mg/Nm³	4596
1-Benzothiophen	mg/Nm³	0
Chinolin	mg/Nm³	0
2-Methylnaphthalin	mg/Nm³	48
Isochinolin	mg/Nm³	0
1-Methylnaphthalin	mg/Nm³	28
Eugenol	mg/Nm³	0
1-Indanon	mg/Nm³	0
Indol	mg/Nm³	0
Biphenyl	mg/Nm³	112
1-Vinylnaphthalin	mg/Nm³	0
Isoeugenol	mg/Nm³	0
2-Vinylnaphthalin	mg/Nm³	0
Acenaphthylen	mg/Nm³	1803
Acenaphthen	mg/Nm³	26
Dibenzofuran	mg/Nm³	222
Fluoren	mg/Nm³	219
Dibenzothiophen	mg/Nm³	0
Anthracen	mg/Nm³	1153
Phenanthren	mg/Nm³	290
Carbazol	mg/Nm³	0
4,5-Mehtylphenanthren	mg/Nm³	129
9-Methylanthracen	mg/Nm³	0
Fluoranthen	mg/Nm³	639
Pyren	mg/Nm³	554
Benzo[a]anthracen	mg/Nm³	116
Chrysen	mg/Nm³	139
Benzo[b]fluoranthen	mg/Nm³	94
Benzo[k]fluoranthen	mg/Nm³	69
Benzo[e]pyren	mg/Nm³	0
Benzo[a]pyren	mg/Nm³	146
Perylen	mg/Nm³	0
Dibenz[a,h]anthracen	mg/Nm³	0
Benzo[g,h,i]perylen	mg/Nm³	63
Indeno[1,2,3-cd]pyren	mg/Nm³	75
Coronen	mg/Nm³	0

4.3.1 Mixture (90/10 wt.-%) of olivine and calcite

In this section, results from gasification test runs of softwood with a mixture (90/10 wt.-%) of olivine and calcite as bed material in the advanced 100 kW_{th} pilot plant at TU Wien are presented. Figure 21 shows an overview on the temporal courses of gasification temperature in the gasification reactor (GR) at steady state operation during the softwood gasification process with a mixture (90/10 wt.-%) of olivine and calcite as bed material. T_GR15 and T_GR 6 are the temperature at the top and bottom of the gasification reactor in the fluidized bed region, respectively. T_GR1 is the temperature at the bottom of the gasification reactor in the bubbling bed region. During the gasification operation, it was tried to measure the gas composition at the outlet of the gasification reactor (sample point A). Table 17 presents the main results and parameters of the gasification test run. Table 18 and Table 19 display the main gaseous product gas composition and additional product gas component, respectively. Table 20 illustrates the main gaseous flue gas composition of combustion reactor. Table 21 gives detailed information on the tar components measured by gas chromatography coupled with mass spectrometry (GC-MS).

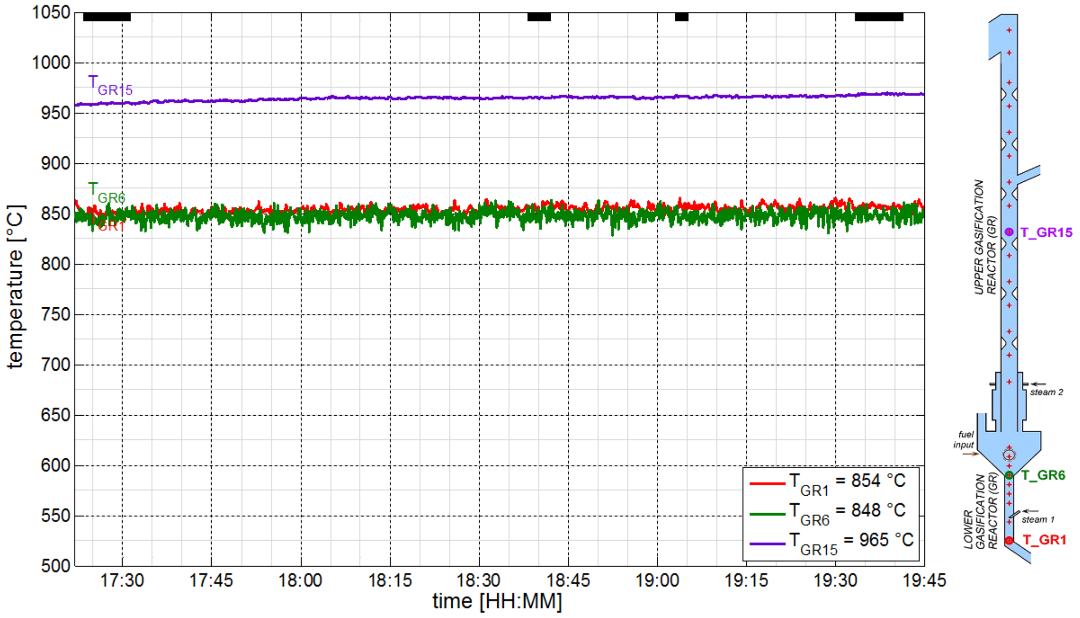

Figure 21: Overview on the temporal courses of gasification temperature for the gasification test run with softwood pellets and a mixture (90/10 wt.-%) of olivine and calcite as bed material

Table 17: Main results and parameters; gasification of softwood with a mixture (90/10 wt.-%) of olivine and calcite as bed material

Parameter	Unit	Gasification reactor	Combustion reactor
Bed material types	µm	100 – 300 (olivine), 300 – 600 (calcite)	
Bed material	wt.-%	90 (olivine), 10 (calcite)	
Overall initial bed material inventory	kg	82	
Feedstock type	-	softwood	-
Feedstock/fuel analysis no.	-	PL-15065-A	-
Feedstock mass flow	kg/h	20.1*	-
Feedstock/fuel power into GR	kW	95*	-
Fuel to CR	kW	-	51*
Heat losses of reactor system (GR & CR)	kW	19*	
Typical temperatures (lower reactor part)	°C	GR6 848	CR4 983
Typical temperatures (upper reactor part)	°C	GR15 965	CR7 954
Water content in the gas stream	vol.-%	37* – 38	14*
Gasification steam to fuel ratio	$kg_{steam}/kg_{fuel,db,af}$	1.0*	
Gasification steam to carbon ratio	$kg_{steam}/kg_{fuel,carbon}$	1.9*	
Product gas volume flow	Nm^3_{db}/h	27*	
Feedstock mass flow, dry & ash free	$kg_{,db,af}/h$	18.6	
Product gas yield	Nm^3_{db} $/kg_{fuel,db,af}$	1.46*	
Steam related H_2O conversion	kg_{H2O}/kg_{H2O}	0.29*	
Fuel related H_2O conversion	$kg_{H2O}/kg_{fuel,db,af}$	0.28*	
Product gas lower heating value (free of char & tar)	MJ/Nm^3_{db}	11.6*	
Product gas power (free of char & tar)	kW	87*	
Cold gas efficiency	%	92*	
Overall cold gas efficiency, novel 100kW test plant	%	60*	
Overall cold gas efficiency, estimated for a 50 MW plant	%	70 – 80	
Product gas, H_2 to CO ratio	-	1.9*	

* via calculation with IPSEpro mass & energy balance

Table 18: Main gaseous product gas composition; gasification of softwood pellets with a mixture (90/10 wt.-%) of olivine and calcite as bed material; sample point A

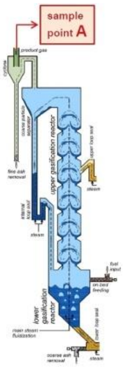

Product gas composition, sample point A				
Parameter	**Unit**	**NGA2000 online**	**PE Arnel GC TU Wien**	**IPSEpro simulation**
H_2 hydrogen	vol.-% $_{db}$	43.6	-	43.9
CO carbon monoxide	vol.-% $_{db}$	21.7	22.7	22.6
CO_2 carbon dioxide	vol.-% $_{db}$	20.6	21.2	21.1
CH_4 methane	vol.-% $_{db}$	9.14	9.39	9.7
C_2H_4 ethylene	vol.-% $_{db}$	-	0.82	0.85
C_2H_6 ethane	vol.-% $_{db}$	-	0.05	0.05
C_3H_8 propane	vol.-% $_{db}$	-	0.00	0.00

Additional gaseous product gas components			
Parameter	**Unit**	**Typical values**	**PE Arnel GC TU Wien**
N_2 nitrogen	vol.-% $_{db}$	0.5 – 2.0	1.27*
sum of C_4-.C_5-hydrocarbons, NH_3, H_2S, HCl & other comp.	vol.-% $_{db}$	0.1 – 2.0**	-

* value because of purging/flushing feedstock hoppers and temp. & press.-measuring points with nitrogen
** value range strongly depends on the fuel composition (see fuel analysis & optional offline gas analysis)

Table 19: Additional product gas component; gasification of softwood pellets with a mixture (90/10 wt.-%) of olivine and calcite as bed material; sample point A from test laboratory for combustion systems from TU Wien; offline tar measurement

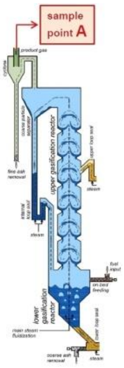

Product gas analytics, measured discontinuous, sample point A		
Parameter	**Unit**	**Solvent: toluene**
Dust content	g/Nm^3 $_{db}$	0.40
Char content	g/Nm^3 $_{db}$	1.19
Tar content GC-MS (without BTEX[1])	g/Nm^3 $_{db}$	4.53
Tar content gravimetric	g/Nm^3 $_{db}$	1.46
Water content, H_2O	vol.-%	38
Tar dew point*	°C	166

*calculated via http://www.thersites.nl/completemodel.aspx
[1] no BTEX measured

Table 20: Main gaseous flue gas composition of the combustion reactor; gasification of softwood pellets with a mixture (90/10 wt.-%) of olivine and calcite as bed material

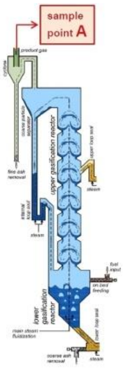

Flue gas composition			
Parameter	**Unit**	**NGA2000 online**	**IPSEpro simulation**
CO_2 carbon dioxide	vol.-% $_{db}$	15.5	15.3
O_2 oxygen	vol.-% $_{db}$	0.93	0.86
CO carbon monoxide	vol.-% $_{db}$	0.0	0.0
N_2 nitrogen	vol.-% $_{db}$	-	82.91
Ar argon	vol.-% $_{db}$	-	0.97
NO nitrogen monoxide	vol.-% ppm $_{db}$	13	0.0
SO_2 sulfur dioxide	vol.-% ppm $_{db}$	27	0.0
NO_2 nitrogen dioxide	vol.-% ppm $_{db}$	0	0.0
N_2O nitrous oxide	vol.-% ppm $_{db}$	6	0.0

Table 21: GC-MS tar components of product gas; gasification of softwood pellets with a mixture (90/10 wt.-%) of olivine and calcite as bed material

Solvent		**Toluene**
Total GC-MS (without BTEX)	**g/Nm^3**	**4.53**
2-Methylpyridin	mg/Nm^3	0
Phenylacetylen	mg/Nm^3	0
3- und 4-Methylpyridin	mg/Nm^3	0
Styrol	mg/Nm^3	73
Mesitylen	mg/Nm^3	0
Phenol	mg/Nm^3	0
Benzofuran	mg/Nm^3	0
1H-Inden	mg/Nm^3	113
2-Methylphenol	mg/Nm^3	0
4-Methylphenol	mg/Nm^3	0
2-Methylbenzofuran	mg/Nm^3	0
2,6-Dimethylphenol	mg/Nm^3	0
2,5&2,4-Dimethylphenol	mg/Nm^3	0
3,5-Dimethylphenol	mg/Nm^3	0
2,3-Dimethylphenol	mg/Nm^3	0
3,4-Dimethylphenol	mg/Nm^3	0
2-Methoxy-4-Methylphenol	mg/Nm^3	0
Naphthalin	mg/Nm^3	2438
1-Benzothiophen	mg/Nm^3	0
Chinolin	mg/Nm^3	0
2-Methylnaphthalin	mg/Nm^3	0
Isochinolin	mg/Nm^3	0
1-Methylnaphthalin	mg/Nm^3	0
Eugenol	mg/Nm^3	0
1-Indanon	mg/Nm^3	0
Indol	mg/Nm^3	0
Biphenyl	mg/Nm^3	55
1-Vinylnaphthalin	mg/Nm^3	0
Isoeugenol	mg/Nm^3	0
2-Vinylnaphthalin	mg/Nm^3	0
Acenaphthylen	mg/Nm^3	664
Acenaphthen	mg/Nm^3	≤ 16
Dibenzofuran	mg/Nm^3	27
Fluoren	mg/Nm^3	27
Dibenzothiophen	mg/Nm^3	0
Anthracen	mg/Nm^3	499
Phenanthren	mg/Nm^3	103
Carbazol	mg/Nm^3	0
4,5-Mehtylphenanthren	mg/Nm^3	23
9-Methylanthracen	mg/Nm^3	0
Fluoranthen	mg/Nm^3	219
Pyren	mg/Nm^3	177
Benzo[a]anthracen	mg/Nm^3	40
Chrysen	mg/Nm^3	57
Benzo[b]fluoranthen	mg/Nm^3	0
Benzo[k]fluoranthen	mg/Nm^3	0
Benzo[e]pyren	mg/Nm^3	0
Benzo[a]pyren	mg/Nm^3	0
Perylen	mg/Nm^3	0
Dibenz[a,h]anthracen	mg/Nm^3	0
Benzo[g,h,i]perylen	mg/Nm^3	0
Indeno[1,2,3-cd]pyren	mg/Nm^3	0
Coronen	mg/Nm^3	0

4.3.2 Mixture (50/50 wt.-%) of olivine and calcite

In this section, results from gasification test runs of softwood with a mixture (50/50 wt.-%) of olivine and calcite as bed material in the advanced 100 kW_{th} pilot plant at TU Wien are presented. Figure 22 shows an overview on the temporal courses of gasification temperature in the gasification reactor (GR) at steady state operation during the softwood gasification process with a mixture (50/50 wt.-%) of olivine and calcite as bed material. T_GR15 and T_GR 6 are the temperature at the top and bottom of the gasification reactor in the fluidized bed region, respectively. T_GR1 is the temperature at the bottom of the gasification reactor in the bubbling bed region. During the gasification operation, it was tried to measure the gas composition at the outlet of the gasification reactor (sample point A). Table 22 presents the main results and parameters of the gasification test run. Table 23 and Table 24 display the main gaseous product gas composition and additional product gas component, respectively. Table 25 illustrates the main gaseous flue gas composition of combustion reactor. Table 26 gives detailed information on the tar components measured by gas chromatography coupled with mass spectrometry (GC-MS).

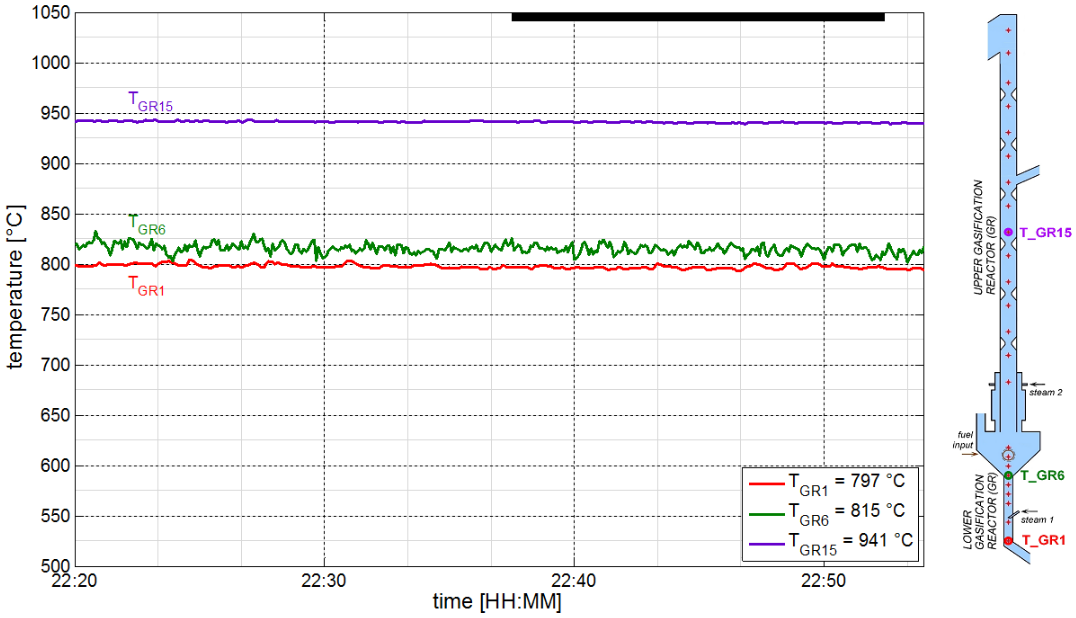

Figure 22: Overview on the temporal courses of gasification temperature for the gasification test run with softwood pellets and a mixture (50/50 wt.-%) of olivine and calcite as bed material:

Table 22: Mail results and parameters; gasification of softwood with a mixture (50/50 wt.-%) of olivine and calcite as bed material

Parameter/Name	Unit	Gasification reactor	Combustion reactor
Bed material types	µm	100 – 300 (olivine), 300 – 600 (calcite)	
Bed material	wt.-%	50 (olivine), 50 (calcite)	
Overall initial bed material inventory	kg	80	
Feedstock type	-	softwood	-
Feedstock/fuel analysis no.	-	PL-15065-A	-
Feedstock mass flow	kg/h	21.4*	-
Feedstock/fuel power into GR	kW	102*	-
Fuel to CR	kW	-	31*
Heat losses of reactor system (GR & CR)	kW	13*	
Typical temperatures (lower reactor part)	°C	GR6 815	CR4 999
Typical temperatures (upper reactor part)	°C	GR15 941	CR7 950
Water content in the gas stream	vol.-%	31*	14*
Gasification steam to fuel ratio	$kg_{steam}/kg_{fuel,db,af}$	0.8*	
Gasification steam to carbon ratio	$kg_{steam}/kg_{fuel,carbon}$	1.5*	
Product gas volume flow	Nm^3_{db}/h	28*	
Feedstock mass flow, dry & ash free	$kg_{,db,af}/h$	19.8	
Product gas yield	Nm^3_{db} $/kg_{fuel,db,af}$	1.42*	
Steam related H_2O conversion	kg_{H2O}/kg_{H2O}	0.32*	
Fuel related H_2O conversion	$kg_{H2O}/kg_{fuel,db,af}$	0.24*	
Product gas lower heating value (free of char & tar)	MJ/Nm^3_{db}	11.4*	
Product gas power (free of char & tar)	kW	89*	
Cold gas efficiency	%	87*	
Overall cold gas efficiency, novel 100kW test plant	%	67*	
Overall cold gas efficiency, estimated for a 50 MW plant	%	70 - 80	
Product gas, H_2 to CO ratio	-	2.1*	

*via calculation with IPSEpro mass & energy balance

Table 23: Main gaseous product gas composition; gasification of softwood pellets with a mixture (50/50 wt.-%) of olivine and calcite as bed material; sample point A

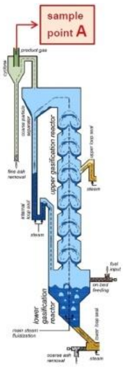

Product gas composition, sample point A				
Parameter	**Unit**	**NGA2000 online**	**PE Arnel GC TU Wien**	**IPSEpro simulation**
H_2 hydrogen	vol.-% $_{db}$	43.3	-	43.8
CO carbon monoxide	vol.-% $_{db}$	20.2	21.0	20.9
CO_2 carbon dioxide	vol.-% $_{db}$	20.0	21.0	20.8
CH_4 methane	vol.-% $_{db}$	9.12	9.42	9.43
C_2H_4 ethylene	vol.-% $_{db}$	-	0.92	0.94
C_2H_6 ethane	vol.-% $_{db}$	-	0.09	0.09
C_3H_8 propane	vol.-% $_{db}$	-	0.00	0.00

Additional gaseous product gas components			
Parameter/Name	**Unit**	**Typical values**	**PE Arnel GC TU Wien**
N_2 nitrogen	vol.-% $_{db}$	0.5 – 2.0	2.33*
Sum of C_4-.C_5-hydrocarbons, NH_3, H_2S, HCl & other comp.	vol.-% $_{db}$	0.1 – 2.0**	-

* value because of purging/flushing feedstock hoppers and temp.&press.-measuring points with nitrogen
** value range strongly fuel analysis & optional offline gas analysis

Table 24: Additional product gas component; gasification of softwood pellets with a mixture (50/50 wt.-%) of olivine and calcite as bed material; sample point A from test laboratory for combustion systems from TU Wien; offline tar measurement

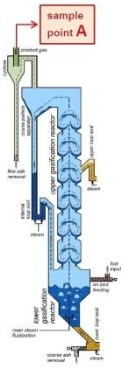

Product gas analytics, measured discontinuous, sample point A		
Parameter	**Unit**	**Solvent: toluene***
Dust content	g/Nm^3 $_{db}$	6.7
Char content	g/Nm^3 $_{db}$	5.7
Tar content GC-MS (without BTEX)	g/Nm^3 $_{db}$	3.504
Tar content gravimetric	g/Nm^3 $_{db}$	0.53
Water content, H_2O	vol.-%	32
Tar dew point**	°C	117

* mean values from two test runs measurements
**calculated via http://www.thersites.nl/completemodel.aspx

Table 25: Main gaseous flue gas composition of the combustion reactor; gasification of softwood pellets with a mixture (50/50 wt.-%) of olivine and calcite as bed material

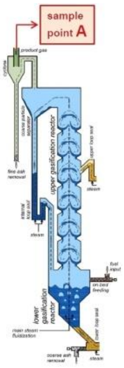

Flue gas composition			
Parameter	**Unit**	**NGA2000 online**	**IPSEpro simulation**
CO_2 carbon dioxide	vol.-% $_{db}$	11.6	13.0
O_2 oxygen	vol.-% $_{db}$	4.4	4.8
CO carbon monoxide	vol.-% $_{db}$	0.0	0.0
N_2 nitrogen	vol.-% $_{db}$	-	81.27
Ar argon	vol.-% $_{db}$	-	0.95
NO nitrogen monoxide	vol.-% ppm $_{db}$	n.a.	0.0
SO_2 sulfur dioxide	vol.-% ppm $_{db}$	n.a.	0.0
NO_2 nitrogen dioxide	vol.-% ppm $_{db}$	n.a.	0.0
N_2O nitrous oxide	vol.-% ppm $_{db}$	n.a.	0.0

Table 26: GC-MS tar components of product gas; gasification of softwood pellets with a mixture (50/50 wt.-%) of olivine and calcite as bed material

Solvent		**Toluene**
Total GC-MS (without BTEX)	**g/Nm³**	**3.504**
2-Methylpyridin	mg/Nm³	0
Phenylacetylen	mg/Nm³	≤ 7
3- und 4-Methylpyridin	mg/Nm³	0
Styrol	mg/Nm³	65
Mesitylen	mg/Nm³	0
Phenol	mg/Nm³	0
Benzofuran	mg/Nm³	0
1H-Inden	mg/Nm³	64
2-Methylphenol	mg/Nm³	0
4-Methylphenol	mg/Nm³	0
2-Methylbenzofuran	mg/Nm³	0
2,6-Dimethylphenol	mg/Nm³	0
2,5&2,4-Dimethylphenol	mg/Nm³	0
3,5-Dimethylphenol	mg/Nm³	0
2,3-Dimethylphenol	mg/Nm³	0
3,4-Dimethylphenol	mg/Nm³	0
2-Methoxy-4-Methylphenol	mg/Nm³	0
Naphthalin	mg/Nm³	2428
1-Benzothiophen	mg/Nm³	0
Chinolin	mg/Nm³	0
2-Methylnaphthalin	mg/Nm³	15
Isochinolin	mg/Nm³	0
1-Methylnaphthalin	mg/Nm³	8
Eugenol	mg/Nm³	0
1-Indanon	mg/Nm³	0
Indol	mg/Nm³	0
Biphenyl	mg/Nm³	25
1-Vinylnaphthalin	mg/Nm³	0
Isoeugenol	mg/Nm³	0
2-Vinylnaphthalin	mg/Nm³	≤ 13
Acenaphthylen	mg/Nm³	328
Acenaphthen	mg/Nm³	46
Dibenzofuran	mg/Nm³	11
Fluoren	mg/Nm³	17
Dibenzothiophen	mg/Nm³	0
Anthracen	mg/Nm³	296
Phenanthren	mg/Nm³	37
Carbazol	mg/Nm³	0
4,5-Mehtylphenanthren	mg/Nm³	8
9-Methylanthracen	mg/Nm³	0
Fluoranthen	mg/Nm³	84
Pyren	mg/Nm³	69
Benzo[a]anthracen	mg/Nm³	≤ 3
Chrysen	mg/Nm³	3
Benzo[b]fluoranthen	mg/Nm³	0
Benzo[k]fluoranthen	mg/Nm³	0
Benzo[e]pyren	mg/Nm³	≤ 3
Benzo[a]pyren	mg/Nm³	0
Perylen	mg/Nm³	0
Dibenz[a,h]anthracen	mg/Nm³	0
Benzo[g,h,i]perylen	mg/Nm³	0
Indeno[1,2,3-cd]pyren	mg/Nm³	0
Coronen	mg/Nm³	0
BTEX components	**g/Nm³**	**17.683**
Benzol	mg/Nm³	17683
Toluol	mg/Nm³	not measurable
Ethylbenzol	mg/Nm³	0
m- und p-Xylol	mg/Nm³	0
o-Xylol	mg/Nm³	0

4.4 Silica sand and mixtures with calcite

4.4.1 Pure silica sand (100 wt.-%)

In this section, results from gasification test runs of softwood with pure silica sand as bed material in the advanced 100 kW_{th} pilot plant at TU Wien are presented. Figure 23 shows an overview on the temporal courses of gasification temperature in the gasification reactor (GR) at steady state operation during the softwood gasification process with pure silica sand as bed material. T_GR15 and T_GR 6 are the temperature at the top and bottom of the gasification reactor in the fluidized bed region, respectively. T_GR1 is the temperature at the bottom of the gasification reactor in the bubbling bed region. During the gasification operation, it was tried to measure the gas composition at the outlet of the gasification reactor (sample point A). Table 27 presents the main results and parameters of the gasification test run. Table 28 and Table 29 display the main gaseous product gas composition and additional product gas component, respectively. Table 30 illustrates the main gaseous flue gas composition of combustion reactor. Table 31 gives detailed information on the tar components measured by gas chromatography coupled with mass spectrometry (GC-MS).

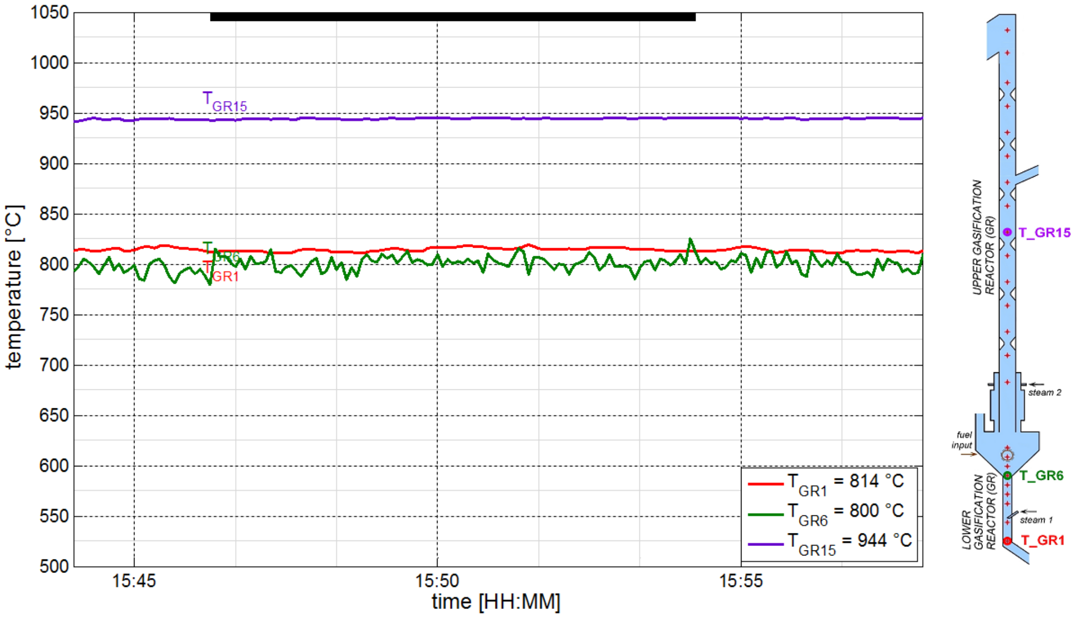

Figure 23: Overview on the temporal courses of gasification temperature; gasification of softwood pellets with pure silica sand as bed material

Table 27: Main results and parameters; gasification of softwood pellets with pure silica sand as bed material

Parameter	Unit	Gasification reactor	Combustion reactor
Bed material types	µm	200 – 400 (silica sand)	
Bed material	wt.-%	100 (silica sand)	
Overall initial bed material inventory	kg	80	
Feedstock type	-	softwood	-
Feedstock/fuel analysis no.	-	PL-15065-A	-
Feedstock mass flow	kg/h	21.3	-
Feedstock/fuel power into GR	kW	100.8	-
Fuel to CR	kW	-	45.9*
Heat losses of reactor system (GR & CR)	kW	20.2*	
Typical temperatures (lower reactor part)	°C	GR6 800	CR4 1014
Typical temperatures (upper reactor part)	°C	GR15 944	CR7 947
Water content in the gas stream	vol.-%	38*	12*
Gasification steam to fuel ratio	$kg_{steam}/kg_{fuel,db,af}$	0.9*	
Gasification steam to carbon ratio	$kg_{steam}/kg_{fuel,carbon}$	1.7*	
Product gas volume flow	Nm^3_{db}/h	26.4*	
Feedstock mass flow, dry & ash free	$kg_{,db,af}/h$	19.7	
Product gas yield	Nm^3_{db} /$kg_{fuel,db,af}$	1.34*	
Steam related H_2O conversion	kg_{H2O}/kg_{H2O}	0.25*	
Fuel related H_2O conversion	$kg_{H2O}/kg_{fuel,db,af}$	0.22*	
Product gas lower heating value (free of char & tar)	MJ/Nm^3_{db}	12.1*	
Product gas power (free of char & tar)	kW	89*	
Cold gas efficiency	%	88*	
Overall cold gas efficiency, novel 100kW test plant	%	60*	
Overall cold gas efficiency, estimated for a 50 MW plant	%	70 - 80	
Product gas, H_2 to CO ratio	-	1.8*	

* via calculation with IPSEpro mass & energy balance

Table 28: Main gaseous product gas composition; gasification of softwood pellets with pure silica sand as bed material; sample point A

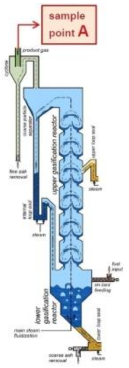

Product gas composition, sample point A				
Parameter	**Unit**	**NGA2000 online**	**PE Arnel GC TU Wien**	**IPSEpro simulation**
H_2 hydrogen	vol.-% $_{db}$	40.4	-	40.4
CO carbon monoxide	vol.-% $_{db}$	21.9	22.6	22.6
CO_2 carbon dioxide	vol.-% $_{db}$	19.4	20.6	20.6
CH_4 methane	vol.-% $_{db}$	10.2	10.1	10.8
C_2H_4 ethylene	vol.-% $_{db}$	-	1.56	1.58
C_2H_6 ethane	vol.-% $_{db}$	-	0.104	0.106
C_3H_8 propane	vol.-% $_{db}$	-	0.00	0.00

Additional gaseous product gas components			
Parameter	**Unit**	**Typical values**	**PE Arnel GC TU Wien**
N_2 nitrogen	vol.-% $_{db}$	0.5 – 2.0	1.44*
Sum of C_4-.C_5-hydrocarbons, NH_3, H_2S, HCl & other comp.	vol.-% $_{db}$	0.1 – 2.0**	-

* value because of purging/flushing feedstock hoppers and temp.& press.-measuring points with nitrogen
** value range strongly depends on the fuel composition (see fuel analysis & optional offline gas analysis

Table 29: Additional product gas component; gasification of softwood pellets with pure silica sand as bed material; sample point A from test laboratory for combustion systems from TU Wien; offline tar measurement

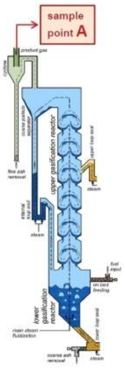

Product gas analytics, measured discontinuous, sample point A		
Parameter	**Unit**	**Solvent: toluen**
Dust content	g/Nm^3_{db}	4.5
Char content	g/Nm^3_{db}	6.1
Tar content GC-MS (without BTEX)	g/Nm^3_{db}	11.887
Tar content BTEX	g/Nm^3_{db}	22.093
Tar content gravimetric	g/Nm^3_{db}	5.21
Water content, H_2O	vol.-%	38
Tar dew point*	°C	211

*calculated via http://www.thersites.nl/completemodel.aspx

Table 30: Main gaseous flue gas composition of the combustion reactor; gasification of softwood pellets with pure silica sand as bed material

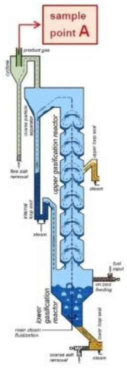

Flue gas composition			
Parameter	**Unit**	**NGA2000 online**	**IPSEpro simulation**
CO_2 carbon dioxide	vol.-% $_{db}$	13	13.34
O_2 oxygen	vol.-% $_{db}$	3.5	3.66
CO carbon monoxide	vol.-% $_{db}$	0.01	0.01
N_2 nitrogen	vol.-% $_{db}$	-	82.03
Ar argon	vol.-% $_{db}$	-	0.96
NO nitrogen monoxide	vol.-% ppm $_{db}$	n.a.	0.0
SO_2sulfur dioxide	vol.-% ppm $_{db}$	n.a.	0.0
NO_2nitrogen dioxide	vol.-% ppm $_{db}$	n.a.	0.0
N_2O nitrous oxide	vol.-% ppm $_{db}$	n.a.	0.0

n.a.: not available

Table 31: GC-MS tar components of product gas; gasification of softwood pellets with pure silica sand as bed material

Solvent		**Toluene**
Total GC-MS (without BTEX)	**g/Nm³**	**11.887**
Pyridin	mg/Nm³	not measurable
2-Methylpyridin	mg/Nm³	0
Phenylacetylen	mg/Nm³	37
3- und 4-Methylpyridin	mg/Nm³	0
Styrol	mg/Nm³	220
Mesitylen	mg/Nm³	0
Phenol	mg/Nm³	0
Benzofuran	mg/Nm³	0
1H-Inden	mg/Nm³	571
2-Methylphenol	mg/Nm³	0
4-Methylphenol	mg/Nm³	0
2-Methylbenzofuran	mg/Nm³	0
2,6-Dimethylphenol	mg/Nm³	0
2,5&2,4-Dimethylphenol	mg/Nm³	0
3,5-Dimethylphenol	mg/Nm³	0
2,3-Dimethylphenol	mg/Nm³	0
3,4-Dimethylphenol	mg/Nm³	0
2-Methoxy-4-Methylphenol	mg/Nm³	0
Naphthalin	mg/Nm³	5149
1-Benzothiophen	mg/Nm³	0
Chinolin	mg/Nm³	0
2-Methylnaphthalin	mg/Nm³	56
Isochinolin	mg/Nm³	0
1-Methylnaphthalin	mg/Nm³	32
Eugenol	mg/Nm³	0
1-Indanon	mg/Nm³	0
Indol	mg/Nm³	0
Biphenyl	mg/Nm³	89
1-Vinylnaphthalin	mg/Nm³	0
Isoeugenol	mg/Nm³	0
2-Vinylnaphthalin	mg/Nm³	44
Acenaphthylen	mg/Nm³	1616
Acenaphthen	mg/Nm³	25
Dibenzofuran	mg/Nm³	184
Fluoren	mg/Nm³	237
Dibenzothiophen	mg/Nm³	0
Anthracen	mg/Nm³	1148
Phenanthren	mg/Nm³	292
Carbazol	mg/Nm³	0
4,5-Mehtylphenanthren	mg/Nm³	132
9-Methylanthracen	mg/Nm³	0
Fluoranthen	mg/Nm³	677
Pyren	mg/Nm³	556
Benzo[a]anthracen	mg/Nm³	118
Chrysen	mg/Nm³	121
Benzo[b]fluoranthen	mg/Nm³	87
Benzo[k]fluoranthen	mg/Nm³	105
Benzo[e]pyren	mg/Nm³	72
Benzo[a]pyren	mg/Nm³	144
Perylen	mg/Nm³	28
Dibenz[a,h]anthracen	mg/Nm³	0
Benzo[g,h,i]perylen	mg/Nm³	69
Indeno[1,2,3-cd]pyren	mg/Nm³	70
Coronen	mg/Nm³	7
BTEX components	**g/Nm³**	**22.093**
Benzol	mg/Nm³	22093
Toluol	mg/Nm³	not measurable
Ethylbenzol	mg/Nm³	0
m- und p-Xylol	mg/Nm³	0
o-Xylol	mg/Nm³	0

4.4.1 Mixture (90/10 wt.-%) of silica sand and calcite

In this section, results from gasification test runs of softwood with a mixture (90/10 wt.-%) of silica sand and calcite as bed material in the advanced 100 kW_{th} pilot plant at TU Wien are presented. Figure 24 shows an overview on the temporal courses of gasification temperature at steady state operation with softwood pellets and a mixture (90/10 wt.-%) of silica sand and calcite as bed material in the gasification reactor (GR). T_GR15 and T_GR 6 are the temperature at the top and bottom of the gasification reactor in the fluidized bed region, respectively. T_GR1 is the temperature at the bottom of the gasification reactor in the bubbling bed region. During the gasification operation, it was tried to measure the gas composition at the outlet of the gasification reactor (sample point A). Table 32 presents the main results and parameters of the gasification test run. Table 33 and Table 34 display the main gaseous product gas composition and additional product gas component, respectively. Table 35 illustrates the main gaseous flue gas composition of combustion reactor. Table 36 gives detailed information on the tar components measured by gas chromatography coupled with mass spectrometry (GC-MS).

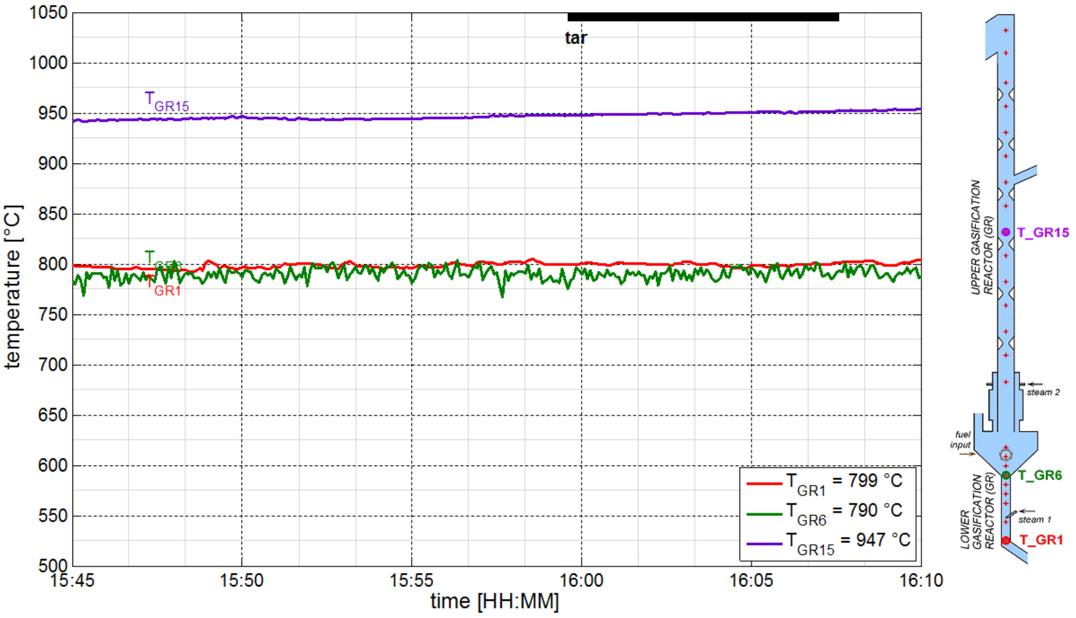

Figure 24: Overview on the temporal courses of gasification temperature; gasification of softwood pellets with a mixture (90/10 wt.-%) of silica sand and calcite as bed material

Table 32: Main results and parameters; gasification of softwood with a mixture (90/10 wt.-%) of silica sand and calcite as bed material

Parameter	Unit	Gasification reactor	Combustion reactor
Bed material types	µm	200-400 (silica), 300-600 (calcite)	
Bed material	wt.-%	90 (silica sand), 10 (calcite)	
Overall initial bed material inventory	kg	80	
Feedstock type	-	softwood	-
Feedstock/fuel analysis no.	-	PL-15065-A	-
Feedstock mass flow	kg/h	21.3	-
Feedstock/fuel power into GR	kW	100.80	-
Fuel to CR	kW	-	65*
Heat losses of reactor system	kW	19*	12
Typical temperatures (lower reactor part)	°C	GR6 790	CR4 1008
Typical temperatures (upper reactor part)	°C	GR15 947	CR7 947.6
Water content in the gas stream	vol.-%	35*	13*
Gasification steam to fuel ratio	$kg_{steam}/kg_{fuel,db,af}$	0.86*	
Gasification steam to carbon ratio	$kg_{steam}/kg_{fuel,carbon}$	1.69*	
Product gas volume flow	Nm^3_{db}/h	27.8*	
Feedstock mass flow, dry & ash free	$kg_{,db,af}/h$	19.7	
Product gas yield	Nm^3_{db} /$kg_{fuel,db,af}$	1.41*	
Steam related H_2O conversion	kg_{H2O}/kg_{H2O}	0.31*	
Fuel related H_2O conversion	$kg_{H2O}/kg_{fuel,db,af}$	0.26*	
Product gas lower heating value (free of char & tar)	MJ/Nm^3_{db}	12.3*	
Product gas power (free of char & tar)	kW	95*	
Cold gas efficiency	%	94.4*	
Overall cold gas efficiency, novel 100kW test plant	%	57.4*	
Overall cold gas efficiency, estimated for a 50 MW plant	%	70 – 80	
Product gas, H_2 to CO ratio	-	1.9*	

* via calculation with IPSEpro mass & energy balance

Table 33: Main gaseous product gas composition; gasification of softwood pellets with a mixture (90/10 wt.-%) of silica sand and calcite as bed material; sample point A

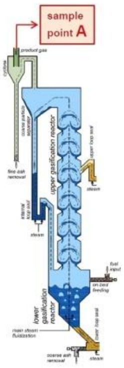

Product gas composition, sample point A				
Parameter	**Unit**	**NGA2000 online**	**PE Arnel GC TU Wien**	**IPSEpro simulation**
H_2 hydrogen	vol.-% $_{db}$	42.2	-	42.3
CO carbon monoxide	vol.-% $_{db}$	22.0	23.1	22.8
CO_2 carbon dioxide	vol.-% $_{db}$	20.4	21.5	21.2
CH_4 methane	vol.-% $_{db}$	10.1	10.6	10.9
C_2H_4 ethylene	vol.-% $_{db}$	-	1.6	1.54
C_2H_6 ethane	vol.-% $_{db}$	-	0.15	0.11
C_3H_8 propane	vol.-% $_{db}$	-	0.00	0.00

Additional gaseous product gas components			
Parameter	**Unit**	**Typical values**	**PE Arnel GC TU Wien**
N_2 nitrogen	vol.-% $_{db}$	0.5 – 2.0	1.02
Sum of C_4-.C_5-hydrocarbons, NH_3, H_2S, HCl& other comp.	vol.-% $_{db}$	0.1 – 2.0**	-

* value because of purging/flushing feedstock hoppers and temp.& press.-measuring points with nitrogen
** value range strongly depends on the fuel composition (see fuel analysis & optional offline gas analysis

Table 34: Additional product gas component; gasification of softwood pellets with a mixture (90/10 wt.-%) of silica sand and calcite as bed material; sample point A from test laboratory for combustion systems from TU Wien; offline tar measurement

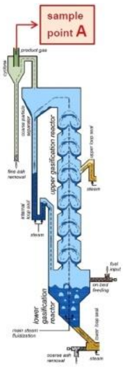

Product gas analytics, measured discontinuous, sample point A		
Parameter/Name	**Unit**	**Solvent: toluene**
Dust content	g/Nm^3 $_{db}$	3.3
Char content	g/Nm^3 $_{db}$	4.2
Tar content GC-MS (without BTEX)	g/Nm^3 $_{db}$	8.917
Tar content BTEX	g/Nm^3 $_{db}$	19.358
Tar content gravimetric	g/Nm^3 $_{db}$	2.15
Water content, H_2O	vol.-%	36
Tar dew point*	°C	181

*calculated via http://www.thersites.nl/completemodel.aspx

Table 35: Main gaseous flue gas composition of the combustion reactor; gasification of softwood pellets with a mixture (90/10 wt.-%) of silica sand and calcite as bed material

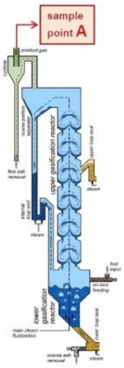

Flue gas composition			
Parameter	**Unit**	**NGA2000 online**	**IPSEpro simulation**
CO_2 carbon dioxide	vol.-% $_{db}$	13.9	14.6
O_2 oxygen	vol.-% $_{db}$	1.02	1.02
CO carbon monoxide	vol.-% $_{db}$	0.6	0.60
N_2 nitrogen	vol.-% $_{db}$	-	0.00
Ar argon	vol.-% $_{db}$	-	0.00
NO nitrogen monoxide	vol.-% ppm $_{db}$	16.41	0.00
SO_2 sulfur dioxide	vol.-% ppm $_{db}$	6.67	0.00
NO_2 nitrogen dioxide	vol.-% ppm $_{db}$	-	0.00
N_2O nitrous oxide	vol.-% ppm $_{db}$	8.20	0.00

*due to additional N_2-flushing of the upper loop seal gravity separator the measured values are lower

Table 36: GC-MS tar components of product gas; gasification of softwood pellets with a mixture (90/10 wt.-%) of silica sand and calcite as bed material

Solvent		**Toluene**
Total GC-MS (without BTEX)	**g/Nm³**	**8.917**
Pyridin	mg/Nm³	not measurable
2-Methylpyridin	mg/Nm³	0
Phenylacetylen	mg/Nm³	22
3- und 4-Methylpyridin	mg/Nm³	0
Styrol	mg/Nm³	232
Mesitylen	mg/Nm³	0
Phenol	mg/Nm³	0
Benzofuran	mg/Nm³	0
1H-Inden	mg/Nm³	688
2-Methylphenol	mg/Nm³	0
4-Methylphenol	mg/Nm³	0
2-Methylbenzofuran	mg/Nm³	0
2,6-Dimethylphenol	mg/Nm³	0
2,5&2,4-Dimethylphenol	mg/Nm³	0
3,5-Dimethylphenol	mg/Nm³	0
2,3-Dimethylphenol	mg/Nm³	0
3,4-Dimethylphenol	mg/Nm³	0
2-Methoxy-4-Methylphenol	mg/Nm³	0
Naphthalin	mg/Nm³	3950
1-Benzothiophen	mg/Nm³	0
Chinolin	mg/Nm³	0
2-Methylnaphthalin	mg/Nm³	42
Isochinolin	mg/Nm³	0
1-Methylnaphthalin	mg/Nm³	24
Eugenol	mg/Nm³	0
1-Indanon	mg/Nm³	0
Indol	mg/Nm³	0
Biphenyl	mg/Nm³	88
1-Vinylnaphthalin	mg/Nm³	0
Isoeugenol	mg/Nm³	0
2-Vinylnaphthalin	mg/Nm³	36
Acenaphthylen	mg/Nm³	1199
Acenaphthen	mg/Nm³	27
Dibenzofuran	mg/Nm³	131
Fluoren	mg/Nm³	216
Dibenzothiophen	mg/Nm³	0
Anthracen	mg/Nm³	833
Phenanthren	mg/Nm³	293
Carbazol	mg/Nm³	0
4,5-Mehtylphenanthren	mg/Nm³	70
9-Methylanthracen	mg/Nm³	0
Fluoranthen	mg/Nm³	456
Pyren	mg/Nm³	345
Benzo[a]anthracen	mg/Nm³	72
Chrysen	mg/Nm³	70
Benzo[b]fluoranthen	mg/Nm³	40
Benzo[k]fluoranthen	mg/Nm³	46
Benzo[e]pyren	mg/Nm³	28
Benzo[a]pyren	mg/Nm³	54
Perylen	mg/Nm³	0
Dibenz[a,h]anthracen	mg/Nm³	0
Benzo[g,h,i]perylen	mg/Nm³	9
Indeno[1,2,3-cd]pyren	mg/Nm³	10
Coronen	mg/Nm³	0
BTEX components	**g/Nm³**	**19.358**
Benzol	mg/Nm³	19358
Toluol	mg/Nm³	not measurable
Ethylbenzol	mg/Nm³	0
m- und p-Xylol	mg/Nm³	0
o-Xylol	mg/Nm³	0

4.4.1 Mixture (50/50 wt.-%) of silica sand and calcite

In this section, results from gasification test runs of softwood with a mixture (50/50 wt.-%) of silica sand and calcite as bed material in the advanced 100 kW_{th} pilot plant at TU Wien are presented. Figure 25 shows an overview on the temporal courses of gasification temperature in the gasification reactor (GR) at steady state operation during the softwood gasification process with a mixture (50/50 wt.-%) of silica sand and calcite as bed material. T_GR15 and T_GR 6 are the temperature at the top and bottom of the gasification reactor in the fluidized bed region, respectively. T_GR1 is the temperature at the bottom of the gasification reactor in the bubbling bed region. During the gasification operation, it was tried to measure the gas composition at the outlet of the gasification reactor (sample point A). Table 37 presents the main results and parameters of the gasification test run. Table 38 and Table 39 display the main gaseous product gas composition and additional product gas component, respectively. Table 40 illustrates the main gaseous flue gas composition of combustion reactor. Table 41 gives detailed information on the tar components measured by gas chromatography coupled with mass spectrometry (GC-MS).

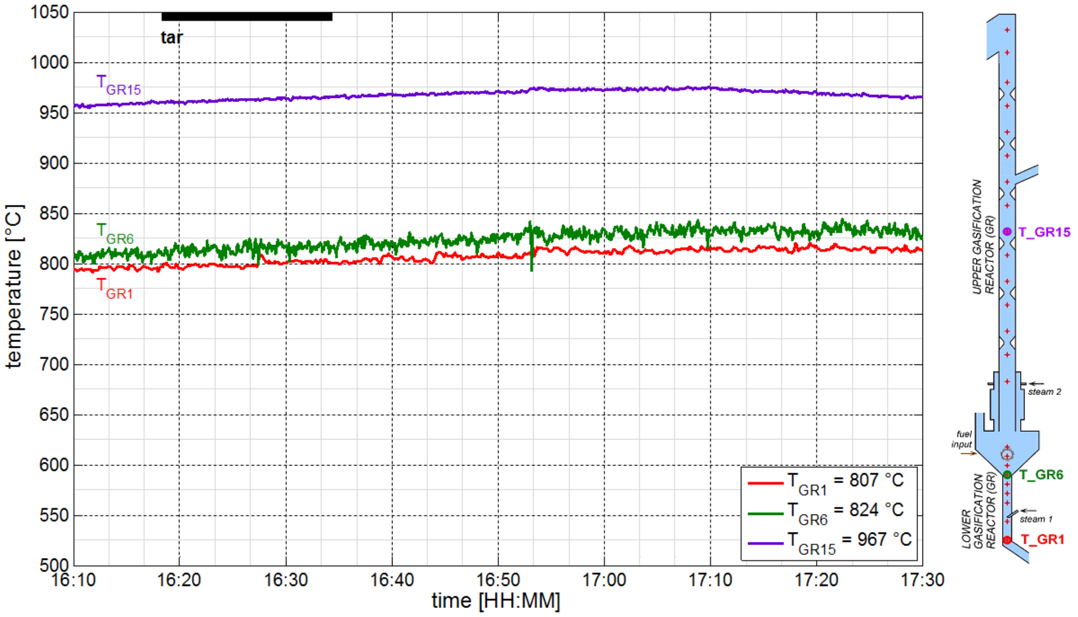

Figure 25: Overview on the temporal courses of gasification temperature; gasification of softwood pellets with a mixture (50/50 wt.-%) of silica sand and calcite as bed material

Table 37: Main results and parameters; gasification of softwood pellets with a mixture (50/50 wt.-%) of silica sand and calcite as bed material

Parameter	Unit	Gasification reactor	Combustion reactor
Bed material types	µm	200 - 400 (silica sand)	
Bed material	wt.-%	50 (silica sand), 50 (calcite)	
Overall initial bed material inventory	kg	80	
Feedstock type	-	softwood	-
Feedstock/fuel analysis no.	-	PL-15065-A	-
Feedstock mass flow	kg/h	21.2	-
Feedstock/fuel power into GR	kW	101	-
Fuel to CR	kW	-	56*
Heat losses of reactor system	kW	16*	10
Typical temperatures (lower reactor part)	°C	GR6 824	CR4 1046
Typical temperatures (upper reactor part)	°C	GR15 967	CR7 974.6
Water content in the gas stream	vol.-%	31*	13*
Gasification steam to fuel ratio	$kg_{steam}/kg_{fuel,db,af}$	0.84*	
Gasification steam to carbon ratio	$kg_{steam}/kg_{fuel,carbon}$	1.66*	
Product gas volume flow	Nm^3_{db}/h	29.3*	
Feedstock mass flow, dry & ash free	$kg_{,db,af}/h$	19.6	
Product gas yield	Nm^3_{db} $/kg_{fuel,db,af}$	1.49*	
Steam related H_2O conversion	kg_{H2O}/kg_{H2O}	0.37*	
Fuel related H_2O conversion	$kg_{H2O}/kg_{fuel,db,af}$	0.32*	
Product gas lower heating value (free of char & tar)	MJ/Nm^3_{db}	11.4*	
Product gas power (free of char & tar)	kW	93*	
Cold gas efficiency	%	93*	
Overall cold gas efficiency, novel 100kW test plant	%	60*	
Overall cold gas efficiency, estimated for a 50 MW plant	%	70 – 80	
Product gas, H_2 to CO ratio	-	2.2*	

* via calculation with IPSEpro mass & energy balance

Table 38: Main gaseous product gas composition; gasification of softwood pellets with a mixture (50/50 wt.-%) of silica sand and calcite as bed material; sample point A

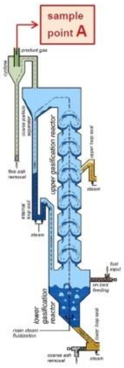

Product gas composition, sample point A				
Parameter	**Unit**	**NGA2000 online**	**PE Arnel GC TU Wien**	**IPSEpro Simulation**
H_2 hydrogen	vol.-% $_{db}$	45.9	-	46.6
CO carbon monoxide	vol.-% $_{db}$	20.6	22.0	21.6
CO_2 carbon dioxide	vol.-% $_{db}$	20.0	21.2	21.0
CH_4 methane	vol.-% $_{db}$	8.7	9.2	9.1
C_2H_4 ethylene	vol.-% $_{db}$	-	0.65	0.64
C_2H_6 ethane	vol.-% $_{db}$	-	0.07	0.075
C_3H_8 propane	vol.-% $_{db}$	-	0.00	0.00

Additional gaseous product gas components			
Parameter/Uame	**Unit**	**Typical values**	**PE Arnel GC TU Wien**
N_2 nitrogen	vol.-% $_{db}$	0.5 – 2.0	0.76
Sum of C_4-.C_5-hydrocarbons, NH_3, H_2S, HCl& other comp.	vol.-% $_{db}$	0.1 – 2.0**	-

* value because of purging/flushing feedstock hoppers and temp.& press.-measuring points with nitrogen

** value range strongly depends on the fuel composition (see fuel analysis & optional offline gas analysis

Table 39: Additional product gas component; gasification of softwood pellets with a mixture (50/50 wt.-%) of silica sand and calcite as bed material; sample point A from test laboratory for combustion systems from TU Wien; offline tar measurement

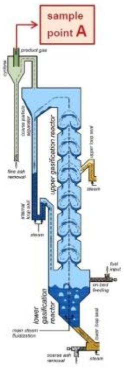

Product gas analytics, measured discontinuous, sample point A		
Parameter/Name	**Unit**	**Solvent: toluene**
Dust content	$g/Nm^3{}_{db}$	8.97
Char content	$g/Nm^3{}_{db}$	5.06
Tar content GC-MS (without BTEX)	$g/Nm^3{}_{db}$	2.452
Tar content BTEX	$g/Nm^3{}_{db}$	8.558
Tar content gravimetric	$g/Nm^3{}_{db}$	0.44
Water content, H_2O	vol.-%	32
Tar dew point*	°C	104

*calculated via http://www.thersites.nl/completemodel.aspx

Table 40: Main gaseous flue gas composition of the combustion reactor; gasification of softwood pellets with a mixture (50/50 wt.-%) of silica sand and calcite as bed material

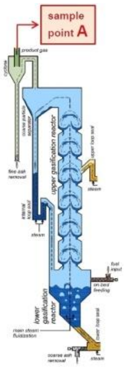

Flue gas composition			
Parameter	**Unit**	**NGA2000 online**	**IPSEpro simulation**
CO_2 carbon dioxide	vol.-% $_{db}$	13.9	15.07
O_2 oxygen	vol.-% $_{db}$	1.02	1.02
CO carbon monoxide	vol.-% $_{db}$	0.6	0.57
N_2 nitrogen	vol.-% $_{db}$	-	0.00
Ar argon	vol.-% $_{db}$	-	0.00
NO nitrogen monoxide	vol.-% ppm $_{db}$	16.41	0.00
SO_2 sulfur dioxide	vol.-% ppm $_{db}$	6.67	0.00
NO_2 nitrogen dioxide	vol.-% ppm $_{db}$	n.a.	0.00
N_2O nitrous oxide	vol.-% ppm $_{db}$	8.20	0.00

n.a.: not available

Table 41: GC-MS tar components of product gas; gasification of softwood pellets with a mixture (50/50 wt.-%) of silica sand and calcite as bed material

Solvent		**Toluene**
Total GC-MS (without BTEX)	**g/Nm^3**	**2.452**
Pyridin	mg/Nm^3	not measurable
2-Methylpyridin	mg/Nm^3	0
Phenylacetylen	mg/Nm^3	0
3- und 4-Methylpyridin	mg/Nm^3	0
Styrol	mg/Nm^3	46
Mesitylen	mg/Nm^3	0
Phenol	mg/Nm^3	0
Benzofuran	mg/Nm^3	0
1H-Inden	mg/Nm^3	58
2-Methylphenol	mg/Nm^3	0
4-Methylphenol	mg/Nm^3	0
2-Methylbenzofuran	mg/Nm^3	0
2,6-Dimethylphenol	mg/Nm^3	0
2,5&2,4-Dimethylphenol	mg/Nm^3	0
3,5-Dimethylphenol	mg/Nm^3	0
2,3-Dimethylphenol	mg/Nm^3	0
3,4-Dimethylphenol	mg/Nm^3	0
2-Methoxy-4-Methylphenol	mg/Nm^3	0
Naphthalin	mg/Nm^3	1712
1-Benzothiophen	mg/Nm^3	0
Chinolin	mg/Nm^3	0
2-Methylnaphthalin	mg/Nm^3	≤ 6
Isochinolin	mg/Nm^3	0
1-Methylnaphthalin	mg/Nm^3	≤ 6
Eugenol	mg/Nm^3	0
1-Indanon	mg/Nm^3	0
Indol	mg/Nm^3	0
Biphenyl	mg/Nm^3	10
1-Vinylnaphthalin	mg/Nm^3	0
Isoeugenol	mg/Nm^3	0
2-Vinylnaphthalin	mg/Nm^3	0
Acenaphthylen	mg/Nm^3	266
Acenaphthen	mg/Nm^3	24
Dibenzofuran	mg/Nm^3	0
Fluoren	mg/Nm^3	8
Dibenzothiophen	mg/Nm^3	0
Anthracen	mg/Nm^3	227
Phenanthren	mg/Nm^3	23
Carbazol	mg/Nm^3	0
4,5-Mehtylphenanthren	mg/Nm^3	0
9-Methylanthracen	mg/Nm^3	0
Fluoranthen	mg/Nm^3	43
Pyren	mg/Nm^3	35
Benzo[a]anthracen	mg/Nm^3	0
Chrysen	mg/Nm^3	0
Benzo[b]fluoranthen	mg/Nm^3	0
Benzo[k]fluoranthen	mg/Nm^3	0
Benzo[e]pyren	mg/Nm^3	0
Benzo[a]pyren	mg/Nm^3	0
Perylen	mg/Nm^3	0
Dibenz[a,h]anthracen	mg/Nm^3	0
Benzo[g,h,i]perylen	mg/Nm^3	0
Indeno[1,2,3-cd]pyren	mg/Nm^3	0
Coronen	mg/Nm^3	0
BTEX components	**g/Nm^3**	**8.558**
Benzol	mg/Nm^3	8558
Toluol	mg/Nm^3	not measurable
Ethylbenzol	mg/Nm^3	0
m- und p-Xylol	mg/Nm^3	0
o-Xylol	mg/Nm^3	0

4.5 Feldspar and mixtures with calcite

4.5.1 Pure feldspar (100 wt.-%)

In this section, results from gasification test runs of softwood with pure feldspar as bed material in the advanced 100 kW_{th} pilot plant at TU Wien are presented. Figure 26 shows an overview on the temporal courses of gasification temperature in the gasification reactor (GR) at steady state operation during the softwood gasification process with pure feldspar as bed material. T_GR15 and T_GR 6 are the temperature at the top and bottom of the gasification reactor in the fluidized bed region, respectively. T_GR1 is the temperature at the bottom of the gasification reactor in the bubbling bed region. During the gasification operation, it was tried to measure the gas composition at the outlet of the gasification reactor (sample point A). Table 42 presents the main results and parameters of the gasification test run. Table 43 and Table 44 display the main gaseous product gas composition and additional product gas component, respectively. Table 45 illustrates the main gaseous flue gas composition of combustion reactor. Table 46 gives detailed information on the tar components measured by gas chromatography coupled with mass spectrometry (GC-MS).

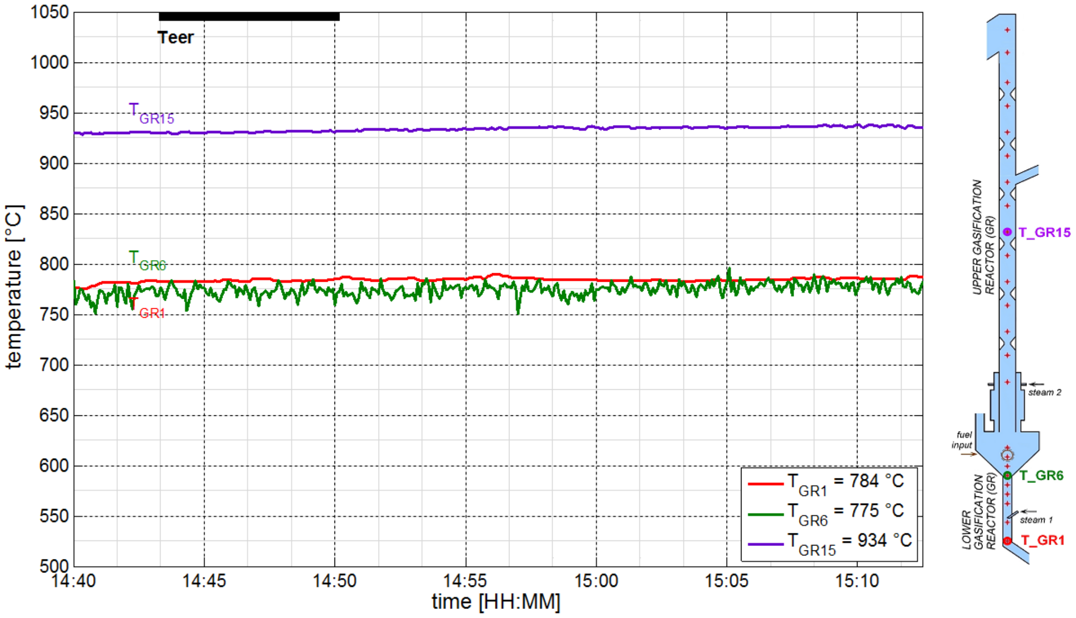

Figure 26: Overview on the temporal courses of gasification temperature; gasification of softwood pellets with pure feldspar as bed material

Table 42: Main results and parameters; gasification of softwood pellets with pure feldspar as bed material

Parameter/name	Unit	Gasification reactor	Combustion reactor
Bed material types	µm	280 – 430 (feldspar)	
Bed material	wt.-%	100 (feldspar)	
Overall initial bed material inventory	kg	80	
Feedstock type	-	softwood	-
Feedstock/fuel analysis no.	-	PL-15065-A	-
Feedstock mass flow	kg/h	21.3	-
Feedstock/fuel power into GR	kW	98	-
Fuel to CR	kW	-	53*
Heat losses of reactor system	kW	17*	12
Typical temperatures (lower reactor part)	°C	GR6 775	CR4 997
Typical temperatures (upper reactor part)	°C	GR15 934	CR7 923
Water content in the gas stream	vol.-%	45*	14*
Gasification steam to fuel ratio	$kg_{steam}/kg_{fuel,db,af}$	0.89*	
Gasification steam to carbon ratio	$kg_{steam}/kg_{fuel,carbon}$	1.80*	
Product gas volume flow	Nm^3_{db}/h	22.9*	
Feedstock mass flow, dry & ash free	$kg_{,db,af}/h$	19.6	
Product gas yield	$Nm^3_{db}/kg_{fuel,db,af}$	1.17*	
Steam related H_2O conversion	kg_{H2O}/kg_{H2O}	0.14*	
Fuel related H_2O conversion	$kg_{H2O}/kg_{fuel,db,af}$	0.12*	
Product gas lower heating value (free of char & tar)	MJ/Nm^3_{db}	13.7*	
Product gas power (free of char & tar)	kW	87.1*	
Cold gas efficiency	%	88.6*	
Overall cold gas efficiency, novel 100kW test plant	%	57.7*	
Overall cold gas efficiency, estimated for a 50 MW plant	%	70 - 80	
Product gas, H_2 to CO ratio	-	1.2*	

* via calculation with IPSEpro mass & energy balance

Table 43: Main gaseous product gas composition; gasification of softwood pellets with pure feldspar as bed material; sample point A

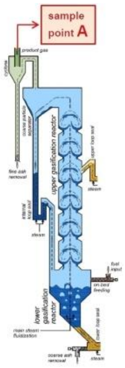

Product gas composition, sample point A				
Parameter/Name	**Unit**	**NGA2000 online**	**PE Arnel GC TU Wien**	**IPSEpro simulation**
H_2 hydrogen	vol.-% $_{db}$	35.6	-	35.7
CO carbon monoxide	vol.-% $_{db}$	29.1	29.2	29.9
CO_2 carbon dioxide	vol.-% $_{db}$	17.1	18.03	17.8
CH_4 methane	vol.-% $_{db}$	12.1	12.03	12.8
C_2H_4 ethylene	vol.-% $_{db}$	-	2.34	2.3
C_2H_6 ethane	vol.-% $_{db}$	-	0.16	0.16
C_3H_8 propane	vol.-% $_{db}$	-	0.00	0.00

Additional gaseous product gas components			
Parameter	**Unit**	**Typical values**	**PE Arnel GC TU Wien**
N_2 nitrogen	vol.-% $_{db}$	0.5 – 2.0	1.22
Sum of C_4-.C_5-hydrocarbons, NH_3, H_2S, HCl& other comp.	vol.-% $_{db}$	0.1 – 2.0**	-

* value because of purging/flushing feedstock hoppers and temp.& press.-measuring points with nitrogen
** value range strongly depends on the fuel composition (see fuel analysis & optional offline gas analysis

Table 44: Additional product gas component; gasification of softwood pellets with pure feldspar as bed material; sample point A from test laboratory for combustion systems from TU Wien; offline tar measurement

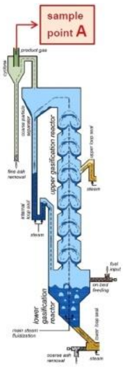

Product gas analytics, measured discontinuous, sample point A		
Parameter	**Unit**	**Solvent: toluene**
Dust content	g/Nm^3 $_{db}$	0.39
Char content	g/Nm^3 $_{db}$	1.08
Tar content GC-MS (without BTEX)	g/Nm^3 $_{db}$	17.099
Tar content BTEX	g/Nm^3 $_{db}$	25.165
Tar content gravimetric	g/Nm^3 $_{db}$	8.26
Water content, H_2O	vol.-%	46
Tar dew point*	°C	215.9

*calculated via http://www.thersites.nl/completemodel.aspx

Table 45: Main gaseous flue gas composition of the combustion reactor; gasification of softwood pellets with pure feldspar as bed material

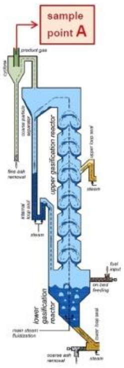

Flue gas composition			
Parameter	**Unit**	**NGA2000 online**	**IPSEpro simulation**
CO_2 carbon dioxide	vol.-% $_{db}$	13.64	15.37
O_2 oxygen	vol.-% $_{db}$	0.398	0.00
CO carbon monoxide	vol.-% $_{db}$	0.125	0.72
N_2 nitrogen	vol.-% $_{db}$	-	0.00
Ar argon	vol.-% $_{db}$	-	0.00
NO nitrogen monoxide	vol.-% ppm $_{db}$	32.3	0.00
SO_2 sulfur dioxide	vol.-% ppm $_{db}$	12.0	0.00
NO_2 nitrogen dioxide	vol.-% ppm $_{db}$	n.a.	0.00
N_2O nitrous oxide	vol.-% ppm $_{db}$	6.00	0.00

n.a.: not available

Table 46: GC-MS tar components of product gas; gasification of softwood pellets with pure feldspar as bed material

Solvent		**Toluene**
Total GC-MS (without BTEX)	**g/Nm³**	**17.099**
Pyridin	mg/Nm³	not measurable
2-Methylpyridin	mg/Nm³	0
Phenylacetylen	mg/Nm³	99
3- und 4-Methylpyridin	mg/Nm³	0
Styrol	mg/Nm³	525
Mesitylen	mg/Nm³	0
Phenol	mg/Nm³	165
Benzofuran	mg/Nm³	59
1H-Inden	mg/Nm³	1931
2-Methylphenol	mg/Nm³	0
4-Methylphenol	mg/Nm³	0
2-Methylbenzofuran	mg/Nm³	0
2,6-Dimethylphenol	mg/Nm³	0
2,5&2,4-Dimethylphenol	mg/Nm³	0
3,5-Dimethylphenol	mg/Nm³	0
2,3-Dimethylphenol	mg/Nm³	0
3,4-Dimethylphenol	mg/Nm³	0
2-Methoxy-4-Methylphenol	mg/Nm³	0
Naphthalin	mg/Nm³	6785
1-Benzothiophen	mg/Nm³	0
Chinolin	mg/Nm³	0
2-Methylnaphthalin	mg/Nm³	175
Isochinolin	mg/Nm³	0
1-Methylnaphthalin	mg/Nm³	97
Eugenol	mg/Nm³	0
1-Indanon	mg/Nm³	0
Indol	mg/Nm³	0
Biphenyl	mg/Nm³	175
1-Vinylnaphthalin	mg/Nm³	≤ 21
Isoeugenol	mg/Nm³	0
2-Vinylnaphthalin	mg/Nm³	99
Acenaphthylen	mg/Nm³	1991
Acenaphthen	mg/Nm³	38
Dibenzofuran	mg/Nm³	399
Fluoren	mg/Nm³	555
Dibenzothiophen	mg/Nm³	0
Anthracen	mg/Nm³	1274
Phenanthren	mg/Nm³	407
Carbazol	mg/Nm³	0
4,5-Mehtylphenanthren	mg/Nm³	218
9-Methylanthracen	mg/Nm³	0
Fluoranthen	mg/Nm³	683
Pyren	mg/Nm³	535
Benzo[a]anthracen	mg/Nm³	165
Chrysen	mg/Nm³	33
Benzo[b]fluoranthen	mg/Nm³	108
Benzo[k]fluoranthen	mg/Nm³	139
Benzo[e]pyren	mg/Nm³	79
Benzo[a]pyren	mg/Nm³	182
Perylen	mg/Nm³	24
Dibenz[a,h]anthracen	mg/Nm³	0
Benzo[g,h,i]perylen	mg/Nm³	87
Indeno[1,2,3-cd]pyren	mg/Nm³	73
Coronen	mg/Nm³	0
BTEX components	**g/Nm³**	**25.165**
Benzol	mg/Nm³	25165
Toluol	mg/Nm³	not measurable
Ethylbenzol	mg/Nm³	0
m- und p-Xylol	mg/Nm³	0
o-Xylol	mg/Nm³	0

4.5.1 Mixture (90/10 wt.-%) of feldspar and calcite

In this section, results from gasification test runs of softwood with a mixture (90/10 wt.-%) of feldspar and calcite as bed material in the advanced 100 kW_{th} pilot plant at TU Wien are presented. Figure 27 shows an overview on the temporal courses of gasification temperature in the gasification reactor (GR) at steady state operation during the softwood gasification process with a mixture (90/10 wt.-%) of feldspar and calcite as bed material. T_GR15 and T_GR 6 are the temperature at the top and bottom of the gasification reactor in the fluidized bed region, respectively. T_GR1 is the temperature at the bottom of the gasification reactor in the bubbling bed region. During the gasification operation, it was tried to measure the gas composition at the outlet of the gasification reactor (sample point A). Table 47 presents the main results and parameters of the gasification test run. Table 48 and Table 49 display the main gaseous product gas composition and additional product gas component, respectively. Table 50 illustrates the main gaseous flue gas composition of combustion reactor. Table 51 gives detailed information on the tar components measured by gas chromatography coupled with mass spectrometry (GC-MS).

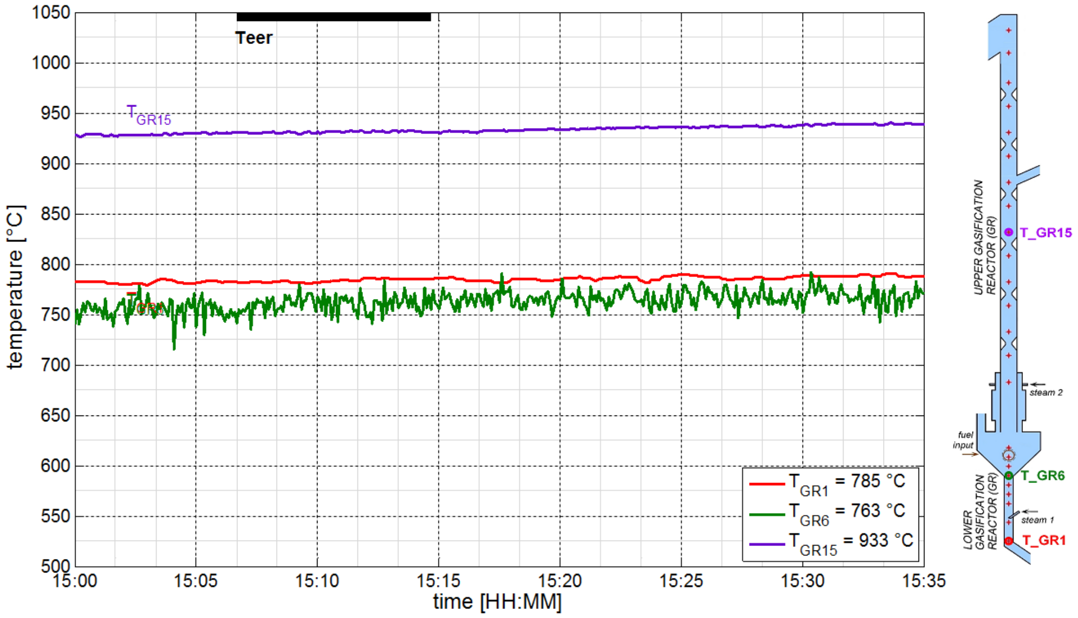

Figure 27: Overview on the temporal courses of gasification temperature for the gasification test run with softwood pellets and a mixture (90/10 wt.-%) of feldspar and calcite as bed material

Table 47: Main results and parameters; gasification of softwood with a mixture (90/10 wt.-%) of feldspar and calcite as bed material

Parameter/Name	Unit	Gasification reactor	Combustion reactor
Bed material types	µm	280 – 430 (feldspar), 300 – 500 (calcite)	
Bed material	wt.-%	90 (Feldspar) – 10 (Calcite)	
Overall initial bed material inventory	kg	80	
Feedstock type	-	softwood	-
Feedstock/fuel analysis no.	-	PL-15065-A	-
Feedstock mass flow	kg/h	20.4	-
Feedstock/fuel power into GR	kW	95.4	-
Fuel to CR	kW	-	61*
Heat losses of reactor system	kW	17*	12
Typical temperatures (lower reactor part)	°C	GR6 763	CR4 991
Typical temperatures (upper reactor part)	°C	GR15 933	CR7 942
Water content in the gas stream	vol.-%	35*	14*
Gasification steam to fuel ratio	$kg_{steam}/kg_{fuel,db,af}$	0.8 *	
Gasification steam to carbon ratio	$kg_{steam}/kg_{fuel,carbon}$	1.7*	
Product gas volume flow	Nm^3_{db}/h	25.7*	
Feedstock mass flow, dry & ash free	$kg_{,db,af}/h$	18.9	
Product gas yield	Nm^3_{db} $/kg_{fuel,db,af}$	1.36*	
Steam related H_2O conversion	kg_{H2O}/kg_{H2O}	0.29*	
Fuel related H_2O conversion	$kg_{H2O}/kg_{fuel,db,af}$	0.24*	
Product gas lower heating value (free of char & tar)	MJ/Nm^3_{db}	12.9*	
Product gas power (free of char & tar)	kW	92.2*	
Cold gas efficiency	%	96.6*	
Overall cold gas efficiency, novel 100kW test plant	%	58.9*	
Overall cold gas efficiency, estimated for a 50 MW plant	%	70 – 80	
Product gas, H_2 to CO ratio	-	1.5*	

* via calculation with IPSEpro mass & energy balance

Table 48: Main gaseous product gas composition; gasification of softwood pellets with a mixture (90/10 wt.-%) of feldspar and calcite as bed material; sample point A

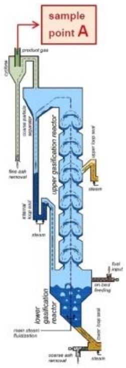

Product gas composition, sample point A				
Parameter	**Unit**	**NGA2000 online**	**PE Arnel GC TU Wien**	**IPSEpro simulation**
H_2 hydrogen	vol.-% $_{db}$	39.6	-	38.9
CO carbon monoxide	vol.-% $_{db}$	23.1	24.4	25.1
CO_2 carbon dioxide	vol.-% $_{db}$	19.7	21.4	20.8
CH_4 methane	vol.-% $_{db}$	11.1	11.6	11.8
C_2H_4 ethylene	vol.-% $_{db}$	-	2.06	2.01
C_2H_6 ethane	vol.-% $_{db}$	-	0.17	0.17
C_3H_8 propane	vol.-% $_{db}$	-	0.00	0.00

Additional gaseous product gas components			
Parameter	**Unit**	**Typical values**	**PE Arnel GC TU Wien**
N_2 nitrogen	vol.-% $_{db}$	0.5 – 2.0	1.13
Sum of C_4-.C_5-hydrocarbons, NH_3, H_2S, HCl& other comp.	vol.-% $_{db}$	0.1 – 2.0**	-

* value because of purging/flushing feedstock hoppers and temp.& press.-measuring points with nitrogen
** value range strongly depends on the fuel composition (see fuel analysis & optional offline gas analysis

Table 49: Additional product gas component; gasification of softwood pellets with a mixture (90/10 wt.-%) of feldspar and calcite as bed material; sample point A from test laboratory for combustion systems from TU Wien; offline tar measurement

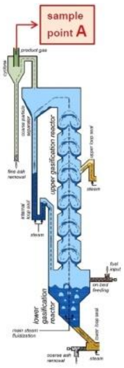

Product gas analytics, measured discontinuous, sample point A		
Parameter	**Unit**	**Solvent: toluene**
Dust content	g/Nm^3 $_{db}$	3.25
Char content	g/Nm^3 $_{db}$	1.88
Tar content GC-MS (without BTEX)	g/Nm^3 $_{db}$	13.386
Tar content BTEX	g/Nm^3 $_{db}$	16.781
Tar content gravimetric	g/Nm^3 $_{db}$	5.38
Water content, H_2O	vol.-%	39
Tar dew point*	°C	201.4

*calculated via http://www.thersites.nl/completemodel.aspx

Table 50: Main gaseous flue gas composition of the combustion reactor; gasification of softwood pellets with a mixture (90/10 wt.-%) of feldspar and calcite as bed material

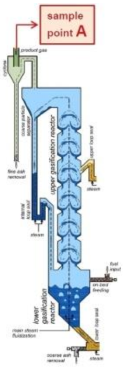

Flue gas composition			
Parameter	**Unit**	**NGA2000 online**	**IPSEpro simulation**
CO_2 carbon dioxide	vol.-% $_{db}$	13.83	15.14
O_2 oxygen	vol.-% $_{db}$	0.02	0.00
CO carbon monoxide	vol.-% $_{db}$	0.49	0.53
N_2 nitrogen	vol.-% $_{db}$	-	0.00
Ar argon	vol.-% $_{db}$	-	0.00
NO nitrogen monoxide	vol.-% ppm $_{db}$	10.2	0.00
SO_2 sulfur dioxide	vol.-% ppm $_{db}$	21.8	0.00
NO_2 nitrogen dioxide	vol.-% ppm $_{db}$	n.a.	0.00
N_2O nitrous oxide	vol.-% ppm $_{db}$	7.7	0.00

n.a.: not available

Table 51: GC-MS tar components of product gas; gasification of softwood pellets with a mixture (90/10 wt.-%) of feldspar and calcite as bed material

Solvent		**Toluene**
Total GC-MS (without BTEX)	**g/Nm³**	**13.386**
Pyridin	mg/Nm³	not measurable
2-Methylpyridin	mg/Nm³	0
Phenylacetylen	mg/Nm³	46
3- und 4-Methylpyridin	mg/Nm³	0
Styrol	mg/Nm³	383
Mesitylen	mg/Nm³	0
Phenol	mg/Nm³	0
Benzofuran	mg/Nm³	≤ 19
1H-Inden	mg/Nm³	1248
2-Methylphenol	mg/Nm³	0
4-Methylphenol	mg/Nm³	0
2-Methylbenzofuran	mg/Nm³	0
2,6-Dimethylphenol	mg/Nm³	0
2,5&2,4-Dimethylphenol	mg/Nm³	0
3,5-Dimethylphenol	mg/Nm³	0
2,3-Dimethylphenol	mg/Nm³	0
3,4-Dimethylphenol	mg/Nm³	0
2-Methoxy-4-Methylphenol	mg/Nm³	0
Naphthalin	mg/Nm³	4770
1-Benzothiophen	mg/Nm³	0
Chinolin	mg/Nm³	0
2-Methylnaphthalin	mg/Nm³	97
Isochinolin	mg/Nm³	0
1-Methylnaphthalin	mg/Nm³	52
Eugenol	mg/Nm³	0
1-Indanon	mg/Nm³	0
Indol	mg/Nm³	0
Biphenyl	mg/Nm³	152
1-Vinylnaphthalin	mg/Nm³	0
Isoeugenol	mg/Nm³	0
2-Vinylnaphthalin	mg/Nm³	83
Acenaphthylen	mg/Nm³	1760
Acenaphthen	mg/Nm³	36
Dibenzofuran	mg/Nm³	231
Fluoren	mg/Nm³	443
Dibenzothiophen	mg/Nm³	0
Anthracen	mg/Nm³	1679
Phenanthren	mg/Nm³	482
Carbazol	mg/Nm³	0
4,5-Mehtylphenanthren	mg/Nm³	129
9-Methylanthracen	mg/Nm³	0
Fluoranthen	mg/Nm³	668
Pyren	mg/Nm³	501
Benzo[a]anthracen	mg/Nm³	147
Chrysen	mg/Nm³	137
Benzo[b]fluoranthen	mg/Nm³	85
Benzo[k]fluoranthen	mg/Nm³	104
Benzo[e]pyren	mg/Nm³	62
Benzo[a]pyren	mg/Nm³	138
Perylen	mg/Nm³	19
Dibenz[a,h]anthracen	mg/Nm³	0
Benzo[g,h,i]perylen	mg/Nm³	53
Indeno[1,2,3-cd]pyren	mg/Nm³	45
Coronen	mg/Nm³	0
BTEX components	**g/Nm³**	**16.781**
Benzol	mg/Nm³	16781
Toluol	mg/Nm³	not measurable
Ethylbenzol	mg/Nm³	0
m- und p-Xylol	mg/Nm³	0
o-Xylol	mg/Nm³	0

4.5.1 Mixture (50/50 wt.-%) of feldspar and calcite

In this section, results from gasification test runs of softwood with a mixture (50/50 wt.-%) of feldspar and calcite as bed material in the advanced 100 kW_{th} pilot plant at TU Wien are presented. Figure 28 shows an overview on the temporal courses of gasification temperature in the gasification reactor (GR) at steady state operation during the softwood gasification process with a mixture (50/50 wt.-%) of feldspar and calcite as bed material. T_GR15 and T_GR 6 are the temperature at the top and bottom of the gasification reactor in the fluidized bed region, respectively. T_GR1 is the temperature at the bottom of the gasification reactor in the bubbling bed region. During the gasification operation, it was tried to measure the gas composition at the outlet of the gasification reactor (sample point A). Table 52 presents the main results and parameters of the gasification test run. Table 53 and Table 54 display the main gaseous product gas composition and additional product gas component, respectively. Table 55 illustrates the main gaseous flue gas composition of combustion reactor. Table 56 gives detailed information on the tar components measured by gas chromatography coupled with mass spectrometry (GC-MS).

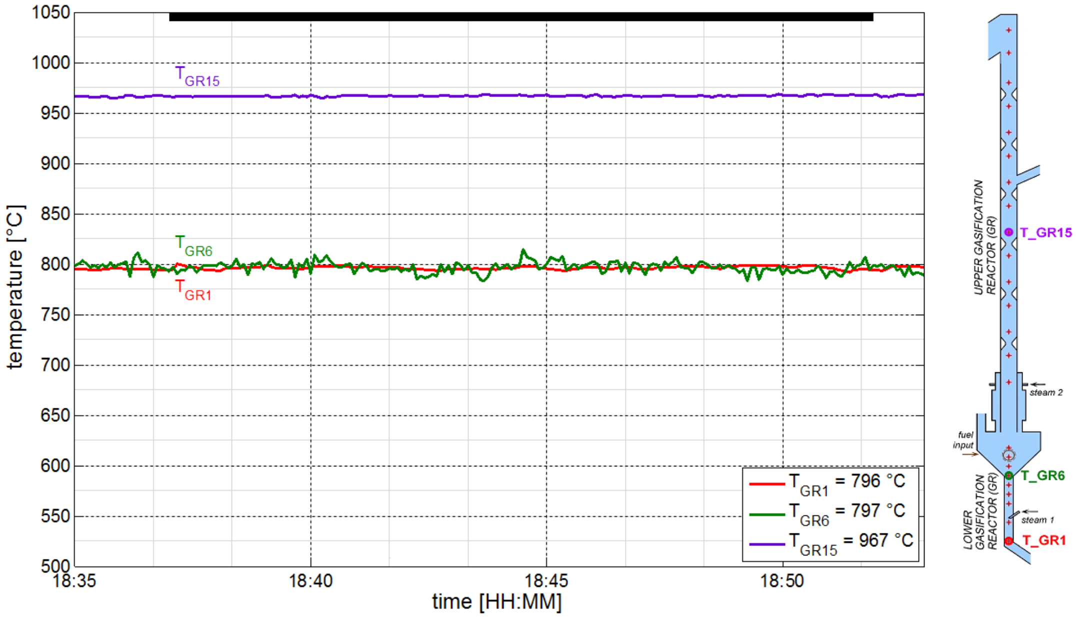

Figure 28: Overview on the temporal courses of gasification temperature; gasification of softwood pellets with a mixture (50/50 wt.-%) of feldspar and calcite as bed material

Table 52: Main results and parameters; gasification of softwood pellets with a mixture (50/50 wt.-%) of feldspar and calcite as bed material

Parameter	Unit	Gasification reactor	Combustion reactor
Bed material types	µm	280 – 430 (feldspar), 300 – 600 (calcite)	
Bed material	wt.-%	50 (feldspar), 50 (calcite)	
Overall initial bed material inventory	kg	80	
Feedstock type	-	softwood	-
Feedstock/fuel analysis no.	-	PL-15065-A	-
Feedstock mass flow	kg/h	21.3	-
Feedstock/fuel power into GR	kW	101	-
Fuel to CR	kW	-	44*
Heat losses of reactor system (GR & CR)	kW	20*	
Typical temperatures (lower reactor part)	°C	GR6 797	CR4 1057
Typical temperatures (upper reactor part)	°C	GR15 967	CR7 977
Water content in the gas stream	vol.-%	31*	11*
Gasification steam to fuel ratio	$kg_{steam}/kg_{fuel,db,af}$	0.8*	
Gasification steam to carbon ratio	$kg_{steam}/kg_{fuel,carbon}$	1.5*	
Product gas volume flow	Nm^3_{db}/h	28*	
Feedstock mass flow, dry & ash free	$kg_{,db,af}/h$	19.7	
Product gas yield	Nm^3_{db} $/kg_{fuel,db,af}$	1.44*	
Steam related H_2O conversion	kg_{H2O}/kg_{H2O}	0.33*	
Fuel related H_2O conversion	$kg_{H2O}/kg_{fuel,db,af}$	0.26*	
Product gas lower heating value (free of char & tar)	MJ/Nm^3_{db}	11.4*	
Product gas power (free of char & tar)	kW	90*	
Cold gas efficiency	%	89*	
Overall cold gas efficiency, novel 100kW test plant	%	62*	
Overall cold gas efficiency, estimated for a 50 MW plant	%	70 – 80	
Product gas, H_2 to CO ratio	-	2.1*	

* via calculation with IPSEpro mass & energy balance

Table 53: Main gaseous product gas composition; gasification of softwood pellets with a mixture (50/50 wt.-%) of feldspar and calcite as bed material; sample point A

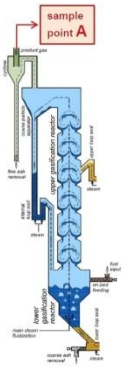

Product gas composition, sample point A				
Parameter	**Unit**	**NGA2000 online**	**PE Arnel GC TU Wien**	**IPSEpro simulation**
H_2 hydrogen	vol.-% $_{db}$	45.6	-	45.8
CO carbon monoxide	vol.-% $_{db}$	20.2	21.0	21.5
CO_2 carbon dioxide	vol.-% $_{db}$	19.5	20.4	20.9
CH_4 methane	vol.-% $_{db}$	8.63	9.21	9.13
C_2H_4 ethylene	vol.-% $_{db}$	-	0.64	0.69
C_2H_6 ethane	vol.-% $_{db}$	-	0.07	0.07
C_3H_8 propane	vol.-% $_{db}$	-	0.00	0.00

Additional gaseous product gas components			
Parameter	**Unit**	**Typical values**	**PE Arnel GC TU Wien**
N_2 nitrogen	vol.-% $_{db}$	0.5 – 2.0	1.62*
Sum of C_4-.C_5-hydrocarbons, NH_3, H_2S, HCl& other comp.	vol.-% $_{db}$	0.1 – 2.0**	-

* value because of purging/flushing feedstock hoppers and temp.& press.-measuring points with nitrogen
** value range strongly depends on the fuel composition (see fuel analysis & optional offline gas analysis)

Table 54: Additional product gas component; gasification of softwood pellets with a mixture (50/50 wt.-%) of feldspar and calcite as bed material; sample point A from test laboratory for combustion systems from TU Wien; offline tar measurement

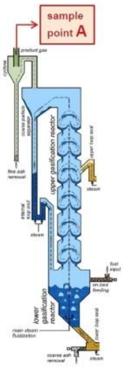

Product gas analytics, measured discontinuous, sample point A		
Parameter/Name	Unit	Solvent: toluene
Dust content	g/Nm^3 $_{db}$	7.9
Char content	g/Nm^3 $_{db}$	5.8
Tar content GC-MS (without BTEX)	g/Nm^3 $_{db}$	2.345
Tar content BTEX	g/Nm^3 $_{db}$	12.236
Tar content gravimetric	g/Nm^3 $_{db}$	0.58
Water content, H_2O	vol.-%	31
Tar dew point*	°C	104

*calculated via http://www.thersites.nl/completemodel.aspx

Table 55: Main gaseous flue gas composition of the combustion reactor; gasification of softwood pellets with a mixture (50/50 wt.-%) of feldspar and calcite as bed material

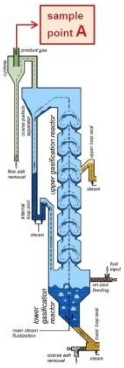

Flue gas composition			
Parameter	**Unit**	**NGA2000 online**	**IPSEpro simulation**
CO_2 carbon dioxide	vol.-% $_{db}$	12.28	13.37
O_2 oxygen	vol.-% $_{db}$	2.85	3.89
CO carbon monoxide	vol.-% $_{db}$	0.0	0.0
N_2 nitrogen	vol.-% $_{db}$	-	81.78
Ar argon	vol.-% $_{db}$	-	0.95
NO nitrogen monoxide	vol.-% ppm $_{db}$	n.a.	0.0
SO_2sulfur dioxide	vol.-% ppm $_{db}$	n.a.	0.0
NO_2nitrogen dioxide	vol.-% ppm $_{db}$	n.a.	0.0
N_2O nitrous oxide	vol.-% ppm $_{db}$	n.a.	0.0

Table 56: GC-MS tar components of product gas; gasification of softwood pellets with a mixture (50/50 wt.-%) of feldspar and calcite as bed material

Solvent		**Toluene**
Total GC-MS (without BTEX)	**g/Nm³**	**2.345**
2-Methylpyridin	mg/Nm³	0
Phenylacetylen	mg/Nm³	0
3- und 4-Methylpyridin	mg/Nm³	0
Styrol	mg/Nm³	37
Mesitylen	mg/Nm³	0
Phenol	mg/Nm³	0
Benzofuran	mg/Nm³	0
1H-Inden	mg/Nm³	47
2-Methylphenol	mg/Nm³	0
4-Methylphenol	mg/Nm³	0
2-Methylbenzofuran	mg/Nm³	0
2,6-Dimethylphenol	mg/Nm³	0
2,5&2,4-Dimethylphenol	mg/Nm³	0
3,5-Dimethylphenol	mg/Nm³	0
2,3-Dimethylphenol	mg/Nm³	0
3,4-Dimethylphenol	mg/Nm³	0
2-Methoxy-4-Methylphenol	mg/Nm³	0
Naphthalin	mg/Nm³	1656
1-Benzothiophen	mg/Nm³	0
Chinolin	mg/Nm³	0
2-Methylnaphthalin	mg/Nm³	0
Isochinolin	mg/Nm³	0
1-Methylnaphthalin	mg/Nm³	0
Eugenol	mg/Nm³	0
1-Indanon	mg/Nm³	0
Indol	mg/Nm³	0
Biphenyl	mg/Nm³	12
1-Vinylnaphthalin	mg/Nm³	0
Isoeugenol	mg/Nm³	0
2-Vinylnaphthalin	mg/Nm³	0
Acenaphthylen	mg/Nm³	231
Acenaphthen	mg/Nm³	22
Dibenzofuran	mg/Nm³	0
Fluoren	mg/Nm³	10
Dibenzothiophen	mg/Nm³	0
Anthracen	mg/Nm³	204
Phenanthren	mg/Nm³	24
Carbazol	mg/Nm³	0
4,5-Mehtylphenanthren	mg/Nm³	0
9-Methylanthracen	mg/Nm³	0
Fluoranthen	mg/Nm³	56
Pyren	mg/Nm³	47
Benzo[a]anthracen	mg/Nm³	0
Chrysen	mg/Nm³	≤ 3
Benzo[b]fluoranthen	mg/Nm³	0
Benzo[k]fluoranthen	mg/Nm³	0
Benzo[e]pyren	mg/Nm³	0
Benzo[a]pyren	mg/Nm³	0
Perylen	mg/Nm³	0
Dibenz[a,h]anthracen	mg/Nm³	0
Benzo[g,h,i]perylen	mg/Nm³	0
Indeno[1,2,3-cd]pyren	mg/Nm³	0
Coronen	mg/Nm³	0
BTEX components	**g/Nm³**	**12.236**
Benzol	mg/Nm³	12236
Toluol	mg/Nm³	not measurable
Ethylbenzol	mg/Nm³	0
m- und p-Xylol	mg/Nm³	0
o-Xylol	mg/Nm³	0

4.6 Discussion

Comparison of influence of used different bed materials during this work as well as effect of calcite admixture to different bed material in the various mass ratios on the performance of DFB steam gasification is presented in this section.

4.6.1 100 wt.-% olivine to 100 wt.-% calcite as bed material

Figure 29 and Figure 30 illustrate the product gas composition as well as the related tar content (consisting of GC-MS tar and gravimetric tar) and calculated tar dew point for gasification of softwood and different mass ratios from 100 wt.-% olivine to 100 wt.-% calcite as bed material. Tar is measured discontinuously by isokinetically taking samples with impinger bottles to condense and dissolve the condensable hydrocarbons. The heavy (high molecular weight) tar compounds represent the mass of tar, which is left after vacuum evaporation of the solvent. These compounds were quantified as gravimetric tar. Tar compounds with a medium molecular weight, like naphthalene, were analyzed by a gas chromatograph coupled with mass spectrometry (GC-MS). The tar dew point is defined as an important value for fouling as well as for long-term operation of biomass gasification systems regarding the impact on downstream equipment. The tar dew points of the detected GC-MS tar compounds were calculated with the calculation tool from the Energy Research Centre of the Netherlands (ECN) [Milne T. A. et al., 1998].

100 wt.-% olivine as bed material caused the product gas, which consisted of the lowest H_2, the lowest CO_2 and the highest CO content compared to other mass ratios of olivine. By increasing the calcite content in the mixture with olivine, the H_2 content enhanced. The maximum value of H_2 was obtained via 100 wt.-% calcite as bed material. In parallel, the CO content decreased. This behavior can be explained by a strong influence of calcium oxide on the enhancement of the homogeneous water gas shift reaction (see Eq. 9) and homogeneous steam reforming reactions (see Eq. 11). The lowest gravimetric tar, GC-MS tar and calculated tar dew point contents were observed by the use of 100 wt.-% calcite as bed material. The CH_4 content had a slightly decreasing by increseing calcite content as bed material. Adding calcite to olivine caused an increasing of CO_2 content, but this increasing remained relatively stable afterwards. Additionally, there was a significiant reduction in the C_2H_4 content, which can be a good indicator for the GC-MS tar content in the product gas [Kitzler H., 2013 and Kern S., 2013]. Consequently, increasing the calcite content in mixing with olivine as bed material leaded to the product gas whit the lowest content of GC-MS tar, gravimetric tar and calculated tar dew point as well as the highest H_2 content.

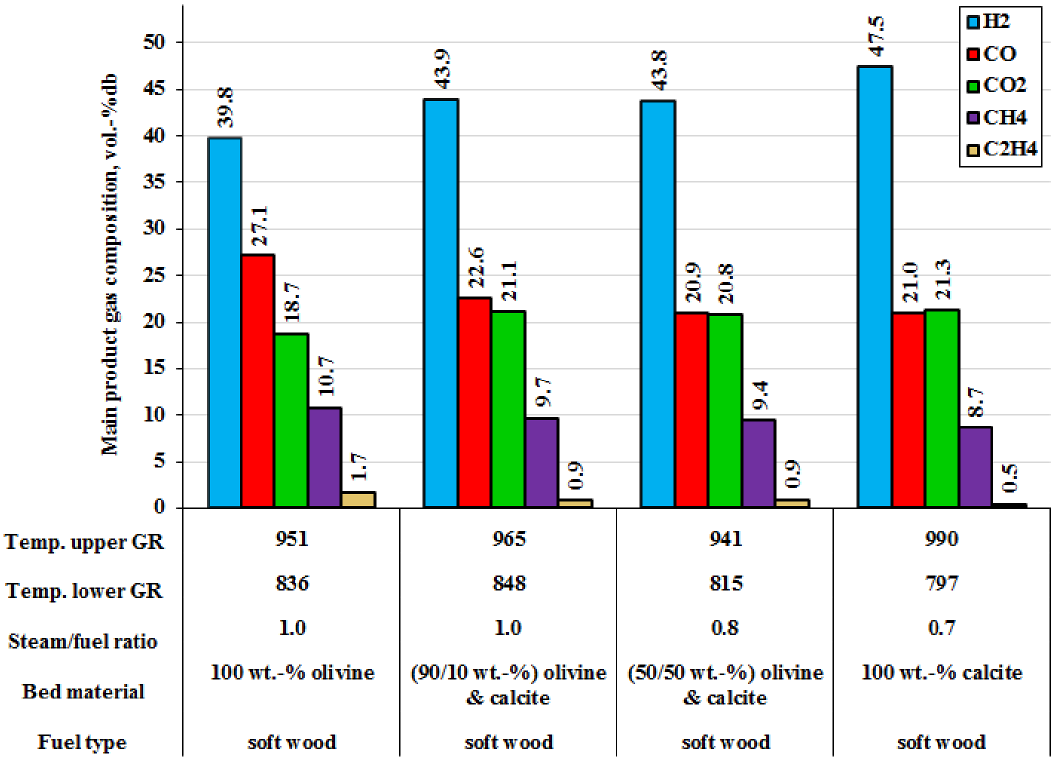

Figure 29: Comparison of product gas composition; gasification of softwood with 100 wt.-% olivine to 100wt.-% calcite as bed material

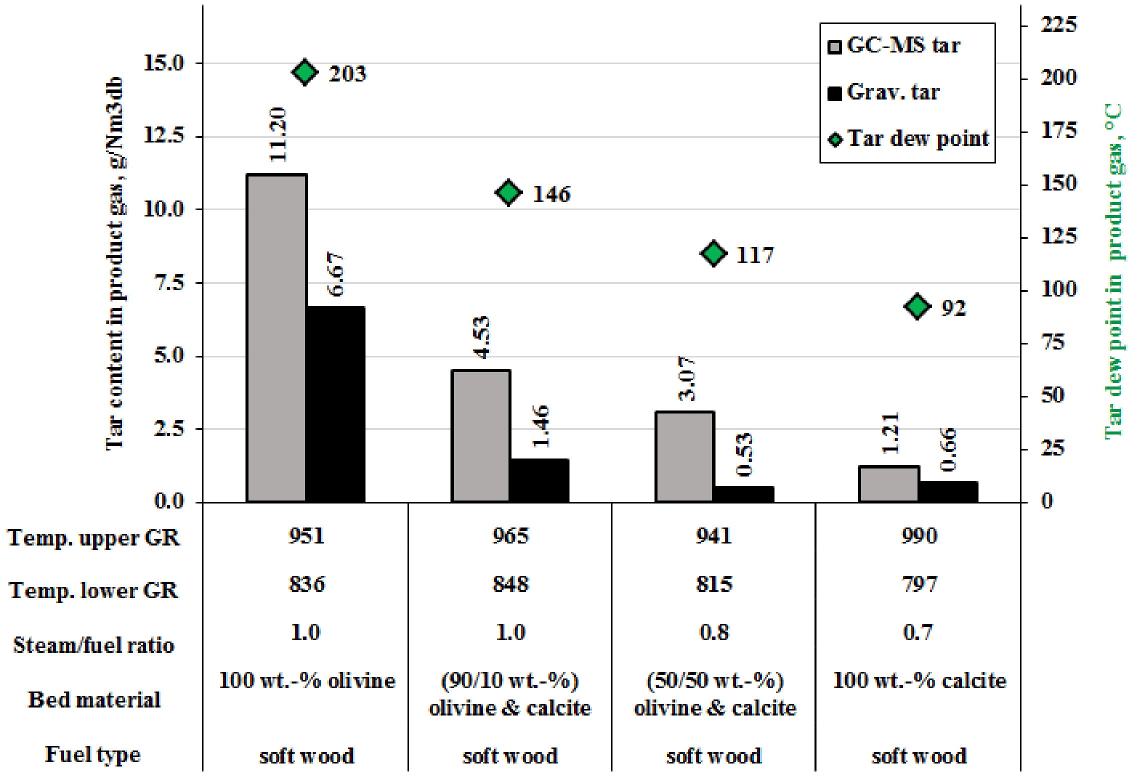

Figure 30: Comparison of tar content and calculated tar dew point of the product gas; gasification of softwood with 100 wt.-% olivine to 100wt.-% calcite as bed material

4.6.2 100 wt.-% silica sand to 100 wt.-% calcite as bed material

Figure 31 and Figure 32 illustarte the product gas composition as well as the related tar content (consisting of GC-MS tar and gravimetric tar) and calculated tar dew point for gasification of softwood and different mass ratios from 100 wt.-% silica sand to 100 wt.-% calcite as bed material. Tar is measured discontinuously by isokinetically taking samples with impinger bottles to condense and dissolve the condensable hydrocarbons. The heavy (high molecular weight) tar compounds represent the mass of tar, which is left after vacuum evaporation of the solvent. These compounds were quantified as gravimetric tar. Tar compounds with a medium molecular weight, like naphthalene, were analyzed by a gas chromatograph coupled with mass spectrometry (GC-MS). The tar dew point is defined as an important value for fouling as well as for long-term operation of biomass gasification systems regarding the impact on downstream equipment. The tar dew points of the detected GC-MS tar compounds were calculated with the calculation tool from the Energy Research Centre of the Netherlands (ECN) [Milne T. A. et al., 1998].

100 wt.-% silica sand as bed material caused the product gas, which consisted of the lowest H_2, the lowest CO_2 and the highest CO content compared to other mass ratios of silica sand. By increasing the calcite content in the mixture with silica sand, the H_2 content enhanced. The maximum value of H_2 was obtained via 100 wt.-% calcite as bed material. In parallel, the CO content decreased. This behavior can be explained by a strong influence of calcium oxide on the enhancement of the homogeneous water gas shift reaction (see Eq. 9) and homogeneous steam reforming reactions (see Eq. 11). The lowest gravimetric tar, GC-MS tar and calculated tar dew point contents were observed by the use of 100 wt.-% calcite as bed material. The CH_4 content had a slightly decreasing by increseing calcite content as bed material. Adding calcite to silica sand caused an increasing of CO_2 content, but this increasing remained relatively stable afterwards. Additionally, there was a significiant reduction in the C_2H_4 content, which can be a good indicator for the GC-MS tar content in the product gas [Kitzler H., 2013 and Kern S., 2013]. Consequently, increasing the calcite content in mixing with silica sand as bed material leaded to the product gas whit the lowest content of GC-MS tar, gravimetric tar and calculated tar dew point as well as the highest H_2 content.

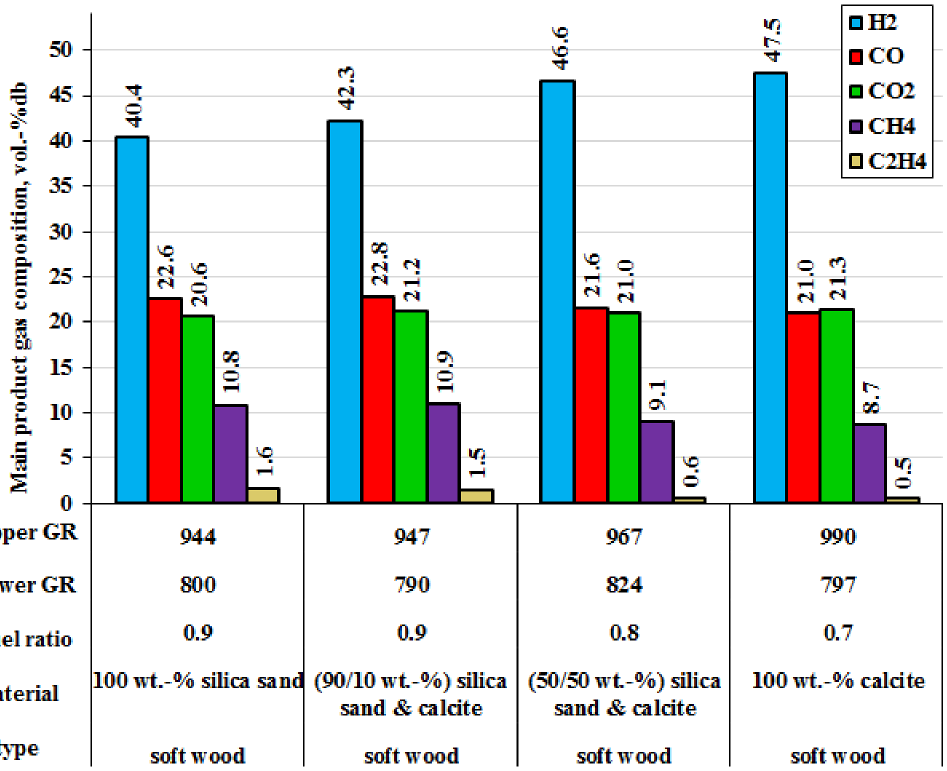

Temp. upper GR	944	947	967	990
Temp. lower GR	800	790	824	797
Steam/fuel ratio	0.9	0.9	0.8	0.7
Bed material	100 wt.-% silica sand	(90/10 wt.-%) silica sand & calcite	(50/50 wt.-%) silica sand & calcite	100 wt.-% calcite
Fuel type	soft wood	soft wood	soft wood	soft wood

Figure 31: Comparison of product gas composition; gasification of softwood with 100 wt.-% silica sand to 100wt.-% calcite as bed material

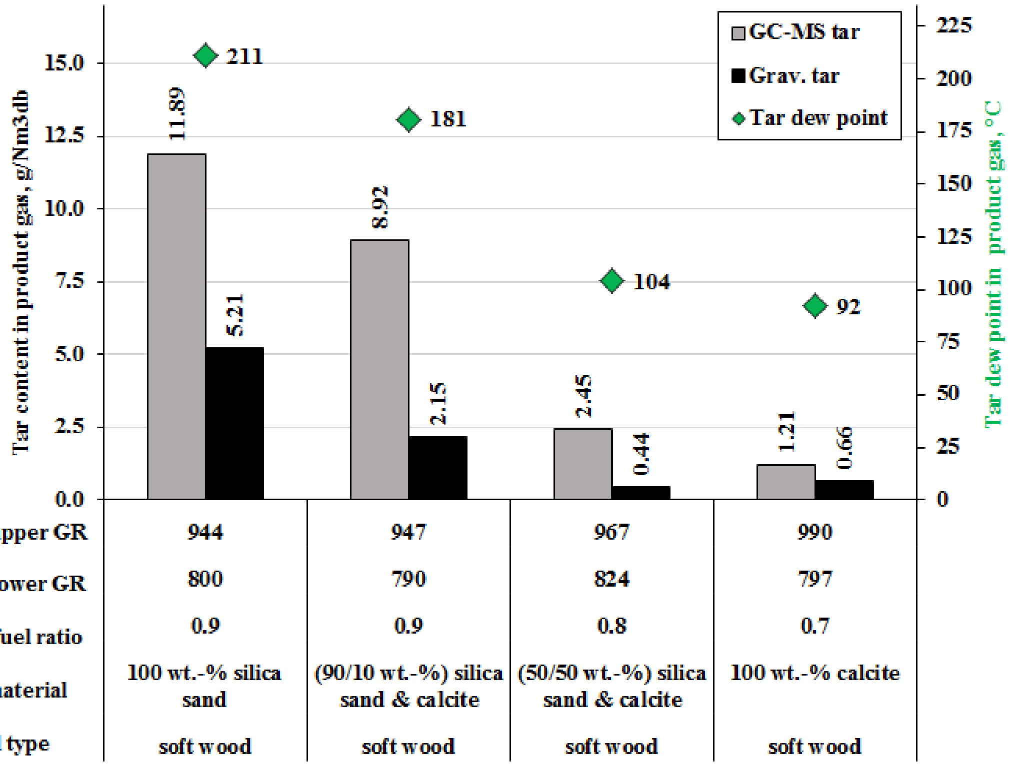

Temp. upper GR	944	947	967	990
Temp. lower GR	800	790	824	797
Steam/fuel ratio	0.9	0.9	0.8	0.7
Bed material	100 wt.-% silica sand	(90/10 wt.-%) silica sand & calcite	(50/50 wt.-%) silica sand & calcite	100 wt.-% calcite
Fuel type	soft wood	soft wood	soft wood	soft wood

Figure 32: Comparison of tar content and calculated tar dew point of the product gas; gasification of softwood with 100 wt.-% silica sand to 100wt.-% calcite as bed material

4.6.3 100 wt.-% feldspar to 100 wt.-% calcite as bed material

Figure 33 and Figure 34 illustarte the product gas composition as well as the related tar content (consisting of GC-MS tar and gravimetric tar) and calculated tar dew point for gasification of softwood and different mass ratios from 100 wt.-% feldspar to 100 wt.-% calcite as bed material. Tar is measured discontinuously by isokinetically taking samples with impinger bottles to condense and dissolve the condensable hydrocarbons. The heavy (high molecular weight) tar compounds represent the mass of tar, which is left after vacuum evaporation of the solvent. These compounds were quantified as gravimetric tar. Tar compounds with a medium molecular weight, like naphthalene, were analyzed by a gas chromatograph coupled with mass spectrometry (GC-MS). The tar dew point is defined as an important value for fouling as well as for long-term operation of biomass gasification systems regarding the impact on downstream equipment. The tar dew points of the detected GC-MS tar compounds were calculated with the calculation tool from the Energy Research Centre of the Netherlands (ECN) [Milne T. A. et al., 1998].

100 wt.-% feldspar as bed material caused the product gas, which consisted of the lowest H_2, the lowest CO_2 and the highest CO content compared to other mass ratios of feldspar. By increasing the calcite content in the mixture with feldspar, the H_2 content enhanced. The maximum value of H_2 was obtained via 100 wt.-% calcite as bed material. In parallel, the CO content decreased. This behavior can be explained by a strong influence of calcium oxide on the enhancement of the homogeneous water gas shift reaction (see Eq. 9) and homogeneous steam reforming reactions (see Eq. 11). The lowest gravimetric tar, GC-MS tar and calculated tar dew point contents were observed by the use of 100 wt.-% calcite as bed material. The CH_4 content had a slightly decreasing by increseing calcite content as bed material. Adding calcite to feldspar caused an increasing of CO_2 content, but this increasing remained relatively stable afterwards. Additionally, there was a significiant reduction in the C_2H_4 content, which can be a good indicator for the GC-MS tar content in the product gas [Kitzler H., 2013 and Kern S., 2013]. Consequently, increasing the calcite content in mixing with faldspar as bed material leaded to the product gas whit the lowest content of GC-MS tar, gravimetric tar and calculated tar dew point as well as the highest H_2 content.

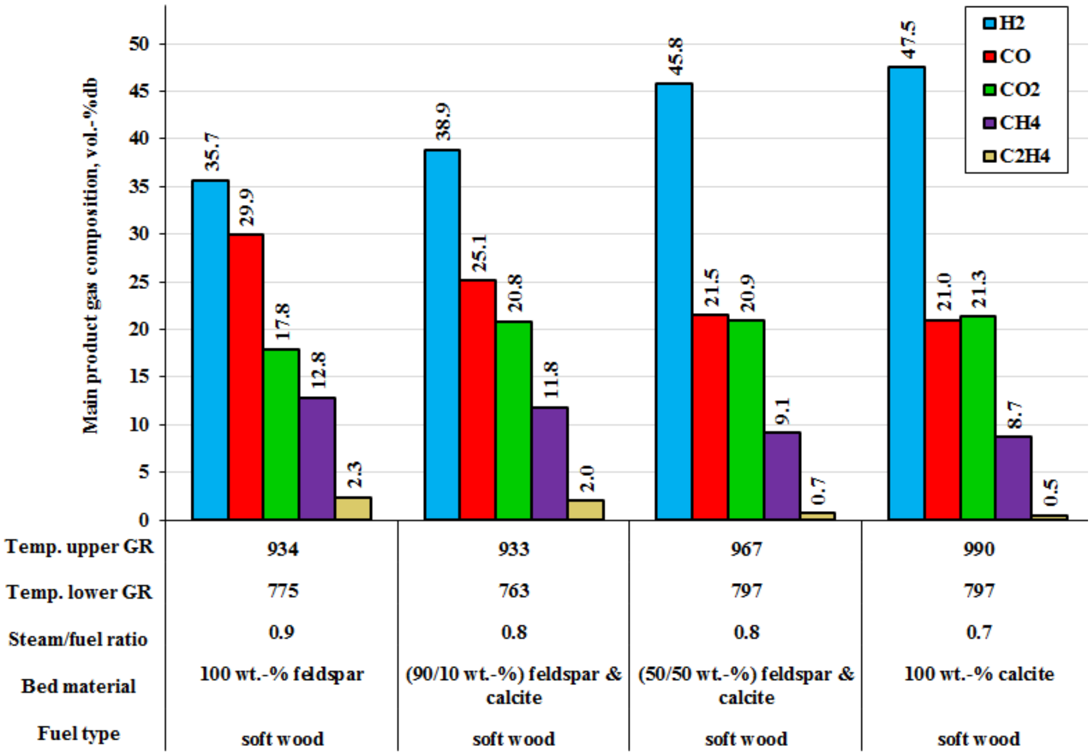

Temp. upper GR	934	933	967	990
Temp. lower GR	775	763	797	797
Steam/fuel ratio	0.9	0.8	0.8	0.7
Bed material	100 wt.-% feldspar	(90/10 wt.-%) feldspar & calcite	(50/50 wt.-%) feldspar & calcite	100 wt.-% calcite
Fuel type	soft wood	soft wood	soft wood	soft wood

Figure 33: Comparison of product gas composition; gasification of softwood with 100 wt.-% feldspar to 100wt.-% calcite as bed material

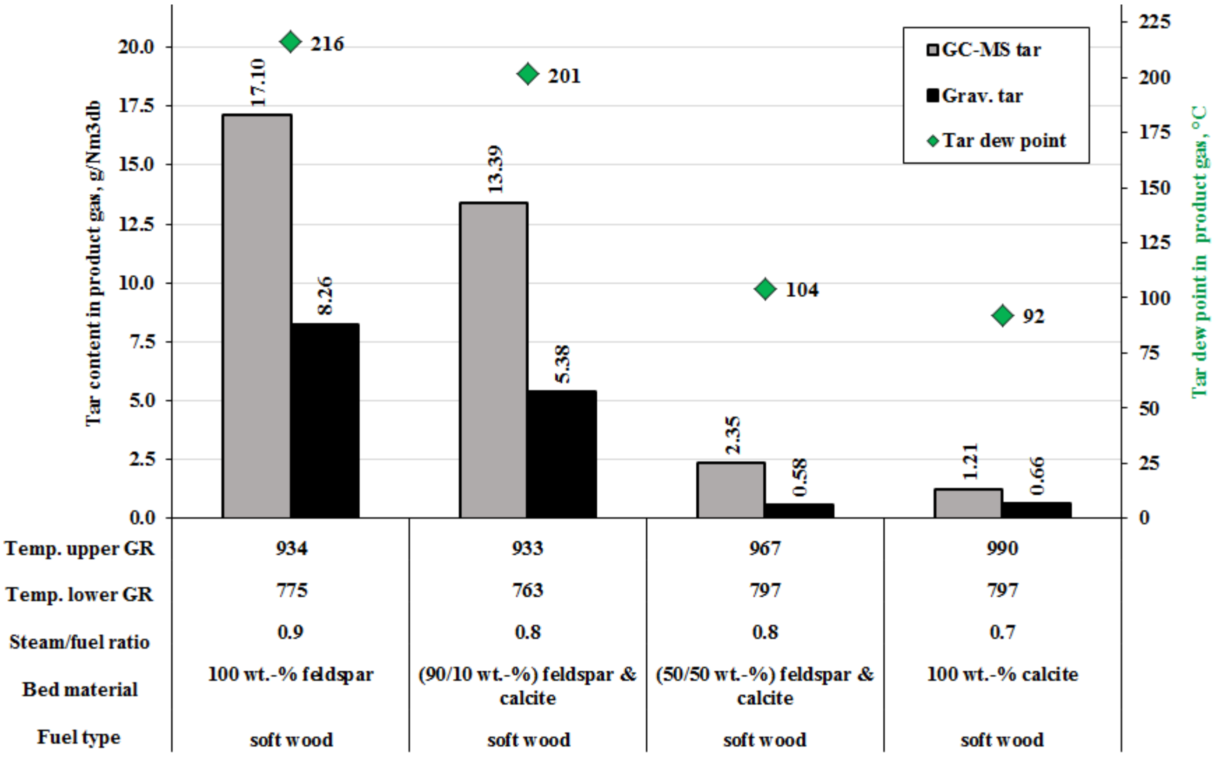

Temp. upper GR	934	933	967	990
Temp. lower GR	775	763	797	797
Steam/fuel ratio	0.9	0.8	0.8	0.7
Bed material	100 wt.-% feldspar	(90/10 wt.-%) feldspar & calcite	(50/50 wt.-%) feldspar & calcite	100 wt.-% calcite
Fuel type	soft wood	soft wood	soft wood	soft wood

Figure 34: Comparison of tar content and calculated tar dew point of the product gas; gasification of softwood with 100 wt.-% feldspar to 100wt.-% calcite as bed material

5 Conclusion and outlook

The current work presented obtained experimental data from ten gasification test runs, which were performed with the advanced 100 kW_{th} DFB steam gasification pilot plant at TU Wien. The aim of this study was to investigate the effect of different pure bed materials as well as the influence of calcite admixtures to other bed materials on the performance of DFB steam gasification. In this respect, olivine, silica sand and feldspar were mixed with calcite in mass ratios of 100/0, 90/10, 50/50 and 0/100. The behavior of calcite as bed material showed positive effects in the DFB gasifier system for steam gasification of softwood pellets. The transformation of calcite ($CaCO_3$) to calcium oxide (CaO) at high temperatures in the reactor system improved the water-gas-shift (WGS) reaction (see Eq. 9) as well as steam reforming of tars (see Eq. 11) inside the gasification reactor. The high catalytic activity of calcite shifted the product gas compositions towards higher hydrogen (H_2) and carbon dioxide (CO_2) and lower carbon monoxide (CO) contents as well as lower tar content (GC-MS tar and gravimetric tar) and lower calculated tar dew points. The investigations showed, that when 100 wt.-% olivine, silica sand or feldspar were used as bed material, thermal effects played a major role regarding tar cracking in the upper gasification reactor. When calcite was added, tar reduction was not only supported by thermal destruction, but also by the favorable catalytic activity of CaO. Calcite, silica sand and feldspar are cheap and worldwide available compared to olivine as bed material currently used in industrial-scale DFB steam gasification plants. Thus, the presented alternative bed materials are predestined for the DFB steam gasification process. In combination with calcite, the missing catalytic properties of alternative bed materials can be balanced and a promising and suitable bed material mixture can be obtained to produce a high-valuable product gas. Summarizing, the positive effects of calcite are as follow:

- Enhancement of catalytic activity by converting calcite into calcium oxide at high temperatures based on the calcination reaction: $\mathrm{CaCO_3} \leftrightarrow \mathrm{CaO} + \mathrm{CO_2}$.
- Increase of hydrogen (H_2) content in the product gas and increase of H_2/CO ratio.
- Decrease of ethylene (C_2H_4) in the product gas, which is a marker for the tar content.
- Significant decrease of GC-MS tar, gravimetric tar and calculated tar dew points.
- The highest H_2 (47.5 vol.-$\%_{db}$) and the lowest tar content (GC-MS: 1.21 g/Nm^3 and grav.: 0.66 g/Nm^3) in the product gas were reached by using pure calcite as bed material.
- Alternative bed materials (silica sand, feldspar, calcite) are cheap and worldwide available.
- No operational limitations occure with the pilot plant at TU Wien (using gravity separators) by using soft bed material such as calcite.
- More investigations are needed on the abrasion resistance for soft bed materials such as calcite for long-term use.

6 Notation

6.1 Abbreviations

Abbreviation	**Description**
af	Ash free
BTEX	Benzol, Tluol, Ethylbenzo and Xylole
CR	Combustion Reactor
daf	Dry and ash free
db	Dry base
DFB	Dual fluidized bed
Eq	Equation
GC-MS	Gas Chromatography coupled with Mass Spectrometry
GR	Gasification Reactor
ILS	Internal Loop Seal
IPSEpro	Process simulation software manufactured by Simtech
LHV	Lower Heating Value
LLS	Lower Loop Seal
Nm^3	Gas cubic meter according to standard conditions (0 °C, 1.013 bar_{abs})
Nm^3_{db}	Gas cubic meter according to standard conditions (0 °C, 1.013 bar_{abs}) on dry basis
Temp	Temparature
ULS	Upper Loop Seal
vol.-%	Percentage by volume
vol.-$\%_{db}$	Percentage by volume on dry basis
wt.-%	Percentage by weight
wt.-$\%_{db}$	Percentage by weight on dry basis

6.2 Symbols

Symbol	Description	Unit
A	Free cross section of the fluidized bed	m^2
A_c	Constricted cross section	m^2
A_c/A	Aperture ratio	-
A_{cs}	Free cross section of the fluidized bed	m^2
A_p	Particle surface	m^2
Ar	Archimedes number	-
C	Carbon	mol
C_2H_4	Ethylene	mol
C_2H_6	Ethane	mol
C_3H_8	Propane	mol
CH_4	Methane	mol
CO	Carbon monoxide	mol
CO_2	Carbon dioxide	mol
C_xH_y	Hydrocarbon, general	mol
$C_xH_yO_z$	Carbonic fuel with oxygen-content, general	mol
d_i	Particle mean diameter of fraction i	µm
d_p	Particle diameter	µm
d_p*	Dimensionless particle diameter	-
$dp/\Delta H$	Pressure gradient	
d_s	Particle surface diameter	µm
d_{sv}	Sauter diameter	µm
d_v	Particle volume diameter	µm
g	Gravity constant, g = 9.81	m/s^2
H	Height of bed	m
H_2	Hydrogen	mol
H_2O	Water	mol
H_L	Height of the layer at the relaxation point	m
i	Number of fraction	-
M	Mass of the total particles	kg
m_f	Mass of dry substance	kg
m_w	Mass of water	kg
N	A known number of particles	-
N_2	Nitrogen	mol
n_i	Number of particles in fraction i	-

O_2	Oxygen	mol
P	Pressure	bar
Re	Reynolds number	-
Re_{c_av}	Reynolds number of U_{c_av}	-
Re_{mf}	Reynolds number of U_{mf}	-
Re_{se}	Reynolds number of U_{se}	-
T	Temperature	°C
U	Velocity	m/s
U*	Dimensionless superficial gas velocity	-
U_0	Superficial gas velocity	m/s
U_c	Critical fluidisation velocity	m/s
U_{mb}	Minimum bubbling velocity	m/s
U_{mf}	Minimum fluidisation velocity	m/s
U_{se}	Fluidisation velocity with significant entrainment of solids	m/s
U_t	Terminal velocity of a single particle	m/s
V_b	Volume of particle matter/fluidised bed	m^3
V_p	Particle volume	m^3
$\dot{V}_g$	Fluidization volume flow	m^3/s
w	Water content	wt.-%
ΔH	Height difference	m
ΔP	Pressure drop	bar
ΔP_b	Pressure drop across a fluidised bed	bar
ε	Void fraction	-
ε_L	Porosity at the relaxation point	-
μ_g	Dynamic gas viscosity	Pa s
ν	Kinematic gas viscosity	m^2/s
ν	Kinematic gas viscosity	m^2/s
π	π number (3.141)	
ρ_g	Gas density	kg/m^3
ρ_p	Particle density	kg/m^3
$(\rho_p-\rho_g)/\rho_g$	Dimensionless density ratio	-
φ	Sphericity of a particle	-
ϕ	Particle volume fraction	-

7 List of Tables

8 List of Figures

9 References

Ammendola P., Chirone R., Ruoppolo G., (2013), “The effect of pelletization on the attrition of wood under fluidized bed combustion and gasification conditions”, in: Proceedings of the Combustion Institute, Vol. 34, pp. 2735-2740

Basu P., (2010), “Book: Biomass Gasification and Pyrolysis: Practical Design and Theory”, Academic press

Benedikt, F., Schmid, J. C., Hofbauer, H., (2017), "Enhanced Dual Fluidized Bed Gasification Using Calcium Oxide as Bed Material", in: Proceedings of the 13th Minisymposium Chemical & Process Engineering, 29 – 30 March 2017, Management Center, Innsbruck, Austria

Bi H. T. and Grace J. R., (1995), “Flow regime diagrams for gas-solid fluidization and upward transport”, International Journal of Multiphase Flow, Vol. 21, No.6, pp. 1229 – 1236

BP, “BP Statistical Review of World Energy”, (2017), 66th edition, available online: bp.com/statisticalreview

Geldart D., (1972), “Types of gas fluidization”, Powder Technology, Vol. 7, pp. 285 – 292

Grace J. R., (1986), “Contacting modes and behavior classification of gas-solid and other two-phase suspensions”, Canadian Journal of Chemical Engineering, Vol. 64, pp. 353 – 363

Grace J. R., Avidan A. A., Knowlton T. M., (1997), “Book: Circulating Fluidized Beds”, Chapman & Hall

Haapala K. R., Sessions J. and Murthy G. S., (2017), “A review and future directions in techno-economic modeling and optimization of upstream forest biomass to bio-oil supply chains”, Renewable & Sustainable Energy Reviews, Vol. 67, pp. 15 – 35

Hofbauer H., (2017), “Skriptum Vorlesung Wirbelschichttechnik“, Institute of Chemical Engineering at TU Wien, Academic press

Hofbauer H., Stoiber H. and Veronik G., (1995), “Gasification of organic material in a novel fluidized bed system”, in: Proceedings of the first SCEJ Symposium on Fluidization, Tokyo, Japan, pp. 291 – 299

Hofbauer H., Veronik G., Fleck T., Rauch R., (1997), “The FICFB - gasification process”, in: Bridgewater A. V., Boocock D., “Developments in thermochemical biomass conversion”, United Kingdom

IEA, International Energy Agency, (2017), www. iea.org

IPCC, Intergovernmental Panel on Climate Change, (2011), “Special reports on renewable energy sources: Summary for policy makers”, in Proceedings of the 11th Session of Working Group III of the IPCC, 5 – 8 May 2011, Abu Dhabi, United Arab Emirates

Jahnig C. E., Campbell D. L., Martin H. Z., (1980),“History of fluidized solids development at Exxon”, Springer publisher, Plenum Press, New York, doi: 0.1007/978-1-4684-1045-7, pp. 3 – 24

Kaltschmitt M., Hartmann H., Hofbauer H., (2009), “Energie aus Biomasse“, Springer publisher, Vienna, doi: 10.1007/978-3-540-85095-3

Kaushal P., Pröll T. and Hofbauer H., (2008), “Model for biomass char combustion in the riser of a dual fluidized bed gasification unit: Part 1 – Model development and sensitivity analysis", Fuel Processing Technology, Vol. 89, pp. 651 – 659

Kern S., (2013), "Gasification and co-gasification of coal, biomass and plastics in a dual fluidized bed System", Ph.D. thesis, Institute of Chemical, Biological and Environmental Engineering, TU Wien

Kern S., Pfeifer C., Hofbauer H., (2013), "Gasification of wood in a dual fluidized bed gasifier: Influence of fuel feeding on process performance", Chemical Engineering Science, Vol. 90, pp. 284–298

Kirnbauer F. and Hofbauer H., (2013), "The mechanism of bed material coating in dual fluidized bed biomass steam gasification plants and its impact on plant optimization", Powder Technology, Vol. 245, pp. 94 – 104

Kitzler H., (2013), "Zweibettwirbelschicht-Dampfvergasung von biogenen, ascheintensiven Brenn- und Reststoffen: Einfluss der Asche auf den Prozess", Ph.D. thesis, Institute of Chemical, Biological and Environmental, TU Wien

Koppatz S., Hofbauer H. and Pfeiffer C., (2011), "Steam gasification of various feedstocks at a dual fluidized bed gasifier: Impacts of operation conditions and bed materials", Biomass Conversion and Biorefinery, Vol. 1, pp. 39 – 53

Kunii D. and Levenspiel O., (1991), "Book: Fluidization Engineering", Butterworth-Heinemann publisher, 2nd. Edition, USA, ISBN: 978-0-08-050664-7

Kunii D. and Levenspiel, O., (1997), "Circulating fluidized-bed reactors", Chemical Engineering Science, Vol. 52, pp. 2471 – 2482

Levenspiel O., (1998), "Chemical Reaction Engineering", 3rd Edition, ISBN: 978-0-471-25424-9

Lim, K. S., Zhu, J. X., Grace, J. R., (1995), "Hydrodynamics of gas-solid fluidization", Multiphase Flow, Vol. 21, pp. 141 – 193

Mauerhofer, A.M., Benedikt, F., Schmid, J.C. and Hofbauer, H., (2017), "Mixtures of Silica Sand and Calcite as Bed Material for Dual Fluidized Bed Steam Gasification", in: Proceedings of the 10th International Conference on Sustainable Energy & Environmental Protection, 27 – 30 June 2017, Bled, Slovenia

Milne T. A., Abatzoglou N. and Evans R. J., (1998), "Biomass gasifier 'tars': their nature, formation, destruction, and tolerance limits in energy conversion devices", Fuel and energy Abstracts, Vol. 40, pp. 49 – 50

Molina A. and Mondrago F., (1998), "Reactivity of coal gasification with steam and CO_2", Fuel, Vol. 77, pp. 1831 – 1839

Overend R. P., (2002), "Bioenergy production and environmental protection", in: Workshop Proceedings, World Renewable Energy Congress, Cologne, Germany

Parikka M., (2004), "Global biomass fuel resources", Biomass Bioenergy, England, Vol. 27, pp. 613 – 620

Pasteiner H. A., (2015), "Cold Flow Investigations on a Novel Dual Fluidized Bed Steam Gasification Test Plant", Master thesis, TU Wien

Rapagna S., Jand N., Kiennemann A. and Foscolo P. U., (2000), "Steam-gasification of biomass in a fluidized-bed of olivine particles", Biomass Bioenergy, Vol. 19, pp. 187 – 197

Ruiz J. C., Juarez M. C., Morales M. P., Munoz P. and Mendivil M. A., (2013), “Biomass gasification for electricity generation: review of current technology barriers”, Renewable and Sustainable Energy Reviews, Vol. 18, pp. 174 – 183

Schmid J. C., (2014), “Development of a novel dual fluidized bed gasification system for increased fuel flexibility”, Doctoral thesis, TU Wien

Schmid J. C., Wolfesberger U., Koppatz S., Pfeifer C., and Hofbauer H., (2012a), “Variation of Feedstock in a Dual Fluidized Bed Steam Gasifier-Influence on Product Gas, Tar Content, and Composition”, TU Wien, Institute of Chemical Engineering, Wiley online library (wileyonlinelibrary.com), doi 10.1002/ep.11607

Schmid, J.C., Kolbitsch, M., Fuchs, J., Benedikt, F., Müller, S. and Hofbauer, H., (2016), “Steam gasification of exhausted olive pomace with a dual fluidized bed pilot plant at TU Wien”, technical report for the EU-project PHENOLIVE, 29 February 2016, Institute of Chemical Engineering, TU Wien

Schmid, J.C., Pröll, T., Pfeifer, C., Rauch, R. and Hofbauer, H., (2012b), “Cold flow model investigation on a modified riser with enhanced gas-solid contact - locating the regions of operation in a fluidization regime map”, in: Proceedings of the 21st International Conference on Fluidized Bed Combustion (FBC), 3 – 6 June 2012, Naples, Italy, ISBN978-88-89677-83-4, pp.80 – 87

Schuster G., Löffler G., Weigl K. and Hofbauer H., (2001), “Biomass steam gasification-an extensive parametric modeling study”, Bio resource Technology, Vol. 77, pp. 71 – 79

State of the World’s Forests, (2001), www.fao.org

Stieß M., (2008), “Mechanische Verfahrenstechnik-Partikeltechnologie 1“, Konstanz, Springer

Swisher J. N., (1994), “Forestry and biomass energy projects bottom-up comparisons of CO_2 storage and costs”, Biomass and Bioenergy, Vol: 6, pp. 359 – 368

UNDP, United Nations Development Program, (2001), “Energy for sustainable development: a policy agenda”, Cambridge University Press, New York, USA, ISBN: 92-1-126145-7

Van der Stelt M. J. C., Gerhauser H., Kiel J. H. A. and Ptasinski K. J., (2011), “Biomass upgrading by torrefaction for the production of biofuels: a review”, Biomass Bioenergy , Vol. 35, pp. 3748 – 3762

Vassilev V. and Vassileva C., (2015), “Advantages and disadvantages of composition and properties of biomass in comparison with coal: An overview”, Fuel, Vol. 158, pp. 330 – 350

WBA Global Bioenergy Statistics, (2017), online available: www.worldbioenergy.org

World Energy Council, (2017), available online: world energy resources bioenergy in 2017

Zainal Z. A., Rifau A., Quadi G. A. and Seetharamu K. N., (2002), “Experimental investigation of a downdraft biomass gasifier”, Biomass Bioenergy. Vol. 23, pp. 283 – 289

Van Swaaij W., Kersten S., and Palz W., “Book: Biomass Power for the World – Transformations to Effective Use”, 1st edition, Pan Stanford Publishing, Singapore, ISBN: 978981461388

10 Appendix

PAPER 1:

(in context with this master thesis)

Mauerhofer A. M., Hassanli F., Schmid J. C., Hofbauer H., (2018), **“Influence of Alternative Bed Materials on Dual Fluidized Bed Steam Gasification”**, in: Proceedings of the 14th Minisymposium Chemical and Process Engineering, 4. – 5. April 2018, Linz, Austria

PAPER 2:

(as additional work beside to the context of this master thesis)

Hassanli F., Halajisani A., Schmid J. C., Rahimpour M. R., (2018), **“Investigation and recovery of flare gas using a membrane separation unit to enhance methanol synthesis production in the presence of catalyst deactivation”,** in: Proceedings of the VIENNA young SCIENTISTS SYMPOSIUM (VSS), 7. – 8. June 2018, Vienna, Austria

PAPER 1:

14th Minisymposium Chemical and Process Engineering, 4. – 5. April 2018, Linz, Austria

Influence of Alternative Bed Materials on Dual Fluidized Bed Steam Gasification

A. M. Mauerhofer[1,*], F. Hassanli[1], J. C. Schmid[1], H. Hofbauer[1]

1: Institute of Chemical, Environmental and Biological Engineering, TU Wien, Austria
* Correspondent author: anna.mauerhofer@tuwien.ac.at

Keywords: quartz, feldspar, limestone, fluidized bed, gasification, softwood

Introduction

The demand for electricity, heat and fuels all over the world increases. To enable a sustainable production of energy and energy carriers in the future alternative technologies and fuels beside fossils are topics of current research. Thus, the thermo-chemical conversion of biogenic fuels presents a promising way to enhance an eco-friendly, efficient and sustainable supply of these goods in daily life. The dual fluidized bed (DFB) steam gasification presented in Fig. 1 has long been a main subject of research at TU Wien. The DFB steam gasification comprises two interconnected reactors: A gasification reactor (GR) and a combustion reactor (CR). Thereby, solid fuel is converted into a nitrogen-free product gas, which mainly consists of hydrogen (H_2), carbon monoxide (CO), carbon dioxide (CO_2), methane (CH_4) and ethylene (C_2H_4). This product gas is source material for different applications. On the one hand, it can be utilized in gas engines, turbines or fuel cells to generate heat and electricity. And on the other hand it can be used as syngas for producing e.g. hydrogen, methane, chemicals, Fischer-Tropsch Diesel [1] or mixed alcohols [2].

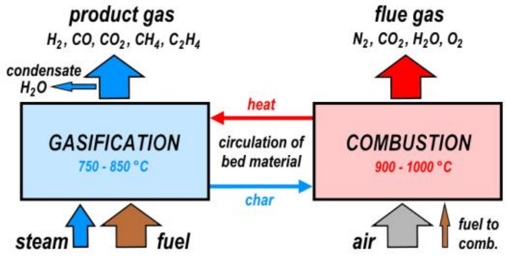

Fig. 1 Basic principle of the DFB steam gasification

The gasification and the combustion reactors are connected by circulating bed material. Through this bed material circulation, the transport of heat from the combustion reactor to the gasification reactor, which is necessary for the ongoing endothermic gasification reaction, can be assured. A typical biogenic fuel for steam gasification is wood. The fuel for the combustion reactor is mainly provided by the residues from the gasification process, the so called char. Through the circulating bed material, char is transported to the combustion reactor and burnt with air. To control the gasification temperature and to balance the heat losses of the pilot plant, additional fuel can be introduced into the combustion reactor. The first 100 kW$_{th}$ dual fluidized bed steam gasification pilot plant at TU Wien was realized in the 1990s [3]. Afterwards this technology has been demonstrated at industrial scale. In 2002, a demonstration plant with a fuel capacity of 8 MW$_{th}$ in Güssing, Austria was constructed [4]. Six years later, in 2008, a 8.5 MW$_{th}$ plant in Oberwart, Austria [5] was built followed by a 15 MW$_{th}$ plant in Senden, Germany. In 2014, a plant with a fuel power of 32 MW$_{th}$ was realized in Gothenburg, Sweden [6]. Olivine sand is used as bed material in all of these plants. Olivine is relatively expensive because the bed material has to be continuously replaced. Thus, alternative bed materials are of interest for the operation of industrial sized plants.

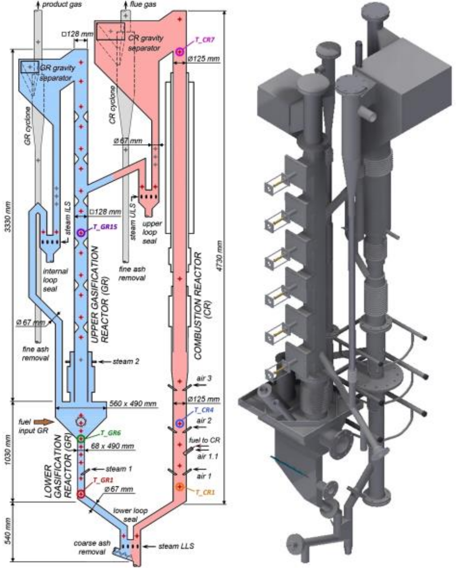

Fig. 2 Sketch with indicating dimensions (left) and 3D drawing of the reactor system (right)

Fig. 2 displays the actual reactor concept of the advanced design of the DFB gasification plant at TU Wien. The gasification reactor is divided into two parts: The lower part is designed as bubbling bed and the upper part is operated as a counter-current column for gas and solids with turbulent fluidized zones for tar cracking. Therefore, the upper counter-current column is equipped with constrictions, which cause an increased hold-up of bed material over the height of the reactor. This results in an extended residence time as well as an increased gas-solid contact of catalytic active bed material particles with product gas. Another favorable effect of the advanced design correlates to the separation system on top of the reactors. Through the replacement of cyclones by gravity separators, the use of softer materials like limestone is possible. Due to the fact, that limestone has a low abrasion resistance, the separation with gravity separators instead of cyclones compensates this unfavorable characteristics. Arising fines with a size of 5 – 80 µm after the gravity separators are removed via cyclones.

Experimental Setup and Methods

During the experiments a process control system measured and recorded data of all relevant flow rates, temperatures and pressures as well as gas compositions (Rosemount NGA2000) of the 100 kW$_{th}$ pilot plant. C_2H_4 was analyzed every 12 minutes by a gas chromatograph (Perkin Elmer ARNEL – Clarus 500). The product gas had to be filtered by a glass wool filter and washed with rapeseed methyl ester (RME) to remove condensable components like water and tar before it was measured online. A detailed explanation of the setup and measurement devices are reported in the work of Kolbitsch [7]. Tar was measured in an isokinetic and discontinuous way with impinger bottles to condense and dissolve condensable hydrocarbons. The solvent, which was used for measuring the tar content was toluene instead of isopropanol, which is typically used, because of the higher solubility of tar in toluene compared to isopropanol. In addition to the measurement of the tar content, the measurement of the water content was possible at same time by using toluene as solvent. However, by using toluene as solvent, its identification was excluded and the measurement of xylene and benzene was difficult with this setup. Due to that fact, the tar contents are presented without benzene, toluene and xylene (BTX). Within this paper, the focus lies on the use of different bed materials and mixtures of bed materials. The experiments, which are presented in the following were carried out with limestone, quartz and feldspar as bed materials. Limestone is mainly composed of calcium carbonate ($CaCO_3$). But limestone has a low abrasion resistance compared to commercially applied bed materials like olivine sand for fluidized bed applications. Quartz conversely showed a good abrasion resistance and owned much higher heat transfer properties. In an additional experimental campaign, feldspar with a very high share of potassium was also used. An alternative bed material (mixture) instead of the relatively expensive olivine is needed. Quartz and feldspar are cheap bed materials with high abrasion resistance but low catalytic activity for tar cracking/reforming reactions. Limestone is also cheap and worldwide available but has a low abrasion resistance. Limestone is catalytically highly active, because it forms CaO in the gasification system at high temperatures. CaO enhances tar cracking/reforming reactions significantly. By the use of mixtures of bed materials, the supplementing properties of different bed materials may fulfill the necessary requirements for the gasification. In Tab. 1 the compositions of the investigated bed materials are shown.

Tab. 1 Investigated bed materials

		bed material type	
parameter	**unit**	**limestone**	**quartz**
Al_2O_3	**wt.-%**	**-**	**0.1**
BaO	**wt.-%**	**-**	**-**
$CaCO_3$	**wt.-%**	**95-97**	**-**
CaO	**wt.-%**	**-**	**-**
Fe_2O_3	**wt.-%**	**0.1-0.3**	**0.04**
K_2O	**wt.-%**	**-**	**-**
MgO	**wt.-%**	**-**	**-**
$MgCO_3$	**wt.-%**	**1.5-4.0**	**-**
Na_2O	**wt.-%**	**-**	**-**
NiO	**wt.-%**	**-**	**-**
P_2O_5	**wt.-%**	**-**	**-**
SiO_2	**wt.-%**	**0.4-0.6**	**99.8**
TiO_2	**wt.-%**	**-**	**-**
Al_2O_3+Cr_2O_3+Mg_3O_4	**wt.-%**	**-**	**-**
hardness	**Mohs**	**3**	**7**
particle density	**kg/m³**	**2650, 1500***	**2650**
trace elements	**wt.-%**	**-**	**-**

*particle density after full calcination

All experiments, which are presented within this work were carried out with softwood pellets according to the Austrian standard ÖNORM M 7135 with a diameter of 6 mm. The proximate and ultimate analysis of the used softwood pellets is given in Tab. 2

Tab. 2 proximate and ultimate analysis of softwood

parameter	**unit**	**Softwood**
ash content	wt.-%$_{db}$	0.2
carbon (C)	wt.-%$_{db}$	50.7
hydrogen (H)	wt.-%$_{db}$	5.9
nitrogen (N)	wt.-%$_{db}$	0.2
sulphur (S)	wt.-%$_{db}$	0.005
chlorid (Cl)	wt.-%$_{db}$	0.005
oxygen (O)	wt.-%$_{db}$	43.0
volatiles	wt.-%$_{db}$	85.4
fixed C	wt.-%$_{db}$	14.6
water content	wt.-%	7.2
LHV (dry)	MJ/kg$_{db}$	18.9
LHV (moist)	MJ/kg	17.4

All in all, seven different experiments were carried out. Two main bed materials with good attrition resistance were chosen and mixed with limestone in different mass ratios. The campaigns started with 100 wt.-% of the main bed material, proceed with a 90/10 wt.-% mixture, then using a 50/50 wt.-% mixture and finally compared with 100 wt.-% limestone. This scheme was applied for quartz and feldspar (see Tab. 3). To ensure a comparability between different bed material types softwood was used as fuel in all test runs.

Tab. 3 Presented experiments with different bed material compositions

		Experiment					
bed material	**unit**	**1** **L**	**2** **Q_{100}**	**3** **Q_{90}**	**4** **Q_{50}**	**5** **F_{100}**	**6** **F_{90}**
limestone	wt.-%	100	-	10	50	-	10
quartz	wt.-%	-	100	90	50	-	-
feldspar	wt.-%	-	-	-	-	100	90

L…limestone; Q…quartz; F…feldspar;

The use of the process simulation software IPSEpro enables to calculate mass and energy balances of the data, which were collected during the gasification experiments. IPSEpro is a flowsheet-based process simulation tool and provides the user a stationary process simulation. It enables to validate measured data and therefore represents results in a very high-quality and representative way. A detailed model library for the use of IPSE pro was developed by Pröll and Hofbauer [8]. To describe the gasification process in detail, several important parameters are of interest. Within this paper, the temperatures in the upper and lower gasification reactor and the steam to fuel ratio are shown. The steam to fuel ratio φ_{SF} is presented in Equation **1** and describes the sum of water and steam in relation to the total mass of dry and ash-free fuel, which is introduced into the GR.

$$\varphi_{SF} = \frac{\dot{m}_{steam,GR} + \dot{m}_{H2O,GR,fuel}}{\dot{m}_{GR,fuel,daf}} \qquad \textbf{Equation 1}$$

The water gas shift (WGS) reaction (see Equation 2) is the most important homogeneous gas-gas reaction, which takes place during the gasification process.

$$CO + H_2O \rightleftharpoons CO_2 + H_2 \qquad \textbf{Equation 2}$$

In Equation 3 the chemical reaction of the steam reforming of hydrocarbons is shown and used for discussing tar decomposition.

$$C_aH_b + a\,H_2O \rightleftharpoons a\,CO + (a + \frac{b}{2})\,H_2 \qquad \textbf{Equation 3}$$

Results and Discussions

Fig. 3 presents the main product gas composition of the gasification test runs with softwood from 100 wt.-% quartz to 100 wt.-% limestone and Fig. 4 displays the main product gas composition of the test runs from 100 wt.-% feldspar to 100 wt.-% limestone.

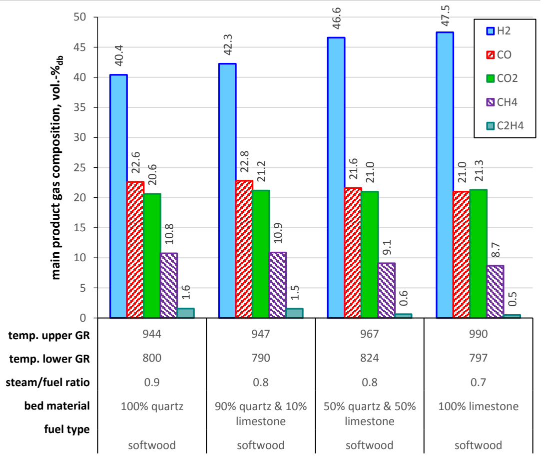

Fig. 3 Main product gas composition of quartz and lin bed materials

By investigating different bed material types during the gasification process a trend could be seen. The H_2 content increased by increasing the limestone content with a maximum value at 100 wt.-% limestone. In parallel, the CO content decreased. This behavior can be explained by an improved WGS reaction (see Equation **2**) through the catalytic activity of calcium oxide (CaO). In literature a comparable effect can be found [9]. The gas compound CH_4 showed a slightly decreasing course. CO_2 increased when limestone was added to the main bed material, but remained relatively stable afterwards.

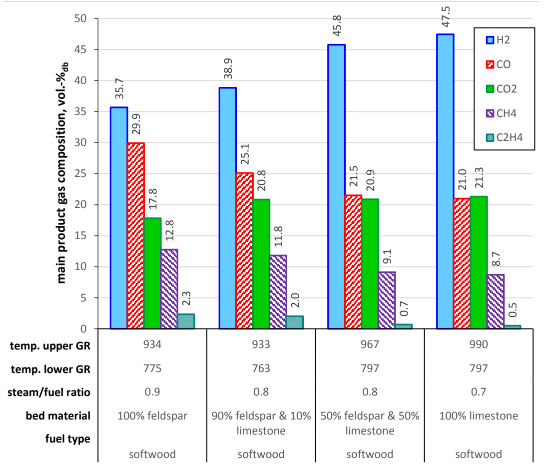

Fig. 4 Main product gas composition of feldspar a limestone as bed materials

In Fig. 5 and Fig. 6 the tar contents as well as the tar dew points from the experiments are shown. The tar dew points were calculated from values of single gas chromatograph coupled with mass spectrometry (GC/MS) tar compounds according to the calculation tool from the Energy Research Centre of the Netherlands [10]. It can be seen, that very high tar contents occurred, when no limestone was added to the main bed material. This could be explained by the low catalytic activity in terms of steam reforming of tar/hydrocarbons. Adding limestone to the bed material, the formation of CO via the steam reforming reaction (see Equation **3**) led to a more intensive run of the WGS reaction, which resulted in higher H_2 contents. Generally, the tar formation could be reduced in line with an increased share of limestone in the bed material mixture. It is apparent, that 50 wt.-% of limestone in the initial bed material mixture led to a significant effect on product gas composition and tar reduction. The tar dew point, which represents an important indicator for formation of deposits in the product gas line, showed a decreasing trend by increasing the limestone content in the bed material mixtures. When investigating 100 wt.-% limestone as bed material, a minimum value for the tar dew point of 92 °C was found.

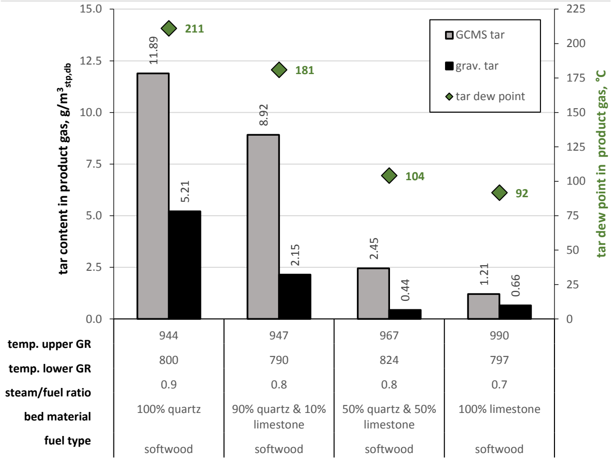

Fig. 5 Tar content of quartz and limestone as bed materials

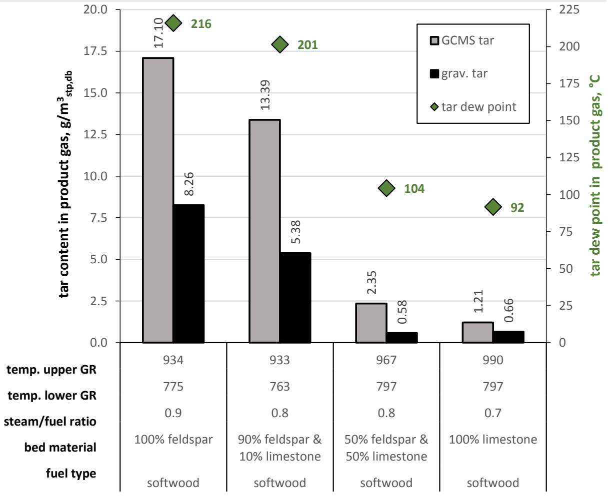

Fig. 6 Tar content of feldspar and limestone as bed materials

Conclusions

The investigations on the dual fluidized bed steam gasification of softwood with alternative bed material mixtures (beside pure olivine sand) in the advanced 100 kW$_{th}$ pilot plant at TU Wien showed a good performance. The catalytic activity of CaO shifted the main product gas compositions to higher H_2 contents as well as lower tar contents and reduced tar dew points. The investigations showed, that when 100 wt.-% quartz or feldspar was used as bed material, thermal effects played a major role regarding tar cracking in the upper gasification reactor. When limestone is added, tar reduction was not only supported by thermal destruction, but also by the favorable catalytic activity of CaO. Summarizing, quartz, feldspar and limestone are cheap and worldwide available compared to olivine. Thus, the presented alternative bed materials are predestined for the dual fluidized bed steam gasification process. In combination with limestone, the missing catalytic properties of alternative bed materials can be balanced and a promising and suitable bed material mixture can be obtained to produce a high-valuable product gas.

List of Abbreviations

Abbreviation	Meaning
BTX	Benzene, toluene and xyle
CR	Combustion reactor
DFB	Dual fluidized bed
ECN	Energy research Centre o Netherlands
GC/MS	Gas chromatograph co with mass spectrometry
GR	Gasification reactor
vol.-%	Volumetric percent
WGS	Water gas shift
wt.-%	Weight percent

List of Subscripts

Subscripts	Meaning
db	Dry basis
daf	Dry and ash free
fuel	
GR	Gasificaiton reactor
steam	
stp	Standard temperature pressure
th	thermal
SF	Steam to fuel

List of symbols

Symbol	Meaning	Unit
a, b	Stoichiometric factors	-
$\dot{m}$	Mass flow	kg/s
φ_{SF}	Steam to fuel ratio	kg_{H2O}/kg_{fuel}

References

[1] S. Müller, P. Groß, R. Rauch, R. Zweiler, C. Aichernig, and M. Fuchs, "Production of diesel from biomass and wind power – Energy storage by the use of the Fischer-Tropsch process," 2017.

[2] G. Weber, R. Rauch, and H. Hofbauer, "Production of mixed alcohols from biomass-derived synthesis gas using a sulfidized molybdenum catalyst," *Proc. Int. Conf. Polygeneration Strateg. (ICPS13), Vienna.*, 2013.

[3] H. Hofbauer, "Gasification of organic material in a novel fluidization bed system. Proc. of the 1st SCEJ Symposium on Fluidization. Tokyo," 1995.

[4] H. Hofbauer, R. Rauch, K. Bosch, R. Koch, and C. Aichernig, "Biomass CHP Plant Güssing - A Success Story," *Expert Meet. Pyrolysis Gasif. Biomass Waste*, 2002.

[5] V. Wilk and H. Hofbauer, "Analysis of optimization potential in commercial biomass gasification plants using process simulation," *Fuel Process. Technol.*, vol. 141, pp. 138–147, 2016.

[6] I. Gunnarsson, "The GoBiGas project - efficient transfer of biomass to biofuels, in Proceedings of the International Seminar on Gasification, Gothenburg, Sweden," 2010.

[7] M. Kolbitsch, "First Fuel Tests at a Novel 100 kWth Dual Fliuidized Bed Steam Gasification Pilot Plant," TU Wien, doctoral thesis, 2016.

[8] T. Pröll and H. Hofbauer, "Development and Application of a Simulation Tool for Biomass Gasification Based Processes," *Int. J. Chem. React. Eng.*, vol. 6, no. 1, p. Article A89, 2008.

[9] S. Koppatz, C. Pfeifer, and H. Hofbauer, "Comparison of the performance behaviour of silica sand and olivine in a dual fluidised bed reactor system for steam gasification of biomass at pilot plant scale," *Chem. Eng. J.*, vol. 175, no. 1, pp. 468–483, 2011.

[10] Energy Research centre of the Netherlands, http://theresites.nl, 2009. (accessed: Oktober 23, 2017)

PAPER 2:
VIENNA young SCIENTISTS SYMPOSIUM (VSS), 7. – 8. June 2018, Vienna, Austria

Investigation and recovery of flare gas using a membrane separation unit to enhance methanol synthesis production in the presence of catalyst deactivation

Fatemeh Hassanli[a,b], Ahmad Halajisani[b], Johannes C. Schmid[a], Mohammad R. Rahimpour[c,d]

[a] E166 Institute of Chemical, Environmental and Bioscience Engineering, TU Wien
[b] School of Chemical Engineering, Collage of Engineering, University of Tehran, Iran
[c] School of Chemical and Petroleum Engineering, Dep. of Chem. Eng., University of Shiraz
[d] Institute of Chemical Engineering and Materials Science, University of California, USA

INTRODUCTION

This research focuses on the recovery of flare gas of the world's largest methanol complex, located in Pars Special Economic Energy Zone of Iran. The work aiming at an increase of methanol production and process efficiency by utilizing flare gas components in an environmentally friendly way. Methanol is produced by the catalytic conversion of the synthesis gas over a commercial catalyst (Figure 1). Important Reactions are shown in Eq. 1-3.

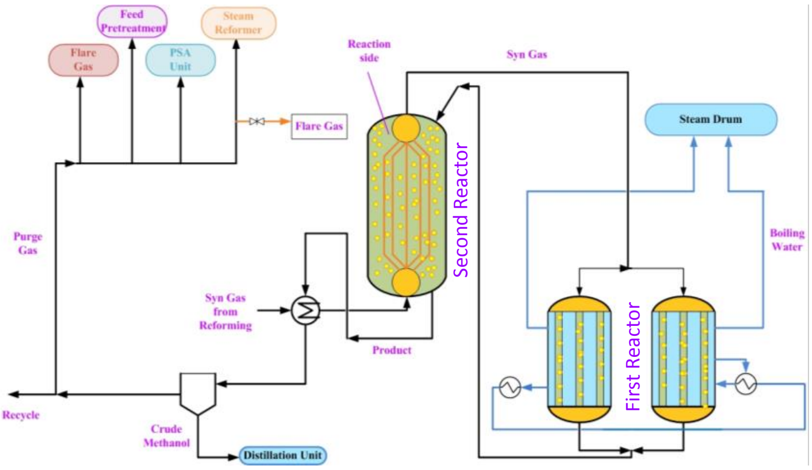

Figure 1: Schematic diagram of the methanol production unit

$$CO + 2H_2 \leftrightarrow CH_3OH \qquad \Delta H_{298} = -90.00\ kJ/mol \qquad \text{Eq. 1}$$
$$CO_2 + 3H_2 \leftrightarrow CH_3OH + H_2O \qquad \Delta H_{298} = -49.43\ kJ/mol \qquad \text{Eq. 2}$$
$$CO_2 + H_2 \leftrightarrow CO + H_2O \qquad \Delta H_{298} = +41.12\ kJ/mol \qquad \text{Eq. 3}$$

MATHEMATICAL MODEL

A one-dimensional steady state model has been used for this fixed-bed reactor to determine the concentration and temperature distributions inside the reactor. To obtain the mole and the energy balance equations, a differential element along the axial direction inside the reactor was considered [1-3]. The simulation of the novel process chain is shown schematically in Figure 2.

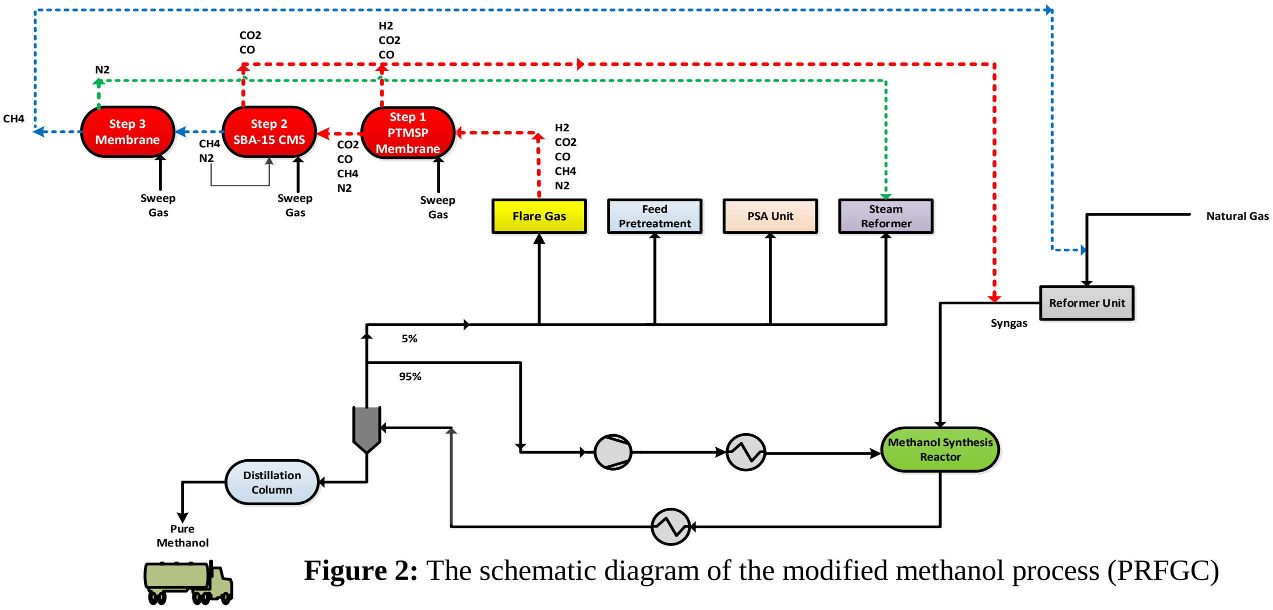

Figure 2: The schematic diagram of the modified methanol process (PRFGC)

RESULTS

The developed steady-state model was validated under industrial conditions and the results of simulation with daily-real plant data were in very good agreement. The achieved simulation results from comparison of Industrial Configuration (IC), Recycle Flare Gas Configuration (RFGC) and purposed strategy, named as Purified Recycle Flare Gas Configuration (PRFGC), are illustrated in Figure 3 & 4.

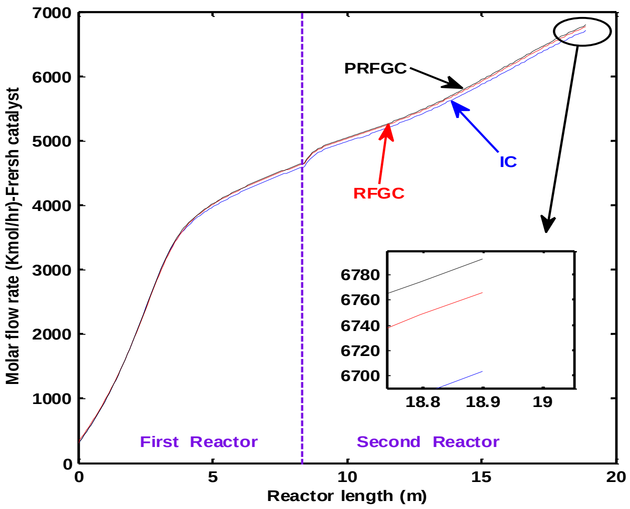

Figure 3: Methanol production along the reactor length

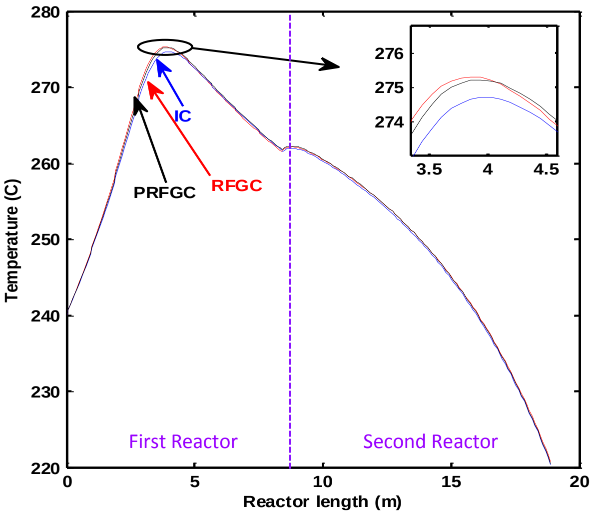

Figure 4: Temperature along the reactor length

Consequently, the methanol production rate obtained from the modified process PRFGC is significantly more than with IC. The reason of lower methanol production in RFGC in comparison with PRFGC is the inert gas increase in the reaction medium. The loss of catalyst activity, which corresponds to the loss of active surface area, is due to thermal sintering in commercial low-pressure $CuO/ZnO/AL_2O_3$ catalysts (Figure 5). The effect of specific catalyst deactivation is considered in the model.

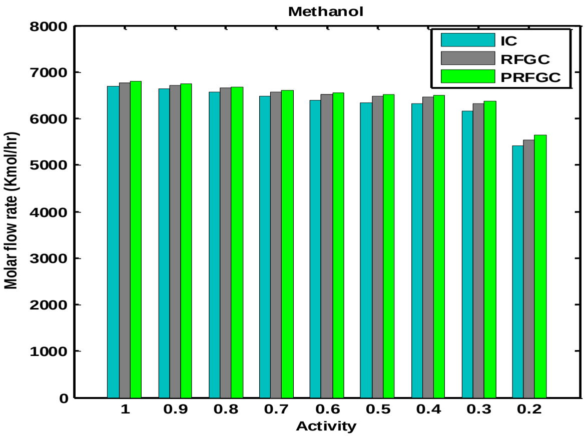

Figure 5: Influence of catalyst activity on the performance of methanol production

CONCLUSION

- A novel recovery-process is presented: PTMSP and SBA-15/CMS membranes are used to separate H_2, CO and CO_2 from the flare gas. An additional membrane separates CH_4 from N_2.
- Up to 17.3 ton/h of flare gas (60% H_2, 20% CO & CO_2, 20% N_2 & CH_4) can be reused.
- 12-14 million US-$ annual profit increase due to the increased methanol production is possible.
- With the modified process chain emission of more than 30300 ton/year of CO_2 to the atmosphere can be prevented by recovering flare gas to the methanol production process.

REFERENCES

[1] G. Graaf, P. Sijtsema, E. Stamhuis, G. Joosten, Chemical equilibria in methanol synthesis, Chemical Engineering Science, 41, pp.2883–2890, (1986).

[2] G. Graaf, H. Scholtens, E. Stamhuis, A. Beenackers, Intra-particle diffusion limitations in low-pressure methanol synthesis, Chemical Engineering Science, 45, pp.773–783, (1990).

[3] L. Hanken, Master's thesis, The Norwegian University of Science and Technology, (1995).